SENSITIVITY ANALYSIS OF TRX-2 LATTICE PARAMETERS WITH EMPHASIS ON EPITHERMAL ^{238}U CAPTURE

EPRI NP-346
(Research Project 612)
ENDF-252

Final Report

March 1977

Prepared by

OAK RIDGE NATIONAL LABORATORY*
P. O. Box X
Oak Ridge, Tennessee 37830

PRINCIPAL INVESTIGATORS
E. T. Tomlinson
G. deSaussure
C. R. Weisbin

(Appendix B written by R. W. Peelle)

*Operated by Union Carbide Corporation Nuclear Division
for the Energy Research and Development Administration

Prepared for

Electric Power Research Institute
3412 Hillview Avenue
Palo Alto, California 94304

and

Energy Research and Development Administration
20 Massachusetts Avenue
Washington, D. C. 20545

EPRI Project Manager
Odelli Ozer

FOREWORD

In order to utilize our nuclear fuel resources most efficiently, it is necessary to have an accurate knowledge of the nuclear properties and cross sections of most materials used in the design of reactor cores. Having such information available on a national standard data file would also be useful for simplifying the dialogue between the utility industry and regulatory agencies and/or vendor organizations. In an attempt to achieve this dual objective, EPRI has been supporting and participating in the activities of the "Cross Section Evaluation Working Group" (CSEWG) responsible for the development of the national reference data library--ENDF/B. Sensitivity analysis is an important tool in the development of such a library since it can provide information on which cross section features are most likely to affect the results of benchmark calculations. In the past such information was obtained in a parametric fashion by doing a series of calculations, each with a modified cross section data base. Such an approach permitted a very limited set of modifications to be tested. Recent advances in computing capability have enabled a few laboratories to implement more powerful methods based on perturbation theory. In particular, the method of sensitivity analysis implemented at Oak Ridge National Laboratory and outlined in Section 8 of this report is capable of simultaneously determining the dependence of a calculated parameter of interest to variations in all relevant cross sections over all energy ranges in great detail. Examples of the resulting "sensitivity profiles" can be seen in Figures 12-31 of this report.

This method of sensitivity analysis has been used extensively by ERDA and the Department of Defense for determining priorities in cross section development for fast breeder reactor and weapons applications. The present project is the first attempt in applying the method to the relatively more complex problem of thermal reactor benchmarks.

The following is a list of the most important results that have been obtained:

(a) The feasibility of utilizing formal sensitivity analysis methods for thermal reactor benchmarks has been demonstrated.

(b) The sensitivity profiles that have been obtained will be used as guidelines for the development of the next version of the national reference data library--

ENDF/B. These profiles provide a quick check for determining the effect of any proposed cross section modification on the calculation of the benchmark experiment considered in this project.

(c) The reevaluation of the resonance data for Uranium-238 carried out as part of this project is expected to help resolve the long standing discrepancy between the calculated and measured capture rates for this material.

(d) The uncertainties inherent in the cross sections of the primary materials of interest to this project have been estimated. When these uncertainties are combined with the calculated sensitivity profiles, the resulting uncertainty in the calculations that can be attributed directly to nuclear data has been shown to be smaller than the uncertainties due to methods approximations. An estimate of the latter can be obtained by comparing the scatter among calculated results reported by different investigators using the same data base.

The limitations of the project are the following:

(a) Only one benchmark experiment has been analyzed. Although the case that has been selected is one of the principal CSEWG thermal benchmarks, the number of materials entering into the composition of this experiment is limited. Additional cases, particularly ones containing plutonium isotopes should also be analyzed.

(b) The method of analysis did not provide for extensive detail to be shown in the thermal energy range of the sensitivity profile.

The above two points are being addressed in a follow-on project with the same contractor (RP975-3).

Odelli Ozer
EPRI Project Manager

ABSTRACT

The main purpose of this study is the determination of the sensitivity of TRX-2 thermal lattice performance parameters to nuclear cross section data, particularly the epithermal resonance capture cross section of ^{238}U. The performance parameters considered are k_{eff}, $^{28}\rho$, $^{25}\delta$, $^{28}\delta$, and CR. An energy-dependent sensitivity profile was generated for each of the performance parameters, to the most important cross sections of the various isotopes in the lattice. Uncertainties in the calculated values of the performance parameters due to estimated uncertainties in the basic nuclear data, deduced in this study, were shown to be small compared to the uncertainties in the measured values of the performance parameter and compared to differences among calculations based upon the same data but with different methodologies.

The ENDF/B-IV ^{238}U cross sections were modified based on recent measurements and analysis not available to the ENDF/B-IV evaluators. The change from ENDF/B-IV to the recommended cross sections was divided in four steps and the performance parameters were recomputed after each step, so that the relative importance of various modifications to the cross sections could be compared.

A tentative adjusted set of cross section data was obtained, which is consistent with the microscopic measurements and minimizes the weighted differences between the calculated and measured values of the performance parameters for TRX-2. The actual adjustments to the recommended data were minimal such that the recommended evaluation, based solely upon differential measurements, could be used without adjustment while maintaining consistent agreement with calculated TRX-2 performance.

ACKNOWLEDGEMENTS

The authors would like to acknowledge the significant contributions made by J. E. White and R. Q. Wright in the preparation of the epithermal cross sections used in this project and O. Ozer for the thermal cross sections. The efforts of J. L. Lucius for the calculation of the generalized sources and sensitivity profiles, L. M. Petrie for the Monte Carlo calculation of the leakage, and J. D. Drischler for obtaining the multigroup covariance files are also greatly appreciated.

The authors also wish to thank D. K. Olsen and R. B. Perez for their aid in obtaining the alternative data sets. Appreciation is also extended to F. G. Perey for recommending the approach used to obtain sensitivities to the resonance parameters. R. W. Peelle developed the covariance file evaluation for $^{235}U(n,f)$. The authors wish to note the important contributions by E. M. Oblow, J. H. Marable, and N. M. Greene in the assessment of the sensitivity profiles and results, and gratefully acknowledge the review of this work by J. D. Hardy, D. R. Finch, P. Rose, and O. Ozer.

This work was sponsored by the Nuclear Power Division of the Electric Power Research Institute.

Finally, the authors wish to extend special thanks to Virginia Glidewell who typed and organized this report.

TABLE OF CONTENTS

LIST OF FIGURES

LIST OF TABLES

I. INTRODUCTION

Calculated overprediction of epithermal ^{238}U capture in water moderated lattices using ENDF/B data has been a long standing problem[1] basic to the prediction of neutron economy and conversion ratio in light water reactors. Measurements of epithermal/thermal ^{238}U capture indicated a 10% discrepancy based upon data testing of ENDF/B-III[2] with an associated 1 to 1-1/2% underprediction of k_{eff}. ENDF/B-IV predictions[3] of the measured integral parameters were significantly improved over those of ENDF/B-III for the uranium systems. However, a significant dispersion in the reported results[3] from independent ENDF/B-IV data testers, illustrated in part in Table 1, has led to the still unsatisfactory situation tabulated below.

Table 1. ENDF/B-IV Data Testing Results for Slightly Enriched Uranium Fueled, Water Moderated Thermal Lattices

	k	$^{28}\rho$[a]	$^{25}\delta$[b]	$^{28}\delta$[c]
Experiment (TRX-1	1.0000	1.324±0.02	0.0995±0.01	0.0934±0.002
ANC	0.9827	1.426	0.1005	0.0957
BAPL	0.9954	1.362	0.0992	0.0948
BNL	0.9880	1.367	0.0993	0.0939
CRNL[f]	0.9824	1.433	0.111	0.0937
EPRI	0.9903	1.344	0.0966	0.0940
GA	0.9855	1.407	0.0982	0.0965
SRL[d]	0.9921	1.365	0.0946	0.0935
Experiment (TRX-2)[e]	1.0000	0.842±0.015	0.0622±0.0007	0.0687±0.002
ANC	0.9893	0.890	0.0615	0.0691
BAPL	0.9996	0.859	0.0610	0.0678
BNL	0.9921	0.846	0.0611	0.0663
CRNL[f]	0.9898	0.882	0.067	0.0661
GA	0.9961	0.881	0.0606	0.0700
SRL[d]	0.9977	0.838	0.0576	0.0642

[a] Ratio of epithermal-to-thermal ^{238}U captures.
[b] Ratio of epithermal-to-thermal ^{235}U fissions.
[c] Ratio of ^{238}U fissions to ^{235}U fissions.
[d] Resonance treatment developed by D. R. Finch.
[e] Uncertainties and nominal values for the TRX-2 experiment have recently been revised by Sher et al.[31] These are not listed in Table 1.
[f] Chalk River National Laboratory.

The TRX-1 and TRX-2 lattices are water moderated thermal assemblies. In particular, the TRX-2 fuel rods were fabricated of uranium metal (enriched to 1.3% ^{235}U, clad in aluminum). The rods were 121.92 cm in length and 0.983 cm in diameter, arranged in hexagonal arrays with a water-to-fuel ratio of 4.02. This resulted[3] in a spectrum considerably softer than the lattice of a typical pressurized water reactor. The lattice was fully reflected and the perimeter was made as circular as possible. The significant differences in calculated performance (Table 1) for these assemblies are not statistical; definitive conclusions cannot be deduced from Table 1 in terms of "average" results. The dispersion among reported calculational results is of the same order as the quoted uncertainty in the integral experiment. Calculated predictions of k_{eff} are from 0.5 to 1.5% low for TRX-1 and vary from excellent agreement to 1% low for TRX-2 depending upon the specific analysis methods used. Similarly, values for $^{28}\rho$ range from 1.5 to 8% high for TRX-1 and from 0.3% low to 6% high for TRX-2 compared to 1σ experimental uncertainties of less than 2%. It appears natural to associate the underprediction of k_{eff} with the overprediction of ^{238}U capture. However, this picture is far too simplistic since it ignores important factors such as ^{235}U fission and leakage which will be discussed in detail later in this report. Other parameters such as $^{25}\delta$ and $^{28}\delta$ depend upon ^{238}U capture only indirectly through its effect on the flux spectrum. These parameters, which are indicative of the ^{235}U fission rate and the leakage treatment, also reflect significant differences between reported data testing from different laboratories.

The differences reported above embody at least two analysis problems common to many applications in reactor physics. First, knowledge of calculation/experiment is usually not sufficient to evaluate whether such data are really discrepant. One must determine the uncertainties associated with each and, if at all possible, separate uncertainties due to methods approximations from those due to nuclear data. Secondly, the ENDF/B-IV data file for ^{238}U does not accurately reflect evaluation of currently available differential measurements between 1 and 100 eV. It is clear that many changes can be made, but it is much less clear which would be significant. Finally, the process of including <u>all</u> information, both differential and integral, in the quantitative analysis process is considered essential to reactor design.

The objective of this project is the determination of a recommended representation of the ^{238}U capture cross section based upon available differential

and specific integral data and the quantitative determination of the sensitivity of thermal uranium lattice (TRX-2) performance parameters to the cross section shape, magnitude, and representation with emphasis on the first four resolved s-wave resonances. Sensitivity profiles and covariance matrices developed for ^{238}U capture and ^{235}U fission permit a first quantitative assessment of performance parameter uncertainties due to concomitant uncertainties in nuclear data. The application of sensitivity methodology to the understanding of epithermal ^{238}U capture is directly responsive to recommendations made at the Seminar on ^{238}U Resonance Capture[4] and illustrative of the powerful role this type of analysis can play in planning and analyzing integral experiments.

II. BACKGROUND AND REPORT ORGANIZATION

Prior to this project initiation, Askew,[1] Bhat,[5] Hardy,[6] Rothenstein[7] and others had already suggested that uncertainties in the capture widths of the first few ^{238}U levels are sufficient to account for the discrepancies between measured and calculated parameters. Recent measurements by Olsen et al.[8] and Liou and Chrien[9] were directed toward a precise determination of the ^{238}U cross sections over the first few levels. In evaluating their measurements relative to ENDF/B-IV, deSaussure et al.[10] note that the ENDF/B-IV file fails to represent correctly the minima in the ^{238}U total cross section, and even leads to negative values because: (1) the ENDF/B-IV treatment neglects the contribution of levels outside the resolved range and (2) it is based on the single level Breit-Wigner approximation which is valid only in the vicinity of the resonance energy. For those reasons, their experimental data was fitted with a multilevel Breit-Wigner cross section formalism and appropriate "background" cross sections were derived with a "picket-fence" model. The results of this study, as well as other recent measurements, and a careful re-evaluation of the results of older measuments suggest smaller radiation widths (in the range of 23 mV) for the first few levels of ^{238}U than those of ENDF/B-IV. As part of this project specific recommendations for the ^{238}U data file (with emphasis below 100 eV) were developed and used. Covariance files for ^{238}U cross sections were evaluated over the entire energy region with emphasis placed on the covariance for the s-wave resolved resonances below 100 eV. Correlations between capture and neutron widths were included where appropriate. Finally, preliminary covariance files were also developed for ^{235}U fission and capture cross sections as well as $^{238}U(n,\gamma)$ and $H(n,\gamma)$ in the thermal group.

In consultation[11] with the CSEWG Thermal Data Testing Subcommittee, the decision was made to perform sensitivity and uncertainty analysis for the TRX-2 lattice. This assembly was selected primarily due to the large number of investigators who have previously analyzed this lattice using various versions of ENDF/B and the associated availability of documentation. The choice of multigroup energy structure for the analysis of TRX-2 was primarily made with respect to the ^{238}U total cross section; the details of this choice is described in Section III. The processing tools used for the multigroup cross section generation are described in Section IV and these tools were applied to the calculational model for TRX-2 discussed in Section V. The ENDF/B-IV multigroup cross section data library so derived was tested according to procedures presented in Section VI. With this data file at hand, performance parameters were calculated and are presented in Section VII along with the associated fluxes and adjoints. Subsequently, the sensitivity profiles which are defined in Section VIII were computed. These curves are presented in Section IX for each of five performance parameters and all important components of the nuclear data field. The sensitivities enable one to project changes to performance parameters consequent to hypothesized changes in the nuclear data. Credible alternative ^{238}U data sets based upon recent measurement and re-evaluation are described in Section X. The sensitivity coefficients were used to establish the changes in TRX-2 performance which would be anticipated if this new evaluation were adopted. These alternative data set results are illustrated in Section XI. The generation of evaluated covariance files is described in Section XII and the associated processed multigroup covariance files for ^{235}U are given in Section XIII. These covariance files were used to estimate uncertainties in calculated TRX-2 performance as presented in Section XIV. Section XV describes our inferred cross section values consistent with differential and TRX-2 data. Lastly, the overall project conclusions are discussed in Section XVI.

III. MULTIGROUP ENERGY STRUCTURE SELECTION

In order to assess the sensitivity of the parameters of interest to the magnitude and formalism of the s-wave ^{238}U resonances below 100 eV, it was appropriate to employ an extremely fine energy group structure in this energy region. Each of the four resonances (6.67, 20.9, 36.8, and 66.2 eV) was spanned by approximately 24 energy groups which not only provided the capability of examining these resonances in detail, but also minimized

the approximations made in resonance self-shielding. It should be noted, however, that the resonance structure of other materials and/or reaction types [e.g., $^{235}U(n,f)$] was not considered in any detail in selecting the group boundaries. The contributions of the resonance levels above 66 eV are also not treated in great detail.

The first 23 group energy boundaries (10^7 eV < E < 10^2 eV) were chosen to produce groups of equal lethargy width (i.e., $\Delta u = 0.5$). The following 107 group energy boundaries were selected according to the aforementioned criterion. Cross sections in the epithermal and fast energy ranges were generated using MINX[12]/SPHINX[13]/AMPX.[14] Cross sections for the single thermal group (E < 0.625 eV) (no upscatter cross section) were provided by EPRI.[15] These included detailed self-shielding, upscattering, and bound atom cross section effects not presently considered in the MINX[12] code. The energy grid used in this analysis is presented in Table 2, and a comparison of the multigroup cross section and the ENDF/B ^{238}U total cross section point data are shown in Fig. 1. Note the fine resolution around the first four resolved resonances.

IV. MULTIGROUP CROSS SECTION GENERATION

The multigroup cross sections for hydrogen, oxygen, aluminum, ^{235}U and ^{238}U derived from ENDF/B-IV were processed using the MINX/SPHINX/AMPX system which has previously been tested on various fast reactor benchmarks.[16-18] Prior to actual cross section generation, the system was applied to a number of TEDIUM[19] isotopes to detect whether any numerical anomalies would arise from the use of an extremely fine energy mesh; none were found. A flow diagram depicting the relationship between the processing codes involved is presented in Fig. 2. The function of each module is discussed in chronological processing order.

The point cross sections for each of the ENDF/B-IV materials (Mat. #1269, 1276, 1193, 1261, and 1262) were reconstructed using the RESEND[20] module of MINX with reconstruction, linearization, and thinning tolerances of 0.5%. This method proved satisfactory for all materials except ^{238}U (1262). The extremely large number of points (approximately 93,000 for the capture cross section) generated made the cost of Doppler broadening and linearization of the various proposed data sets prohibitive. Prior thinning with the code LINEAR[21] was used to linearize and thin the ^{238}U RESEND data to a manageable number of points

Table 2. 131 Group Energy Boundaries for the EPRI ^{238}U Sensitivity Study

Group	Upper Energy (eV)	Group	Upper Energy (eV)
1	1.00000+7	47	6.61366+1
2	6.06531+6	48	6.61270+1
3	3.67879+6	49	6.60980+1
4	2.23130+6	50	6.60700+1
5	1.35335+6	51	6.59900+1
6	8.20850+5	52	6.58700+1
7	4.97871+5	53	6.55100+1
8	3.01974+5	54	6.52300+1
9	1.83156+5	55	6.50400+1
10	1.11090+5	56	6.46200+1
11	6.73795+4	57	6.38000+1
12	4.08677+4	58	6.32200+1
13	2.47875+4	59	5.30000+1
14	1.50344+4	60	3.97000+1
15	9.11882+3	61	3.87600+1
16	5.53084+3	62	3.81850+1
17	3.35463+3	63	3.78100+1
18	2.03468+3	64	3.75200+1
19	1.23410+3	65	3.72100+1
20	7.48518+2	66	3.69800+1
21	4.53999+2	67	3.69146+1
22	2.75364+2	68	3.68491+1
23	1.67017+2	69	3.68300+1
24	1.01310+2	70	3.68108+1
25	9.36000+1	71	3.67917+1
26	9.30000+1	72	3.67725+1
27	9.12800+1	73	3.67534+1
28	9.06250+1	74	3.66767+1
29	8.97500+1	75	3.66000+1
30	8.87500+1	76	3.65000+1
31	8.39200+1	77	3.63800+1
32	8.32000+1	78	3.60955+1
33	8.18000+1	79	3.57800+1
34	8.00000+1	80	3.54900+1
35	6.86800+1	81	3.51200+1
36	6.79800+1	82	3.46000+1
37	6.75000+1	83	2.30000+1
38	6.68700+1	84	2.24500+1
39	6.65900+1	85	2.19500+1
40	6.63800+1	86	2.15800+1
41	6.62200+1	87	2.13000+1
42	6.61975+1	88	2.11000+1
43	6.61750+1	89	2.10000+1
44	6.61654+1	90	2.09626+1
45	6.61558+1	91	2.09252+1
46	6.61462+1	92	2.09152+1

Table 2 (Cont'd.)

Group	Upper Energy (eV)	Group	Upper Energy (eV)
93	2.09053+1	113	6.78000+0
94	2.08953+1	114	6.71000+0
95	2.08854+1	115	6.69690+0
96	2.08754+1	116	6.68387+0
97	2.08377+1	117	6.67830+0
98	2.08000+1	118	6.67280+0
99	2.07600+1	119	6.66720+0
100	2.06000+1	120	6.66170+0
101	2.04000+1	121	6.65616+0
102	2.01500+1	122	6.64310+0
103	2.00000+1	123	6.63000+0
104	1.98000+1	124	6.56000+0
105	1.92600+1	125	6.40000+0
106	1.05000+1	126	6.25000+0
107	9.93000+0	127	6.15000+0
108	8.06000+0	128	5.95000+0
109	7.51000+0	129	5.50000+0
110	7.19000+0	130	1.00000+0
111	7.01000+0	131	6.25000-1
112	6.90000+0		1.00000-5

(approximately 33,000). Point cross sections for the alternative ^{238}U data sets (to be discussed in Section X) were created using the NPTXS module of the AMPX code system. The NPTXS module employs a user-controlled energy mesh to describe the resonances reconstruction. This procedure generally results in significantly fewer energy points than the RESEND algorithm but with only qualitative accuracy estimates.

The thinned and linearized point cross section data sets for all the materials generated were then group averaged and the Bondarenko factors calculated for various background cross sections using the MINX code. The weight function used for the averaging process consisted of a Maxwellian at $300^{o}K$ in the thermal range with an upper energy cutoff of 0.625 eV coupled to a 1/E spectrum joined to a fission spectrum at high energies. (The breakpoint was taken to be 67 keV and the temperature of the fission spectrum was taken to be 1.27 MeV corresponding to the ENDF/B-IV value for the thermal fissions in ^{235}U.) The thermal cross sections generated during this process were not used because of the inability of the MINX code to perform upscatter corrections. The upscatter corrected and self-shielded thermal data, including bound atom effects, used in this study was supplied by EPRI.[15] These were obtained from a 30-group THERMOS[22] calculation.

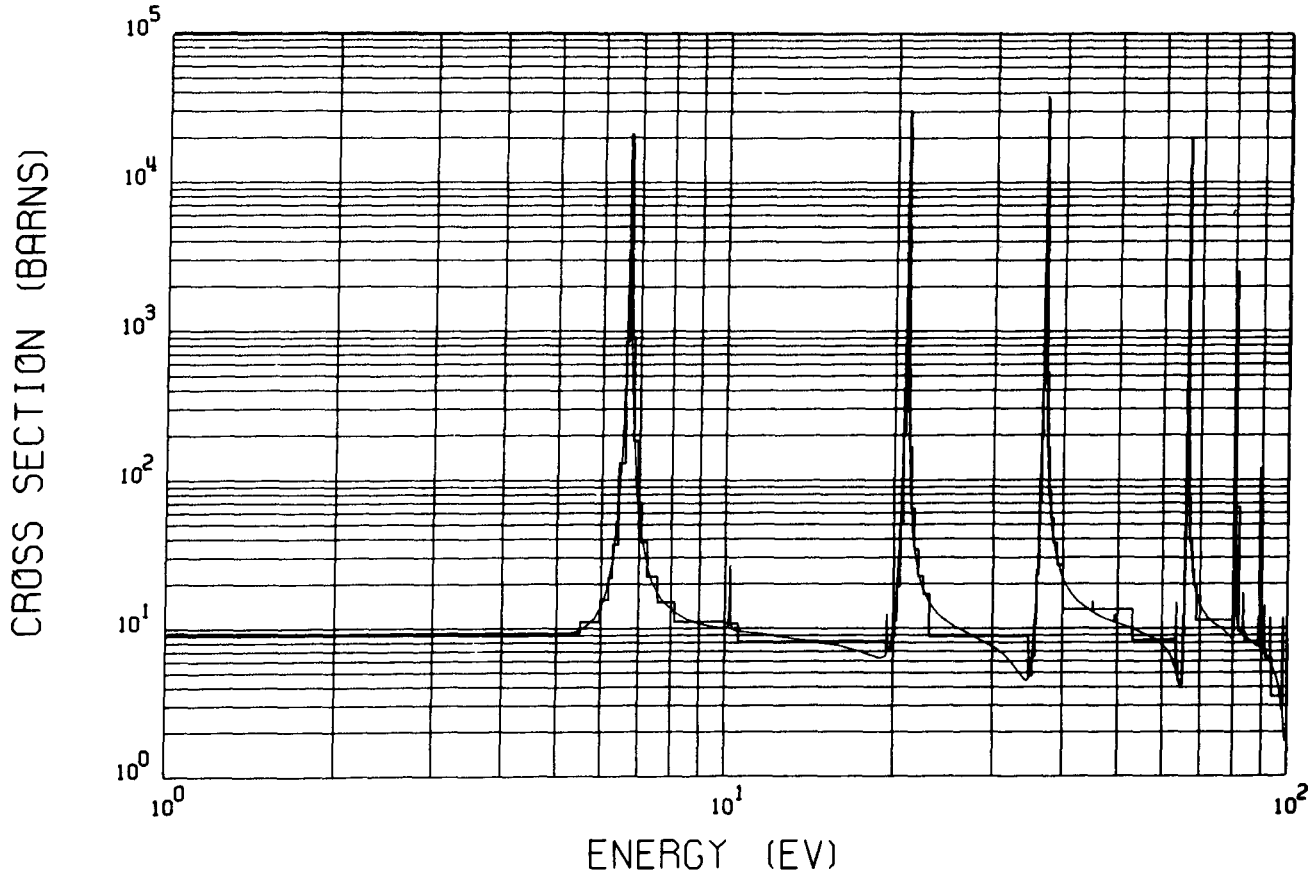

Fig. 1. The ^{238}U Total Cross Section from 1 to 100 eV; Multigroup vs Point Data.

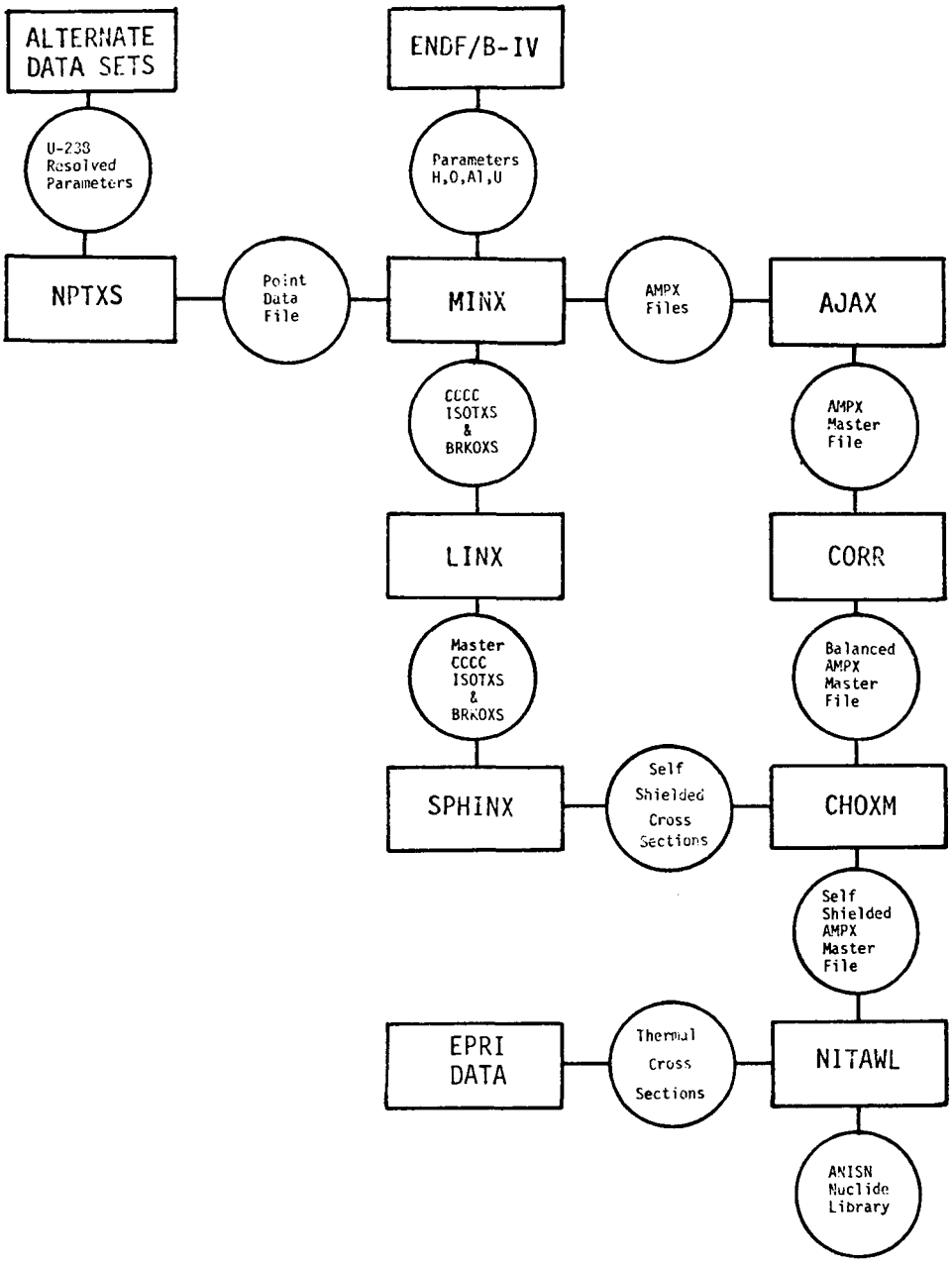

Fig. 2. Flow Chart of the Cross Section Generating System.

The scattering cross section for all the energy groups above thermal were expanded through P_1 except for hydrogen. The hydrogen scattering matrices were expanded through order 5. This was done to correctly account for the forward peaked angular distribution of neutrons scattering from hydrogen in the laboratory system leading to an energy distribution appropriate for the fine energy mesh used in this study. Later results indicated that a P_3 expansion would have been sufficient. The thermal cross section data consisted of a transport corrected P_0 set. (In practice, this was run as P_1, with the P_1 component set to zero.) This involved the assumption that all anisotropic scattering effects can be accounted for by use of the transport cross section instead of the total cross section.

This multigroup averaging process generated three cross section data files: ISOTXS and BRKOXS files and an AMPX master file. The first two files are standard reactor physics interface data files which are used in programs which perform Bondarenko self shielding. The AMPX file is a much more general interface containing all multigroup constants including partial reactions, transfer matrices, etc. The AMPX master files for inelastic scattering for each nuclide were then merged in the AJAX module and their scattering matrices normalized to the total inelastic scattering cross section in the CORR module. The ISOTXS and BRKOXS files were merged using the LINX[23] code in preparation for input to SPHINX.

The SPHINX program was used to perform the interpolation for the appropriate background cross section and temperature to generate the applicable self-shielded cross sections for the epithermal energy region. The f-factors were calculated using Eqs. (1) as an approximation[24] to the Dancoff factor for an infinite lattice of cylindrical pins in a tri-angular pitch array.

$$C = \exp(-\tau\Sigma_m\bar{\ell}V_1/V_0)/[1+(1-\tau)\Sigma_m\bar{\ell}V_1/V_0] \tag{1a}$$

where

$$\tau = [\sqrt{\pi}/(2\sqrt{3})\ \sqrt{1+V_1/V_0} - 1]/(V_1/V_0) - 0.12 \tag{1b}$$

$$\bar{\ell} = 2R_F$$

V_0 = volume of fuel, V_1 - volume of moderator

The volume ratio is calculated from concentric fuel and moderator cylinders whose radii are input to the subroutine. The mean chord length is also computed from these parameters (see Fig. 3). The Dancoff function, ε, is then used to obtain a modified microscopic background cross section. The self-shielded cross sections were then folded with the remaining infinitely dilute multigroup data from the merged AMPX master file using the CHOXM module of AMPX. The entire self-shielded library was then processed through the NITAWL module to produce a cross section library in an ANISN[25] format. An isotope weighted fission spectrum was generated using the XLACS module in AMPX.

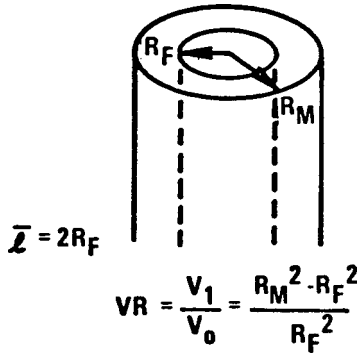

Fig. 3. Cylindrical Cell Using Sauer's Approximation for the Dancoff Correction in a Hexagonal Lattice.

V. DISCUSSION OF THE CALCULATIONAL MODEL

A. The Reactor Model

A calculation model consisted of a single cylindrical cell with dimensions in accordance with the benchmark specifications.[26] These are repeated here for completeness in Table 3. A white isotropic boundary condition was applied at the outer cell boundary to simulate an infinite array. Neither a white nor a reflected boundary condition (the only two options in ANISN) is exact for one-dimensional cylindrical geometry. The white boundary condition assumes that the flux is isotropic on the cell boundary. The reflected boundary condition assumes reflection on a cylindrical boundary which is not the physical situation.

Table 3. The Cylindricized Calculation Model of the TRX-2 Hexagonal Lattice

Region	Outer Radius (cm)	Isotope	Concentration atoms/barn-cm
Fuel	0.4915	^{235}U ^{238}U	0.0006253 0.047205
Void	0.5042	-	-
Clad	0.5753	^{23}Al	0.06025
Moderator	1.14109	^{1}H ^{16}O	0.06676 0.03338
Total Buckling = 0.005469 cm^{-2}			

However, there was virtually no dependence of the calculational results on the choice of boundary conditions (a difference of approximately 0.01% in all parameters). The group flux near the cells outer boundary was the only calculated quantity to change (approximately 1.0%).

A S_{16} Gauss Legendre quadrature set was used for all ANISN calculations. The spatial mesh is presented in Table 4. Extremely fine intervals were used near the outer boundary of the fuel zone (Zone 1) in order to account for the spatial self-shielding effects of the fuel, especially in the energy groups near the lower resolved resonances in ^{238}U.

Initially three eigenvalue calculations were performed to assess the effects of the interaction of fine energy mesh and the higher order scattering in hydrogen, $S_{16}P_1$, $S_{16}P_3$, and $S_{16}P_5$. There was no noticable spectral shift between the P_3 and the P_5 calculation and also no change in the eigenvalue. There was, however, approximately a 1% increase in leakage from the aluminum clad into the water moderator and also a 0.036% decrease in the eigenvalue in going from P_1 to P_3. Thus, it was concluded that a P_1 expansion for hydrogen was inadequate and a P_3 sufficient. All subsequent calculations were performed as $S_{16}P_5$ calculations because of the insignificant cost of including the extra scattering moments.

The adequacy of the spatial mesh was tested by comparing the reaction rates calculated by ANISN using various refinements of the mesh. ($^{28}\rho$ is extremely sensitive to errors in the flux caused by "diamond difference breakdown.") The mesh was judged to be adequate when the increased refinement of the mesh produced no change ($< 0.1\%$) in this reaction rate ratio.

Table 4. The Spatial Mesh for the TRX-2 Cell Calculation

Interval	Zone No.	Radius
1	1	0
2	1	4.09091E-02
3	1	8.18181E-02
4	1	1.22727E-01
5	1	1.63636E-01
6	1	2.04545E-01
7	1	2.45454E-01
8	1	2.86364E-01
9	1	3.27273E-01
10	1	3.68182E-01
11	1	4.09091E-01
12	1	4.50000E-01
13	1	4.55000E-01
14	1	4.60000E-01
15	1	4.65000E-01
16	1	4.70000E-01
17	1	4.74000E-01
18	1	4.77000E-01
19	1	4.80000E-01
20	1	4.82000E-01
21	1	4.83000E-01
22	1	4.84000E-01
23	1	4.85000E-01
24	1	4.86000E-01
25	1	4.87000E-01
26	1	4.88000E-01
27	1	4.89000E-01
28	1	4.90000E-01
29	1	4.90500E-01
30	1	4.91000E-01
31	2	4.91500E-01
32	2	4.97850E-01
33	3	5.04200E-01
34	3	5.18420E-01
35	3	5.32640E-01
36	3	5.46860E-01
37	3	5.61080E-01
38	4	5.75300E-01
39	4	6.31879E-01
40	4	6.88458E-01
41	4	7.45037E-01
42	4	8.01616E-01
43	4	8.58196E-01
44	4	9.14775E-01
45	4	9.71354E-01
46	4	1.02793E 00
47	4	1.08451E 00
48		1.14109E 00

B. The Leakage

The initial attempt to use the simplistic leakage model in ANISN, Eq. (2), for energy group g, spatial region i proved to be inadequate due to spectral effects in the leakage. Equation (2) assumes that the flux in each energy group is cosine shaped in the axial direction.

$$(DB^2)_{g,i} = \frac{1}{3\Sigma_{T_{g,i}}} \left[\frac{\pi}{(H + 1.42089/\Sigma_{T_{g,i}}} \right]^2 \qquad (2)$$

Since the cell height, H, is the only input parameter a more sophisticated estimation of the region and energy dependent leakage was made using the three-dimensional Monte Carlo code KENO.[27] A three-dimensional, infinite triangular pitch array with rod spacings of 2.1740 cm and a height of 40.81 cm corresponding to the measured buckling of 0.00549 cm^{-2} was calculated using the 131 group self-shielded cross section library. The region and energy dependent leakages were calculated, normalized to the flux and edited.

The group and region dependent leakages edited by the Monte Carlo code KENO usually contain a number of zero leakages due to the statistical nature of the calculation. This is particularly true for fine (narrow) energy groups or groups with large total cross sections.

The following procedure was implemented to synthesize leakages for the statistically zero leakage groups. The method is approximate, but is an improvement over the current procedure of using the zero leakages and searching for a k_{eff}.

It is known that the leakage normalized to the flux (DB^2) varies approximately as follows:

$$DB^2 \sim \frac{1}{\Sigma_{TR}} \qquad (3)$$

where Σ_{TR} is the region dependent macroscopic transport cross section. If the geometric buckling, B^2, is assumed to be independent of the transport cross section, Σ_{TR}, it follows that:

$$DB^2 \times \Sigma_{TR} = c \qquad (4)$$

where c is constant.

Since ANISN usually uses the total cross section, Σ_T, rather than the transport cross section, Eq. (4) is further approximated by Eq. (5).

$$DB^2 \times \Sigma_T = c \tag{5}$$

If this equality is assumed to hold for each energy group, g, then it follows that:

$$\frac{(DB^2)_g}{(DB^2)_{g-1}} = \frac{\Sigma_T^{g-1}}{\Sigma_T^g} \tag{6}$$

or

$$(DB^2)_g = (DB^2)_{g-1} \left[\frac{\Sigma_T^{g-1}}{\Sigma_T^g} \right] \tag{7}$$

The weight functions, $\Sigma_T^{g-1}/\Sigma_T^g$, are easily calculated from a macroscopic cross section library for each region and group. The DB^2 values from KENO must then be edited to remove the terms with poor statistics (i.e., 100% deviation in the flux or leakage). This cropped leakage set is then folded with the synthesis factors to compute the complete leakage set. These leakages were then input into ANISN by augmenting the total cross section in each group and region by the calculated DB^2 values. The problem is then run with this new cross section set in the zero buckling mode.

VI. CROSS SECTION LIBRARY TESTING

At this juncture, an effort was made to assess the validity of the ENDF/B-IV multigroup cross section library. To this end the infinitely dilute capture resonance integral based on ENDF/B-IV was calculated for ^{238}U using both the point data and the multigroup data. Calculated resonance integrals of 278.355 b and 278.352 b were obtained for the point data and the multigroup data, respectively. A lower energy cutoff for the integration of 0.625 eV was assumed. These values agree favorably with an analytic estimate of 278.457 b. A similar calculation was performed for the infinitely dilute fission resonance integral of ^{235}U. Calculated resonance integrals of 265.542 b and 265.460 b were obtained for the point data and the multigroup data,

respectively. As before a lower cutoff of 0.625 eV was assumed. These values also agree with Hardy's[28] value of approximately 265 b. These results indicated that there was no significant error introduced during the multigroup averaging of the infinitely dilute smooth cross sections for the important heavy nuclides.

A second confirmation was obtained using a 218 group cross section library[29] which was developed independently at ORNL using the AMPX system. This library was generated for criticality safety studies and contains 27 thermal groups (E < 0.65 eV) and the upscatter cross sections for the lower 77 groups (E < 3.05 eV). The AMPX data was then collapsed using a calculated weight function similar to that used in THERMOS (i.e., TRX-2 cell calculation fluxes). The results of this collapse and a comparison with the thermal cross sections provided by EPRI is presented in Table 5. The cross sections from both data sets are consistent except for the transport cross sections and the hydrogen and oxygen scattering cross sections.

Table 5. TRX-2 Thermal Data

Region No.	Nuclide	XFISS	XABS	XNUFISS	XTOT	XSC	XTR
			EPRI [THERMOS]				
1	^{235}U	396.778	465.582	959.725	481.331	15.749	490.461
1	^{238}U	0.0	1.925	0.0	10.861	8.936	16.041
2	Al	0.0	0.170	0.0	1.536	1.366	1.458
3	H	0.0	0.256	0.0	32.577	32.321	23.940
3	O	0.0	1.38-4	0.0	5.855	5.854	12.141
			ORNL [AMPX]				
1	^{235}U	397.580	465.755	961.50	480.934	15.179	629.025
1	^{238}U	0.0	1.939	0.0	10.881	8.942	11.412
2	Al	0.0	0.170	0.0	1.517	1.347	1.562
3	H	0.0	0.256	0.0	43.631	43.376	38.364
3	O	0.0	1.3684-4	0.0	3.747	3.747	3.748

The discrepancy in the transport cross sections was found to be in the approximations chosen from those available in AMPX. A P_0 free gas model was used to generate the thermal data for all the nuclides except for hydrogen which was generated from the $S(\alpha,\beta)$ data in ENDF/B-IV, i.e., isotropic scattering from a free gas model was assumed; therefore no higher order scattering data was available to perform the transport correction of the total cross section. The AMPX transport cross sections shown in Table 5 are therefore probably invalid.

A resolution of the discrepancy in the hydrogen and oxygen scattering cross sections is somewhat more elusive. A search of recent literature revealed that the experimental value of the transport cross section for water lies between approximately 2.08 and 2.32 cm^{-1} (see ref. 30). The EPRI and AMPX data give cross sections of 2.34 and 2.69 cm^{-1} respectively. Based on better agreement with experiment, the EPRI thermal cross section data was selected as the better data set and was used throughout the TRX-2 analysis.

Another integral check was made on the cross section library, using the one-dimensional model of a TRX-2 cell. A k_∞ eigenvalue was performed and gave a value of 1.1591 which is in excellent agreement with the 1.1587 value quoted by Hardy.

The final check made of the cross section library was the calculation of k_{eff} using the 218 group (with full upscatter) cross section set and comparison to the results obtained with the 131 group cross section set using the standard ANISN treatment of the leakage. Eigenvalues of 1.05154 and 1.04921 were calculated, respectively. Note that this indicates that thermal transport cross section values for the heavy nuclides are relatively unimportant as the free gas approximations cited earlier are used in the 218 group library. For a given geometry model, independently processed cross section libraries result in equivalent predictions for k_{eff}. Any discrepancies in k_{eff} with other accurate analyses would most likely be due to different treatments of leakage or discrepancies in the thermal cross section.

VII. ENDF/B-IV RESULTS

A. Fluxes and Adjoints

An $S_{16}P_5$ calculation was performed using ANISN and the ENDF/B-IV based multigroup library discussed in the previous sections to generate the forward and adjoint fluxes for the TRX-2 cell. Figures 4, 5, and 6 present the neutron flux spectra at the fuel centerline, the fuel surface, and the moderator center, respectively. The flux at each location has a degraded fission spectrum shape at high energy and a 1/E shape (constant flux/lethargy) below approximately 10 keV with inverse structure corresponding to ^{238}U cross section resonances (Fig. 7). The structure becomes more pronounced as penetration of the fuel increases corresponding to significant spatial self shielding. [Note that the fluxes (and adjoints) have all been plotted on the same scale so that this effect would be clearly observable.] The use of a single thermal group below 0.625 eV has masked the Maxwellian at low energies, but a slight increase in the spectrum is noticeable. The flux peak at approximately 95 eV is due to the cross section minimum below the 102.7 eV resonance.

The adjoint flux spectra at these three locations are illustrated in Figs. 8, 9, and 10. The adjoint flux at each location has a relatively large value at high energies due to fast fissions in ^{238}U. It then decreases with decreasing energy to below the ^{238}U fission threshold. The adjoint spectra begin to rise again with decreasing energy since the ^{238}U capture cross section increases less with decreasing energy than the ^{235}U fission cross section. In general, the adjoint fluxes have a shape corresponding to $\nu\Sigma_f/\Sigma_a$ of the fuel with degradation of the structure by hydrogen scattering becoming more important in spatial regions closer to the water moderator.

The fission spectrum used in the calculation of both the forward and adjoint flux is an isotope weighted distribution as calculated by AMPX.[14]

B. Performance Parameters

The ORNL calculated nominal values for k_{eff}, $^{28}\rho$, $^{25}\delta$, $^{28}\delta$, and CR (^{238}U captures/^{235}U fissions) are presented in Table 6. The measured values are also reported for comparison. The corresponding set of CSEWG data testing results was presented in Table 1 of this report.

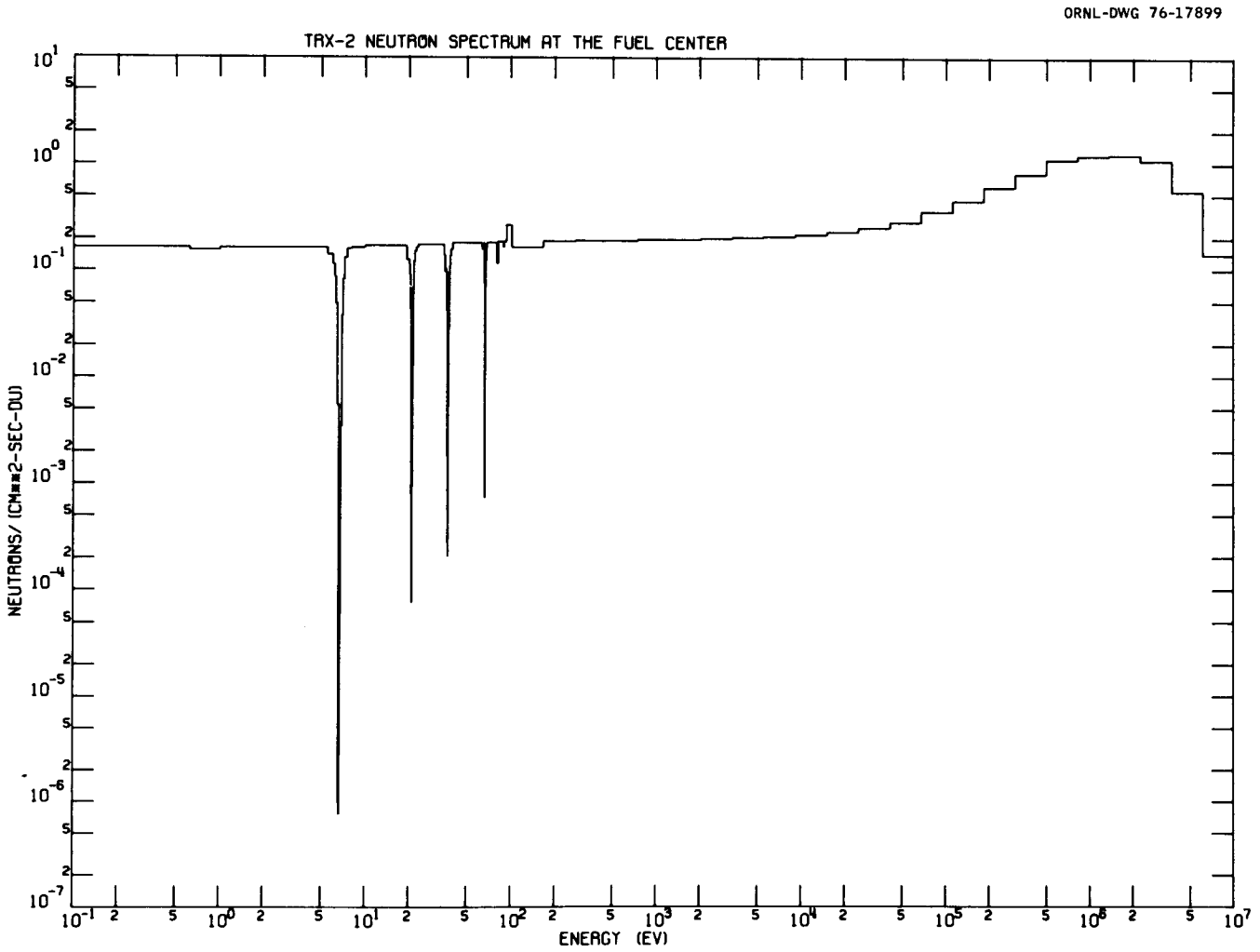

Fig. 4. The TRX-2 Neutron Spectrum at the Center of the Fuel Pin.

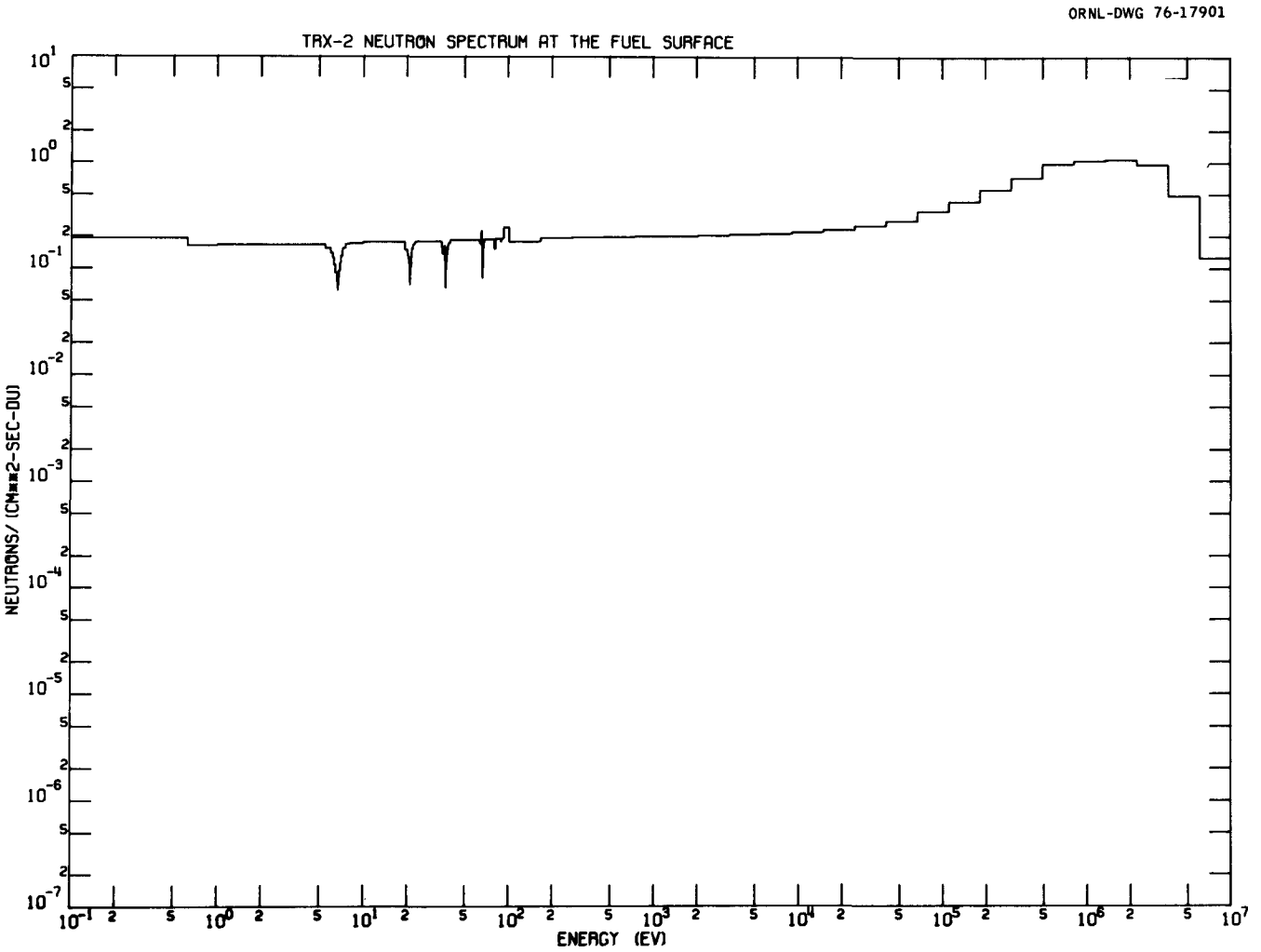

Fig. 5. The TRX-2 Neutron Spectrum at the Fuel-Void Interface.

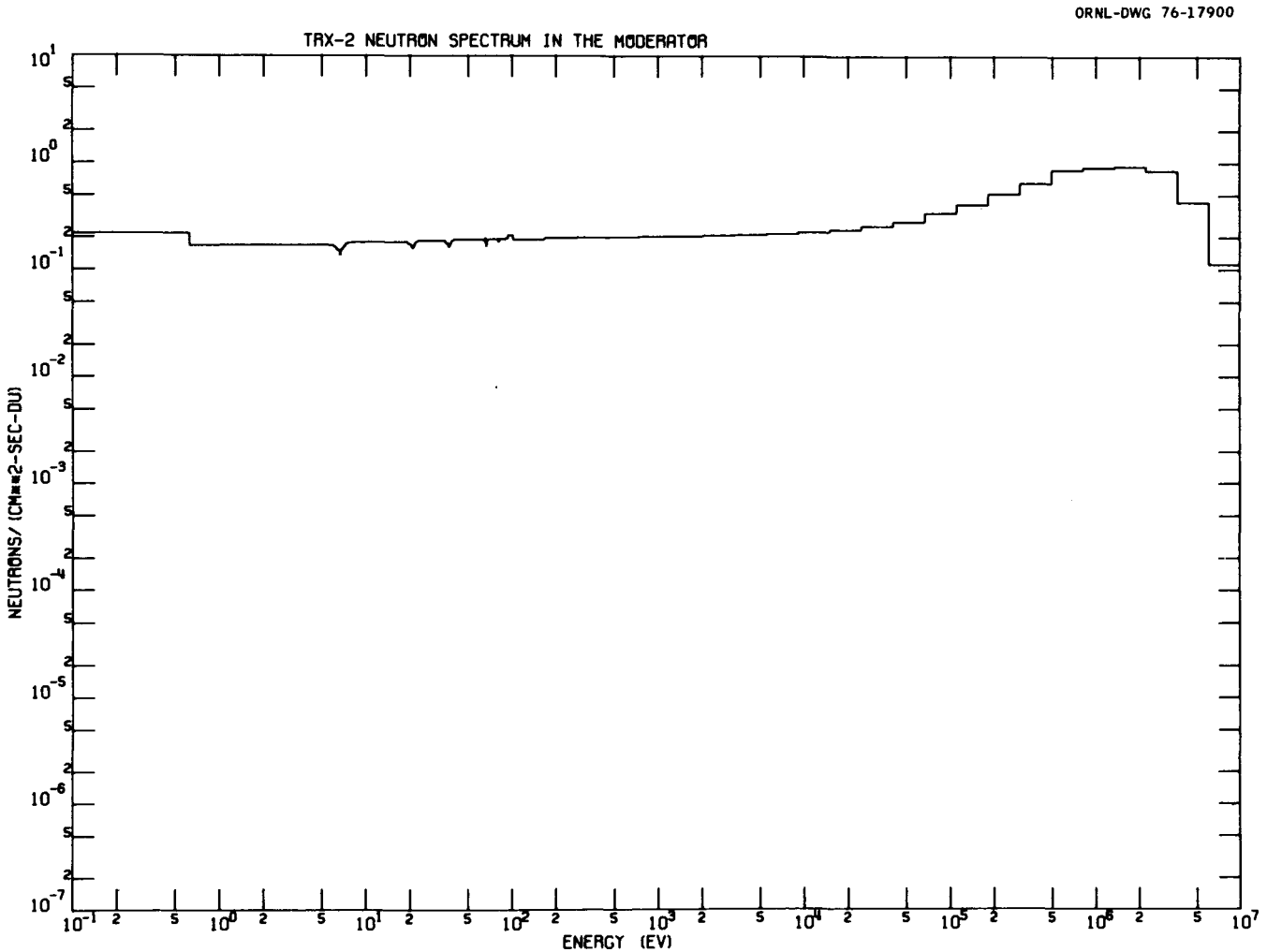

Fig. 6. The TRX-2 Neutron Spectrum in the Water.

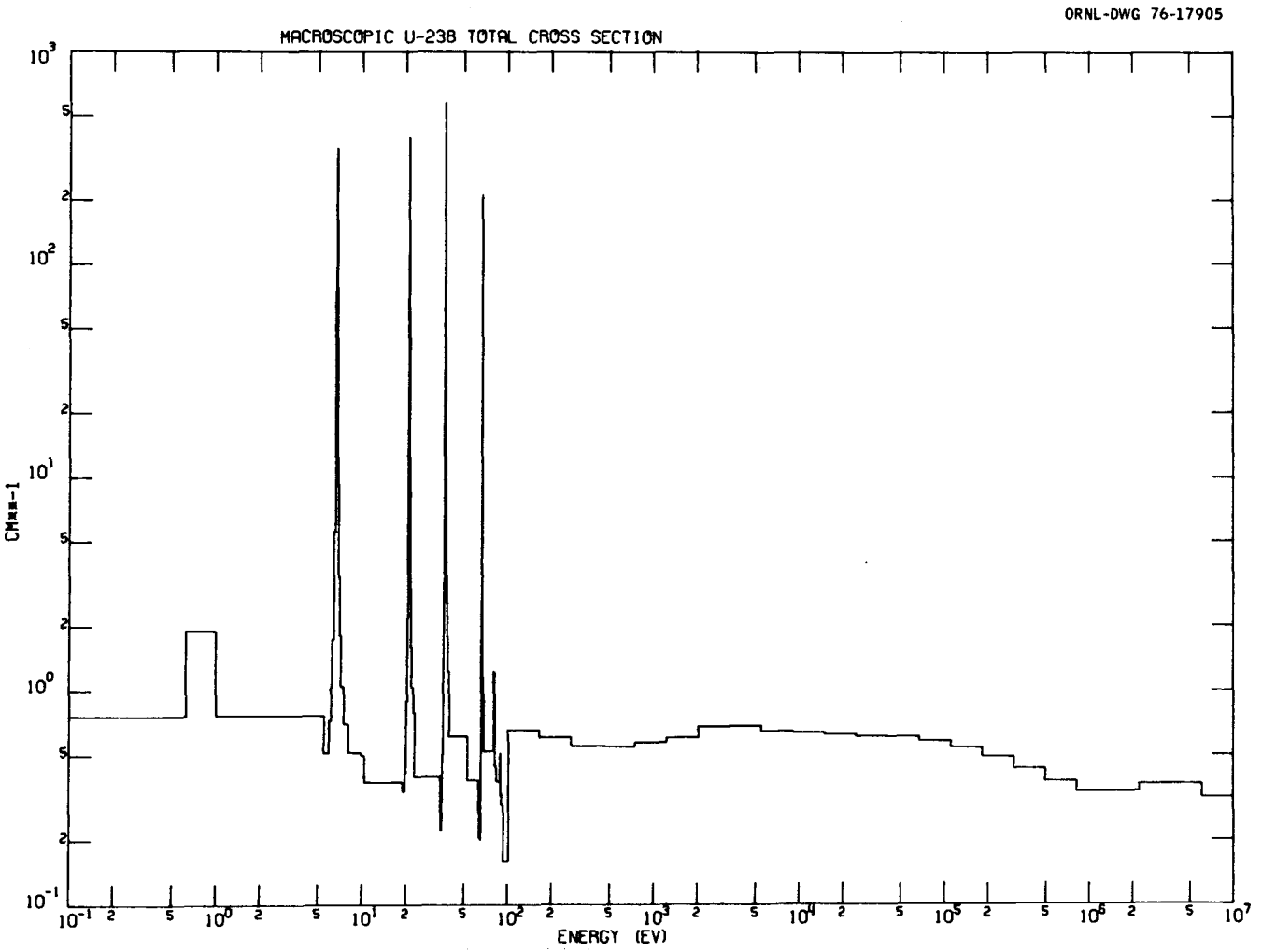

Fig. 7. The Macroscopic ^{238}U Total Cross Section.

(NOTE: The peak in the total cross section at 1 eV is due to an error in the processed ^{238}U scattering cross section. This error was later shown to have no effect on any of the final results of this study. The capture cross section is correct.)

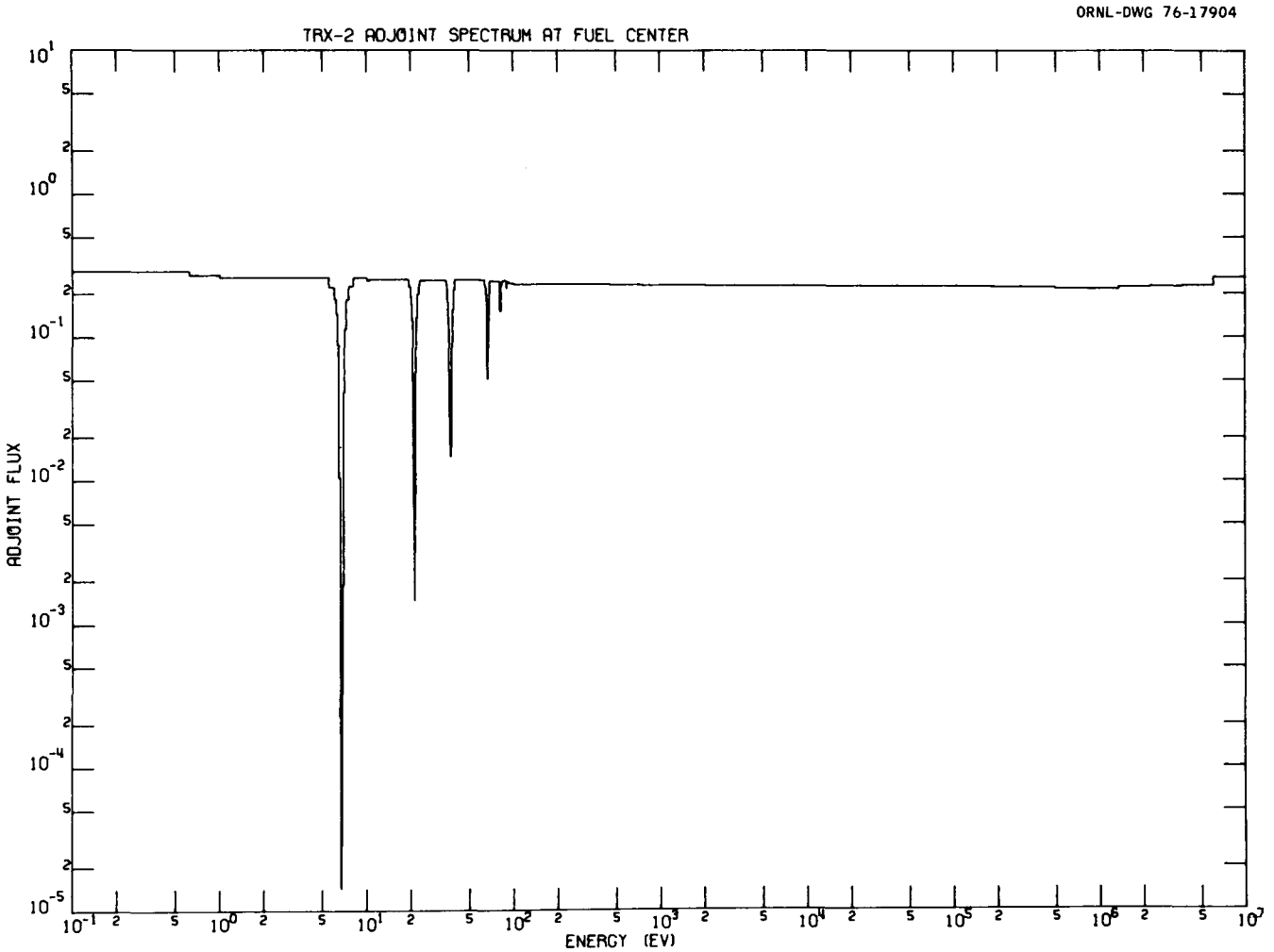

Fig. 8. The TRX-2 Adjoint Spectrum at the Center of the Fuel.

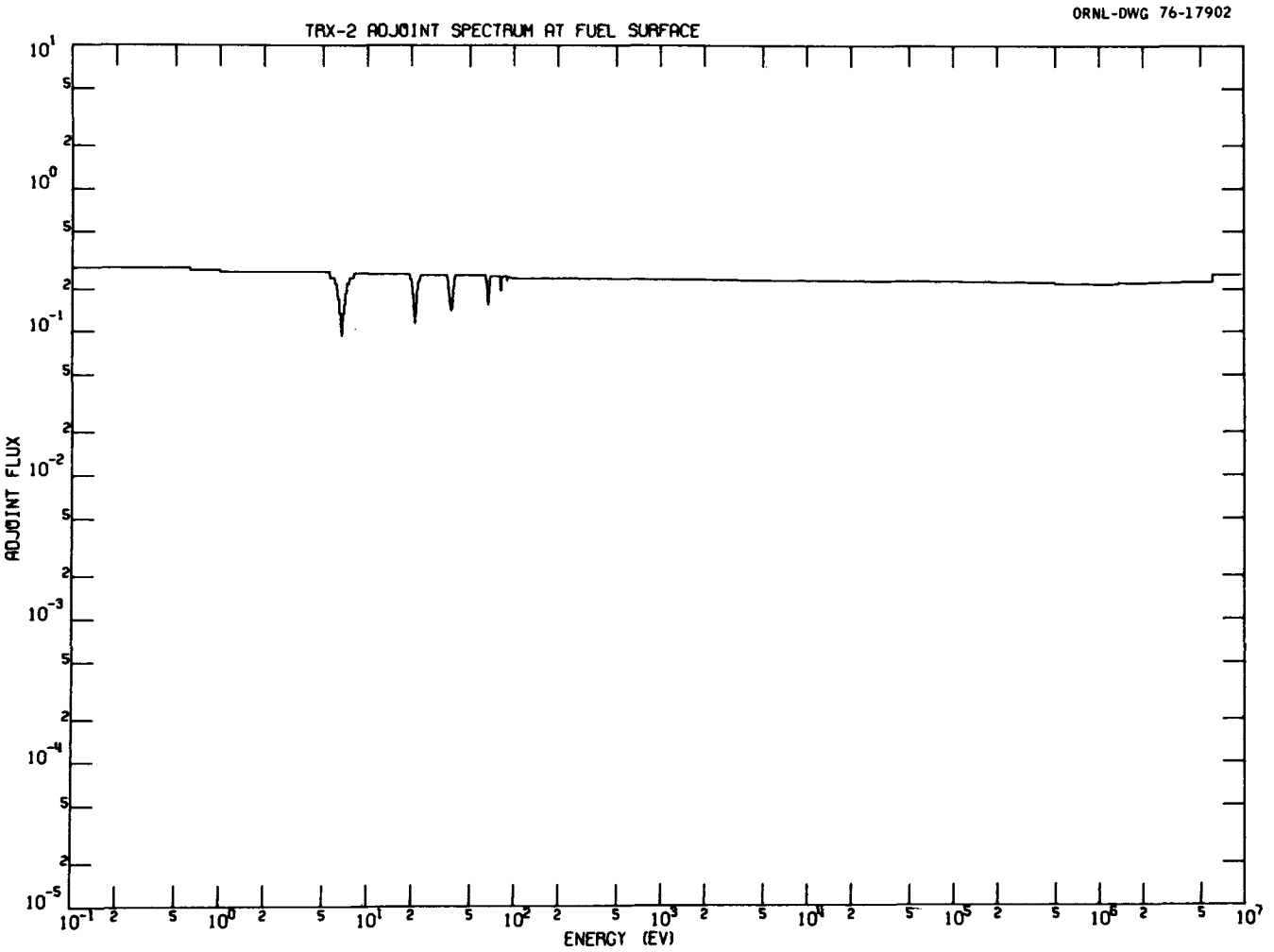

Fig. 9. The TRX-2 Adjoint Spectrum at the Fuel-Void Interface.

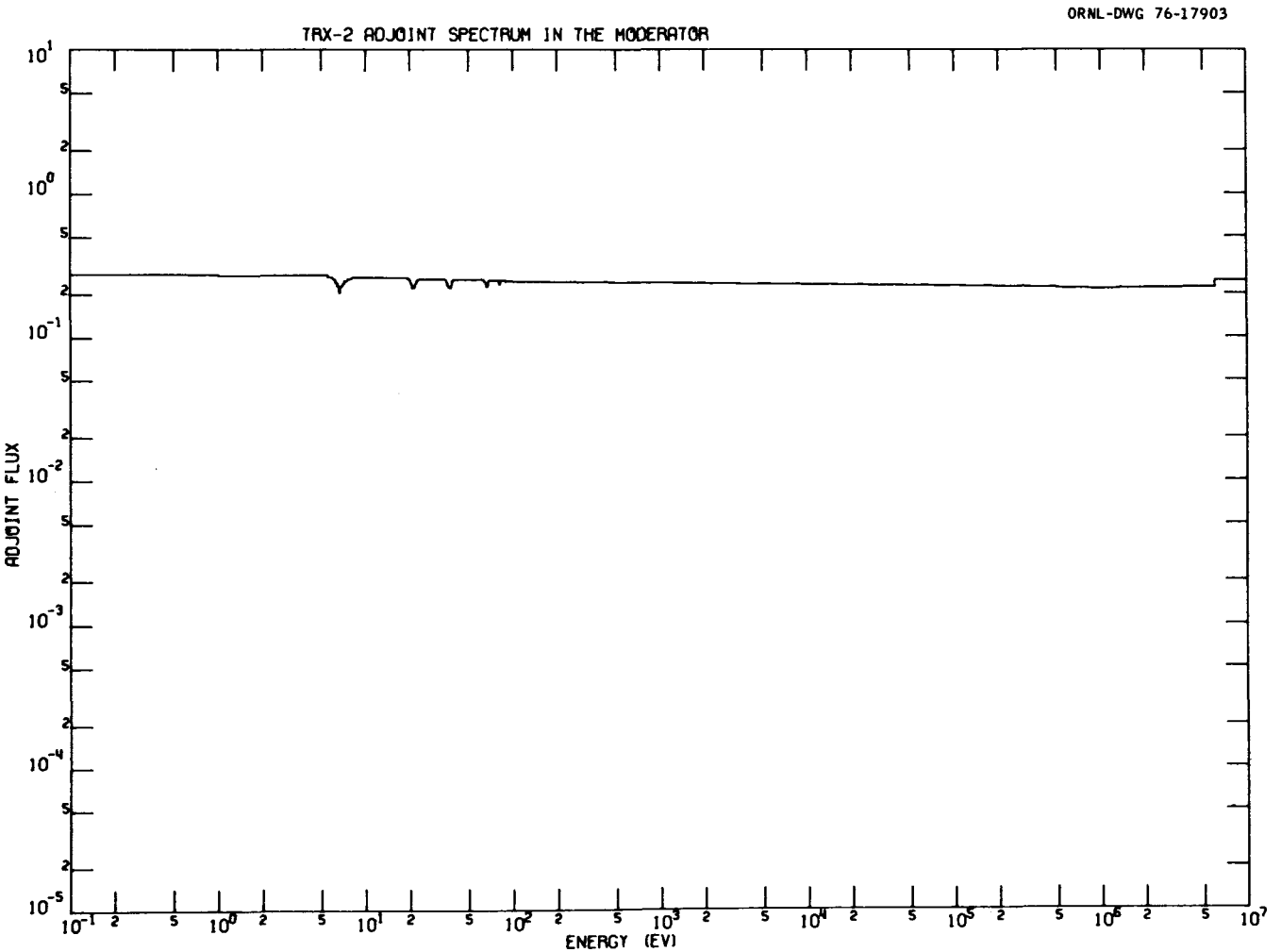

Fig. 10. The TRX-2 Adjoint Spectrum in the Water.

Table 6. TRX-2 Performance Parameters Based Upon ENDF/B-IV

Parameter	Experiment[a]	ORNL Calculation
k_{eff}	1.0000	1.0012
$^{28}\rho$	0.837±0.016	0.867
$^{25}\delta$	0.0614±0.0008	0.0602
$^{28}\delta$	0.0693±0.0035	0.0698
CR	0.647±0.006	0.645

[a]See ref. 31. Note these experimental values reflect the latest available results.

The ORNL calculated eigenvalue (k_{eff}) is aproximately 0.1% higher than unity. A significant calculational uncertainty arises from our assuming a total buckling corresponding to a height of 40.81 cm corresponding to the measured buckling and estimating the energy dependent fast leakage by Monte Carlo. Indeed in a recent communication, J. Hardy[28] indicates that three-dimensional explicit modeling of the actual lattice (as opposed to our one-dimensional calculation with the specified buckling) may reduce the BAPL computed eigenvalue by up to one percent. In addition, the estimated uncertainty (1σ) associated with our equivalent DB^2 values for the prescribed benchmark buckling is approximately 3.5% above 100 keV arising primarily from lack of statistics in the Monte Carlo calculation at high energies. (The uncertainty is much less at lower energies.) Using the computed sensitivities to the group-and region-dependent DB^2 (see Section VIII), the uncertainty in k_{eff} associated with this numerical procedure is approximately ±0.5%. It is clear that these considerations preclude inference of detailed information regarding ^{238}U capture cross sections from calculations of k_{eff}. Fortunately, these leakage and modeling effects have little sensitivity for the calculation of $^{28}\rho$ (<0.1%) which is the focus of the present study. In general, such uncertainties for k_{eff} make our results consistent with most of those reported in Table 1. It is difficult to be more precise at this time, since a quantitative measure of the calculational uncertainty was not provided by any of the data testers. There is no doubt that analysis of uncertainties in various calculations would be a worthy endeavor, but this was considered beyond the scope of this six month study.

The situation for calculating $^{28}\rho$ is different than that for k_{eff} in that there is little sensitivity to leakage effects. The uncertainty in DB^2

referred to above translates to only ∿1% uncertainty in $^{28}\rho$ based upon the sensitivities described in the next section. There is more reason to be confident in the multigroup processed cross section set based upon excellent agreement in the calculation of k_∞ with the independent analysis of Hardy (1.1591 compared to 1.1587), agreement for k_{eff} (1.0515 compared to 1.0492) compared to the NRC 218 group data set (see Section VI) for a given model, and comparison of resonance integrals (278.35 compared to 278.46 for $^{238}U[n,\gamma]$) etc. The ORNL value for $^{28}\rho$ is between 1 and 2σ higher than the quoted experimental value. The value also lies between a significantly dispersed set of reported CSEWG data testing results (e.g., SRL $^{28}\rho$ = 0.839, ANC $^{28}\rho$ = 0.890). Our calculational model was tested with regard to selection of boundary conditions, Legendre order, S_N order, and spatial mesh. Errors incurred due to the choice of these parameters were reduced to less than 0.1% in $^{28}\rho$. We have found in our study that $^{28}\rho$ is extremely sensitive to errors in the flux caused by diamond difference breakdown. [Note the particularly fine spatial mesh required at the fuel moderator interface (Table 4).] Figure 11 illustrates the ^{238}U capture rate per unit lethargy at the fuel-moderator interface in TRX-2. Analysis of this plot reveals that in the epithermal range 70.8% of the captures take place in the first four resonances. With respect to capture in these four resonances, 17.1% takes place near the peak ($E_0 \pm \Gamma_T$), and 53.7% takes place in the wings. Capture in the wings of the resonance becomes relatively more important near the center of the fuel (due to spatial self shielding) but involves a smaller total volume. Although the group structure was tailored to the ^{238}U total cross section, the question of the rigor with which self-shielding effects were treated always remains, particularly when we speak of shielding from other nuclides and reaction types. The authors believe such effects to be negligible for $^{28}\rho$ and estimate the uncertainty in calculated $^{28}\rho$ due to self-shielding treatment to be of the order of 0.3%. Finally, it should be clear from the discussion in the last two paragraphs that predictions of k_{eff} and $^{28}\rho$ are not necessarily fully anti-correlated due to ^{238}U capture since leakage and other effects (e.g., inelastic scattering) can have a major impact on k_{eff} and negligible effect on $^{28}\rho$ (see Section VIII).

The ORNL nominal value of $^{25}\delta$ is approximately 2% lower than the measured value which is quoted with 1% uncertainty. Other CSEWG data testers (except CRNL) also underpredict $^{25}\delta$ (e.g., SRL $^{25}\delta$ = 0.0577). This parameter obviously has high sensitivity to the ^{235}U fission cross section and is also very dependent on the thermal ^{238}U capture cross section (see Section VIII) as well as the H scattering and capture cross sections. The ORNL calculation of

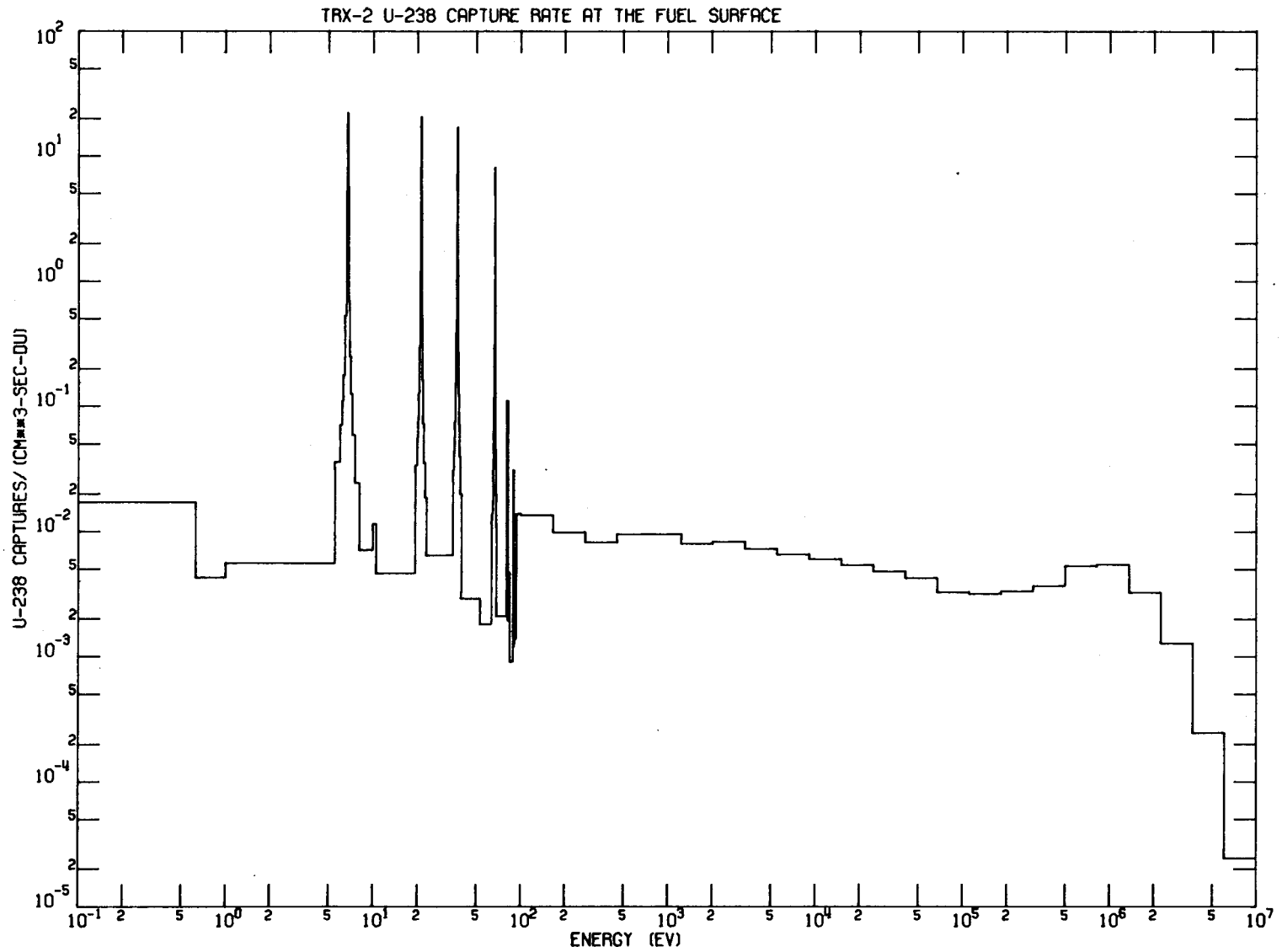

Fig. 11. The TRX-2 ^{238}U Capture Rate at the Fuel-Void Interface.

$^{28}\delta$ is within the experimental uncertainty. Other than GA, most of the other CSEWG data testers tended to underpredict $^{28}\delta$, but were slightly lower than 1σ experimental uncertainty below the quoted experimental value. Again, no calculational uncertainties were available. Finally, Table 6 illustrates that our calculation for the conversion ratio (^{238}U captures to ^{235}U fissions) gives reasonable agreement with experiment and would thus act as a restraint against arbitrary changes in ^{238}U(n,γ) or ^{235}U(n,f) not acting in such a way as to preserve agreement with CR.

An internal consistency check was made among the various performance parameters using the relationship defined in Eq. (8).[4]

$$\frac{c^{28}}{f^{25}} = CR \frac{(1 + {}^{25}\delta)}{(1 + {}^{28}\rho)} \tag{8}$$

where c^{28} and f^{25} are the thermal captures in ^{238}U and thermal fissions in ^{235}U respectively. The values of c^{28}/f^{25} obtained from direct calculation is 0.36625 and the value inferred using Eq. (8) from the experimental data is 0.36627, thus indicating the internal consistency of the results.

VIII. SENSITIVITY PROFILES: DEFINITION

The application of sensitivity analysis to critical benchmark analysis has already been extensively discussed.[33] Suffice it to say that for a rather general class of performance parameters which can be expressed in the form of a homogeneous bilinear ratio, the sensitivity profile, $[dR/R/(d\Sigma(\rho)/\Sigma(\rho)]$ which is the relative change in the response per change in some specific cross section, $\Sigma(\underline{\rho})$ at point $\underline{\rho}$ per unit volume in phase space can be numerically determined.

The resulting formula can be written as:

$$\left(\frac{dR}{R}\right) \Bigg/ \left(\frac{d\Sigma(\underline{\rho})}{\Sigma(\underline{\rho})}\right) \tag{9}$$

$$= \left[\frac{\Sigma(\underline{\rho}) \int \phi^*(\underline{\xi}) \dfrac{dH_1[\Sigma(\underline{\xi})]}{d\Sigma(\underline{\rho})} \phi(\underline{\xi})\, d\underline{\xi}}{\int \phi^*(\underline{\xi})\, H_1[\Sigma(\underline{\xi})]\, \phi(\underline{\xi})\, d\underline{\xi}} - \frac{\Sigma(\underline{\rho}) \int \phi^*(\underline{\xi}) \dfrac{dH_2[\Sigma(\underline{\xi})]}{d\Sigma(\underline{\rho})} \phi(\underline{\xi})\, d\underline{\xi}}{\int \phi^*(\underline{\xi})\, H_2[\Sigma(\underline{\xi})]\, \phi(\underline{\xi})\, d\underline{\xi}} \right]$$

$$- \frac{\Sigma(\underline{\rho})}{R} \left[\int \Gamma^*(\underline{\xi}) \frac{dL[\Sigma(\underline{\xi})]}{d\Sigma(\underline{\rho})} \phi(\underline{\xi})\, d\underline{\xi} + \int \Gamma(\underline{\xi}) \frac{dL^*[\Sigma(\underline{\xi})]}{d\Sigma(\underline{\rho})} \phi^*(\underline{\xi})\, d\underline{\xi} \right]$$

where H_1 and H_2 are suitable operators which depend on the various cross sections and appear in the definition of the response, R,

$$R \equiv \frac{\int \phi^*(\underline{\xi})\, H_1[\Sigma(\underline{\xi})]\phi(\underline{\xi})\, d\underline{\xi}}{\int \phi^*(\underline{\xi})\, H_2[\Sigma(\underline{\xi})]\phi(\underline{\xi})\, d\underline{\xi}} \tag{10}$$

$\phi(\underline{\xi})$ and $\phi^*(\underline{\xi})$ are the forward and adjoint fluxes, respectively, and $\underline{\xi}$ and $d\underline{\xi}$ are the position vector and differential volume element in phase space. (The notation $H[\Sigma(\underline{\xi})]\ \phi(\underline{\xi})$ denotes the application of the operator H on the flux ϕ, the result being a function of point $\underline{\xi}$ in phase space.) $\Gamma(\underline{\xi})$ and $\Gamma^*(\underline{\xi})$ are the generalized forward and adjoint fluxes, respectively, which are solutions to the equations

$$L[\Sigma(\underline{\xi})]\ \Gamma(\underline{\xi}) = \frac{\partial R}{\partial \phi^*(\underline{\xi})} \tag{11}$$

$$L^*[\Sigma(\underline{\xi})]\ \Gamma^*(\underline{\xi}) = \frac{\partial R}{\partial \phi(\underline{\xi})} \tag{12}$$

where L and L* are the normal Boltzmann forward and adjoint operators in the neutron transport equation.

The first bracket of Eq. (9) represent the direct effect, i.e., the induced changes in response due to a change in a cross-section type appearing in the response definition. The last two terms correspond to the flux effect, the change in response due to the effect a cross section change would have on the system flux or adjoint. Once ϕ, ϕ^*, Γ, and Γ^* have been determined, sensitivity functions for any and all elements of the cross section data field for a given problem can be calculated from Eq. (9). Graphical display of this function, called the sensitivity profile, provides a direct measure of the differential rate of change in R as a function of change in Σ and thus the sensitivity of R to Σ.

In general, the sensitivity profile is determined with respect to a cross section group constant, i.e., $dR/R/d\sigma_g/d\sigma_g$, where σ_g is a multigroup cross section for group g. However, in this study, the sensitivity to the basic resonance parameter Γ_x was also of interest. This was determined by using:

$$\frac{dR/R}{d\Gamma_x/\Gamma_x} = \sum_g \frac{dR/R}{d\sigma_g/\sigma_g} \left(\frac{d\sigma_g/\sigma_g}{d\Gamma_x/\Gamma_x} \right) \tag{13}$$

and determining the quantity in parenthesis numerically.

IX. SENSITIVITY PROFILES: RESULTS

In the section below, total sensitivities are tabulated for each of the performance parameters with respect to the multigroup constants in the nuclear data field. They represent a useful figure-of-merit indicating what reactions are likely to be important for a given response. However, since the total sensitivity is often composed of large positive and negative contributions [e.g., the sensitivity of $^{28}\rho$ to $^{238}U(n,\gamma)$], a uniform one percent change over the entire range affecting the numerator and denominator, one must be careful

not to be misled. The graphical displays of the sensitivity profile illustrate the detailed energy dependence.

A. k_{eff}

The sensitivities (space and angle integrated profile) of k_{eff} to various reaction types is given in Table 7. Note that σ_s in this and all subsequent tables refers to total scattering (sum of elastic, inelastic, etc.). The

Table 7. Sensitivities for k_{eff} in the TRX-2 Thermal Lattice

		(dR/R/dσ/σ)			
Nuclide	Item	Group 1[a]	Group 2[b]	Group 3[c]	Group 4[d]
^{235}U	$\bar{\nu}$	0.006	0.002	0.045	0.872
^{235}U	σ_f	0.003	0.001	0.024	0.401
^{238}U	σ_c	-0.012	-0.013	-0.068	-0.173
H	σ_s	0.044	0.025	0.122	-0.009
H	σ_c	-0.00003	-0.00006	-0.005	-0.154
Moderator	DB^2	-0.058	-0.009	-0.023	-0.014
^{235}U	σ_c	-0.002	-0.003	-0.010	-0.082
^{238}U	$\bar{\nu}$	0.075	0.0	0.0	0.0
^{238}U	σ_f	0.048	0.0	0.0	0.0
Fuel	DB^2	-0.015	-0.003	-0.006	-0.004
Clad	DB^2	-0.004	-0.0007	-0.002	-0.001
Aℓ	σ_c	-0.0002	-0.00006	-0.0003	-0.007
^{238}U	σ_s	-0.0003	0.00002	-0.0008	-0.001
O	σ_c	-0.002	0.0	0.0	0.00004
O	σ_s	0.001	0.0003	0.001	-0.0008
Void	DB^2	-0.0009	-0.0003	-0.0008	-0.0003
Aℓ	σ_s	-0.00003	0.00001	0.0001	-0.0002
^{235}U	σ_s	0.0	0.0	0.0	-0.00004

[a] 10 MeV - 67.37 keV.
[b] 67.73 keV - 3.35 keV.
[c] 3.35 keV - 0.625 eV.
[d] 0.625 eV - 10^{-5} eV.

sensitivity to the DB^2 components refers to our treatment of leakage by simulation of the Monte Carlo calculated leakage by an equivalent absorption term added to the total cross section. The importance of leakage is clearly evident; a 10% underprediction of the leakage cross section for the moderator would reduce k_{eff} by approximately one percent. The importance of $^{235}U(\bar{\nu})$, $^{235}U(n,f)$, and $^{238}U(n,\gamma)$ are well known and are here quantified. The importance of the H cross sections is also well known; however, the balance between capture and scattering is delicate as can be seen from Table 7. The role of $^{235}U(n,\gamma)$, $^{238}U(\bar{\nu})$, and $^{238}U(n,f)$ is also significant. The oxygen, aluminum and scattering reactions with heavy nuclides are of little importance.

Figures 12, 13, and 14 illustrate the energy dependence of the three reaction types with the highest sensitivities, namely $^{235}U(\bar{\nu})$, $^{235}U(n,f)$, and $^{238}U(n,\gamma)$. A comprehensive library[34] of all energy dependent profiles pertaining to the TRX-2 thermal lattice has been compiled for distribution. The overwhelming importance of the $^{235}U(\bar{\nu})$ and $^{235}U(n,f)$ occurs in the thermal group. (Note the graph is extended from the 0.1 eV point plotted down to 10^{-5} eV with the same value of sensitivity/lethargy since the thermal group spans the range from 10^{-5} eV to 0.625 eV.) Figure 14 clearly illustrates the relatively large sensitivity to the wings of the first few ^{238}U resolved resonances compared to the value at the self-shielded peak. In each of the figures to follow, dashed lines represent positive values while solid lines correspond to negative sensitivities.

B. Epithermal/Thermal ^{238}U Capture ($^{28}\rho$)

The sensitivities of $^{28}\rho$ to various reaction types are presented in Table 8. In particular, note that the five reaction types with the highest sensitivties all effect $^{28}\rho$ indirectly. Figures 15, 16, and 17 illustrate the energy dependence of the three reaction types with the highest sensitivities, namely H scattering, ^{235}U fission and H capture. The hydrogen scattering has, as classical reactor theory has described in the four-factor formula, important consequences on the probability of avoiding resonance capture. ^{235}U fission and H capture at thermal compete effectively with the thermal ^{238}U capture cross section. The total sensitivity for ^{238}U capture is relatively small because it results from the difference of two large sensitivities of opposite sign (negative in the thermal region and positive in the epithermal region). The energy dependent sensitivity profile for ^{238}U capture is presented in Fig. 18.

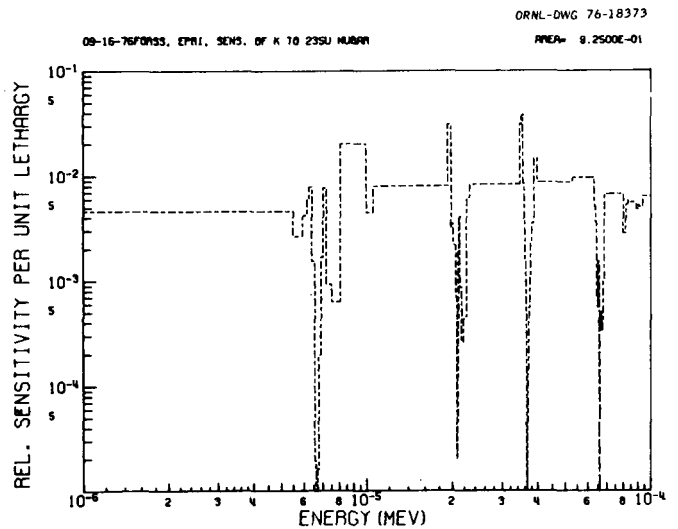

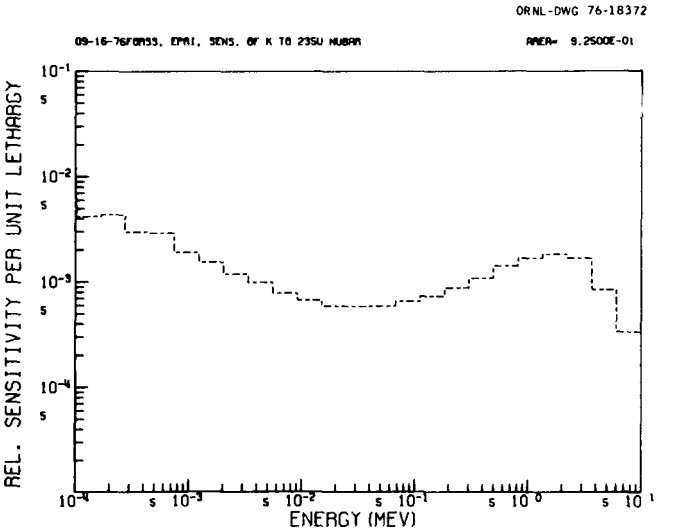

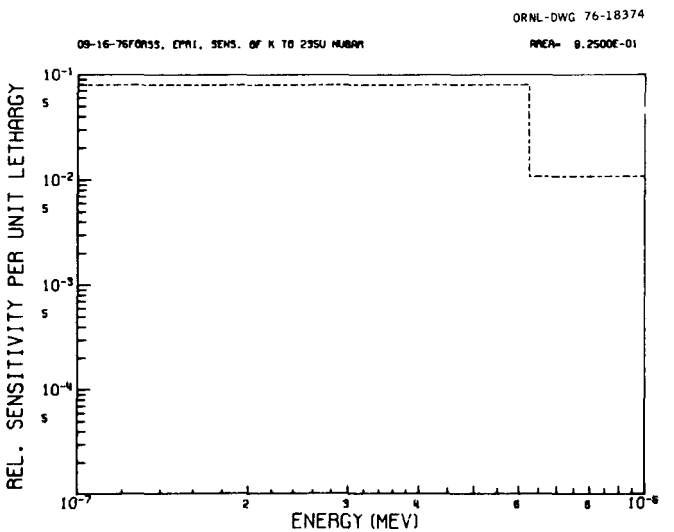

Fig. 12. The Energy Dependent Sensitivity Profile of k_{eff} in TRX-2 to ν of ^{235}U.

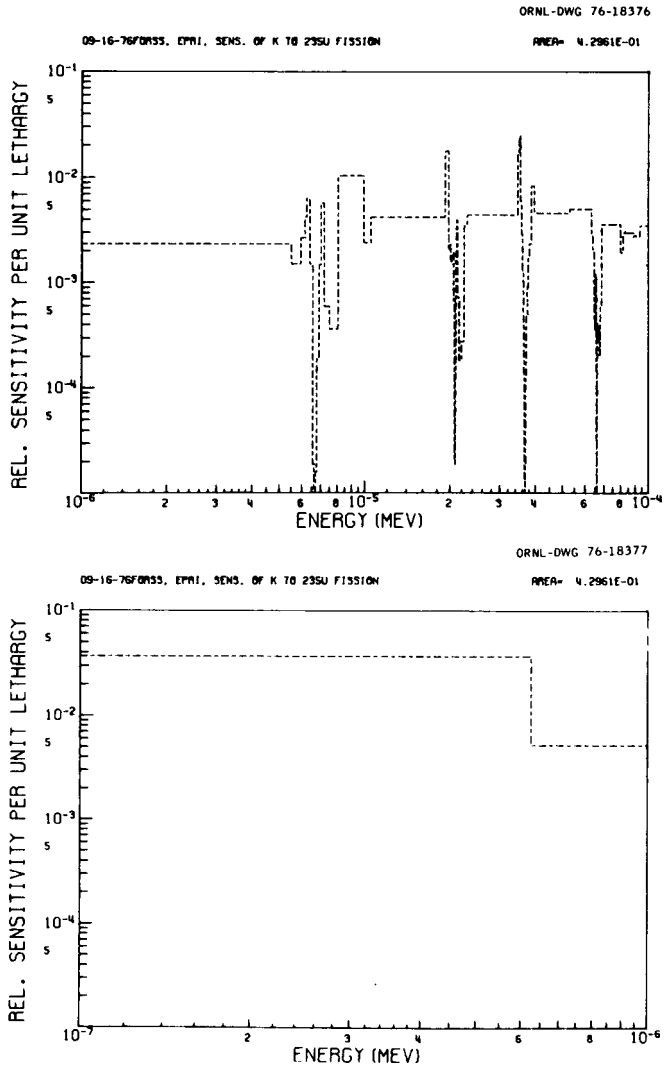

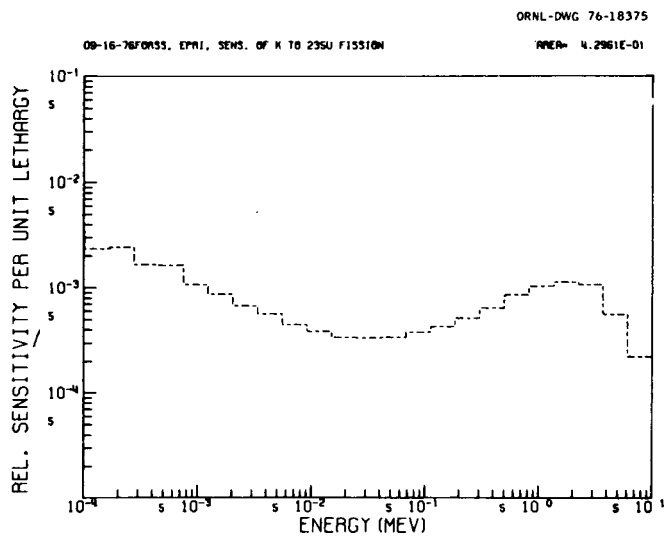

Fig. 13. The Energy Dependent Sensitivity Profile of k_{eff} in TRX-2 to $^{235}U(n,f)$.

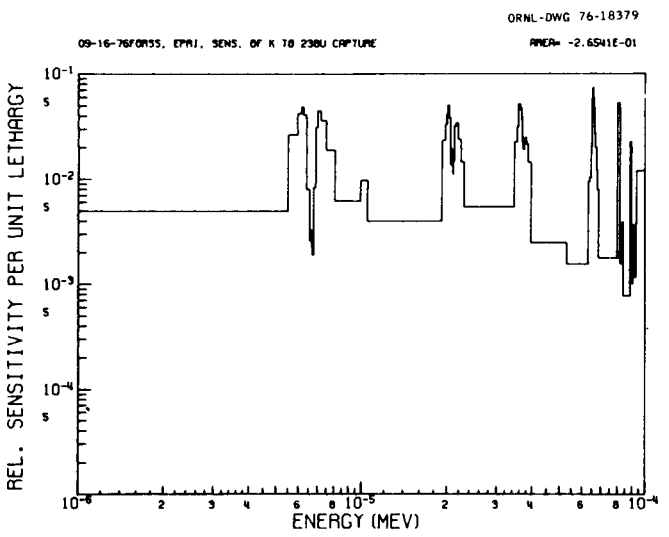

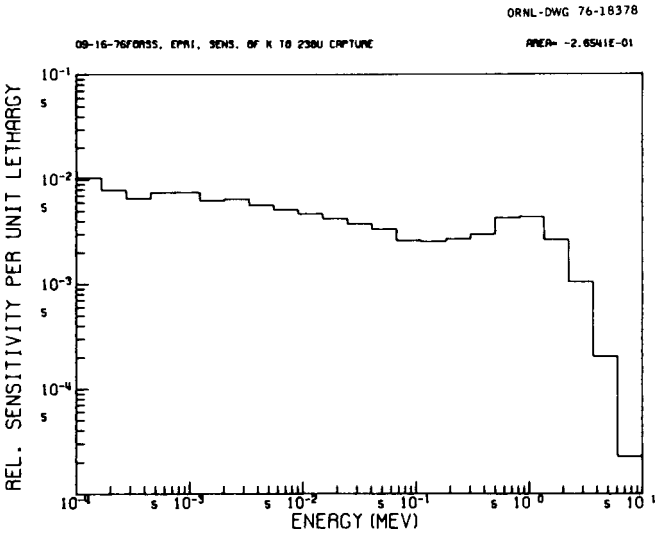

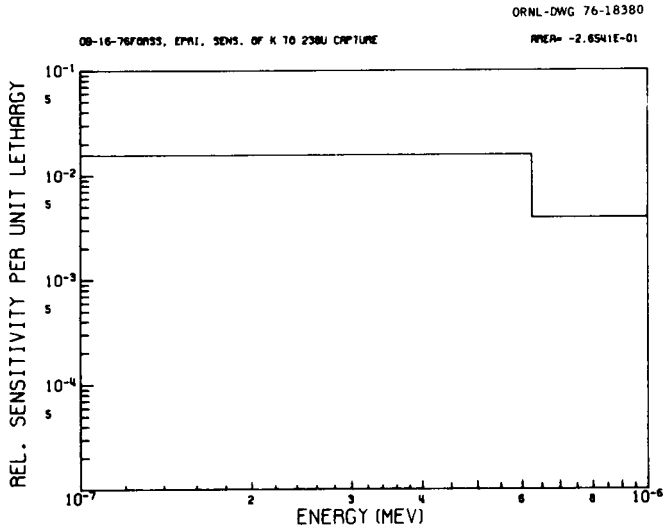

Fig. 14. The Energy Dependent Sensitivity Profile of k_{eff} in TRX-2 to $^{238}U(n,\gamma)$.

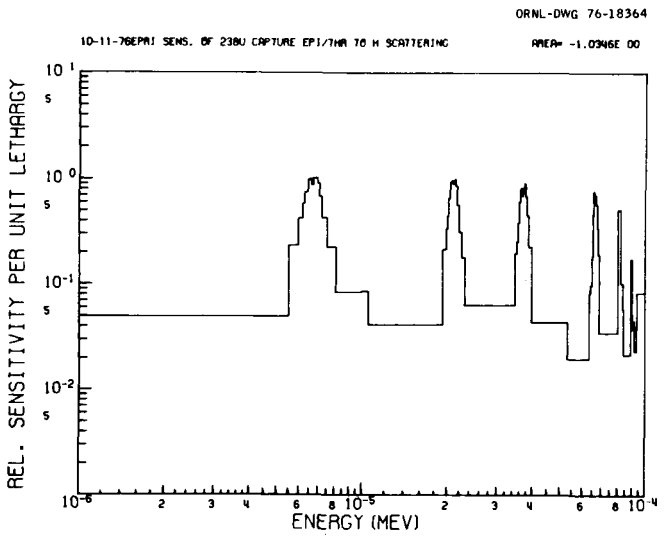

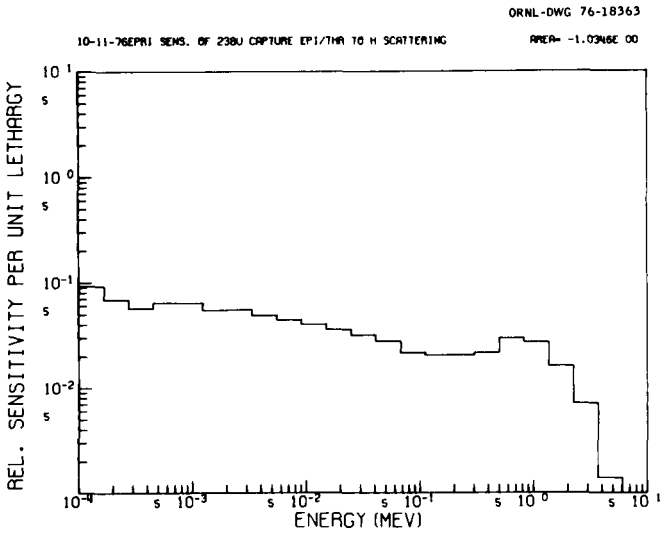

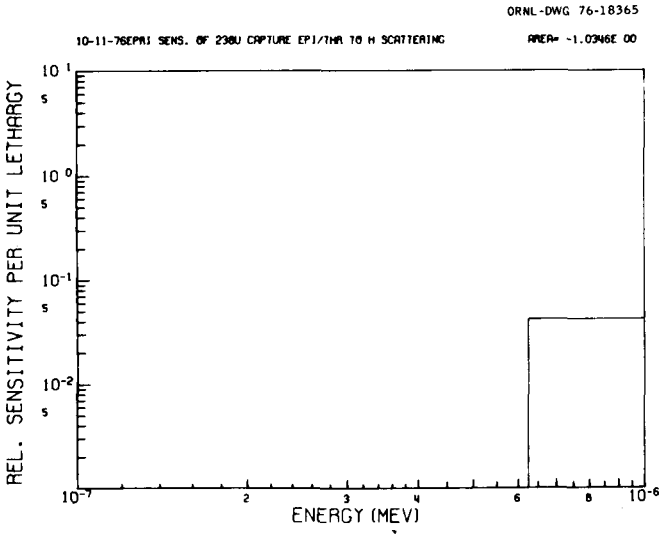

Fig. 15. The Energy Dependent Sensitivity Profile of $^{28}\rho$ in TRX-2 to H(n,n).

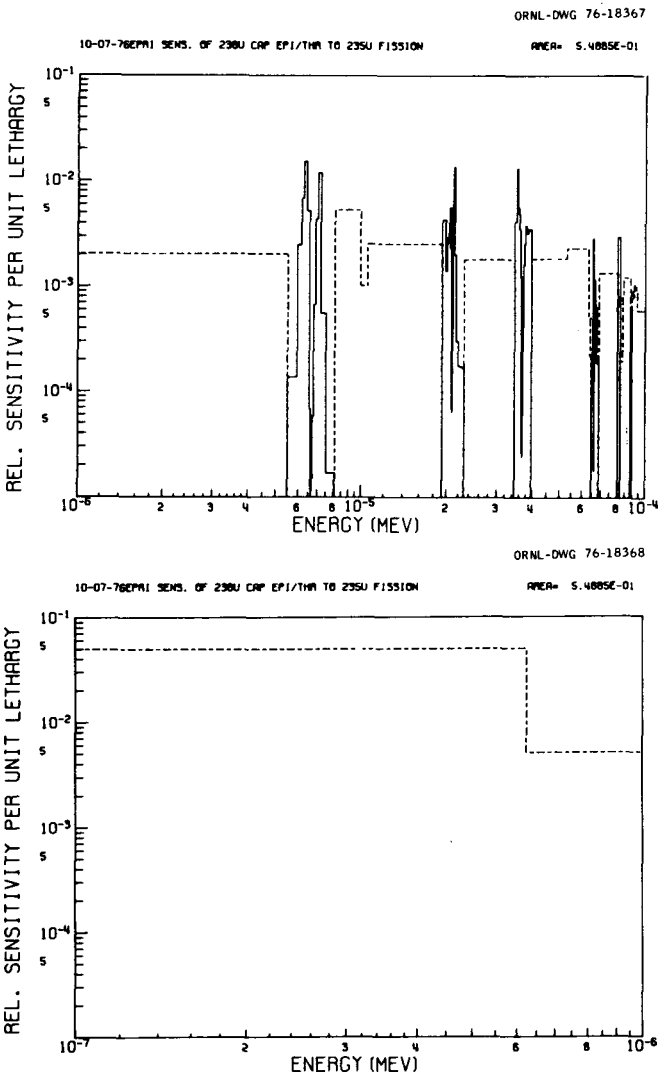

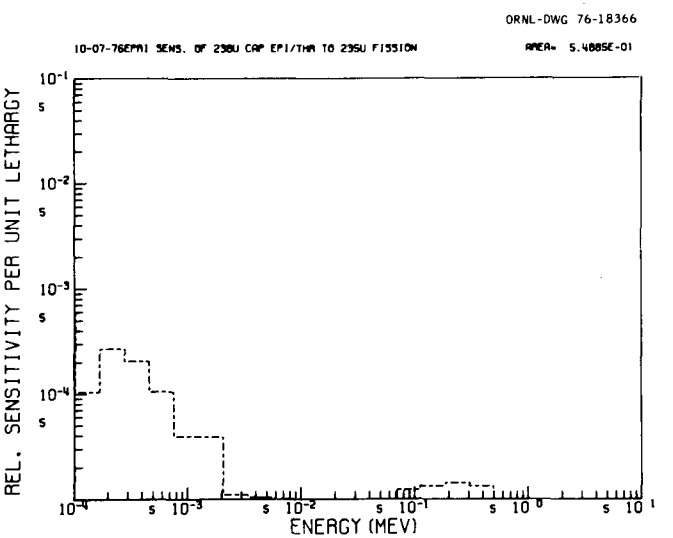

Fig. 16. The Energy Dependent Sensitivity Profile of $^{28}\rho$ in TRX-2 to $^{235}U(n,f)$.

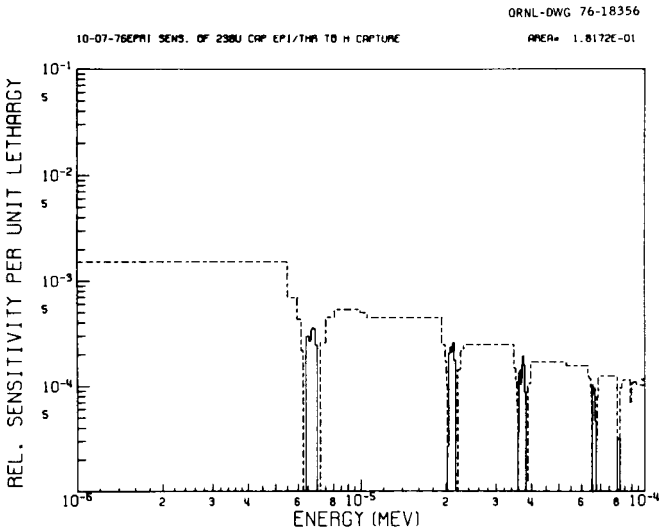

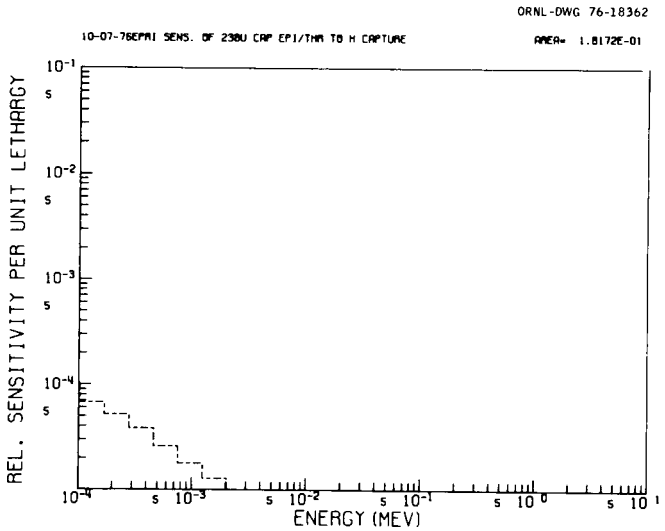

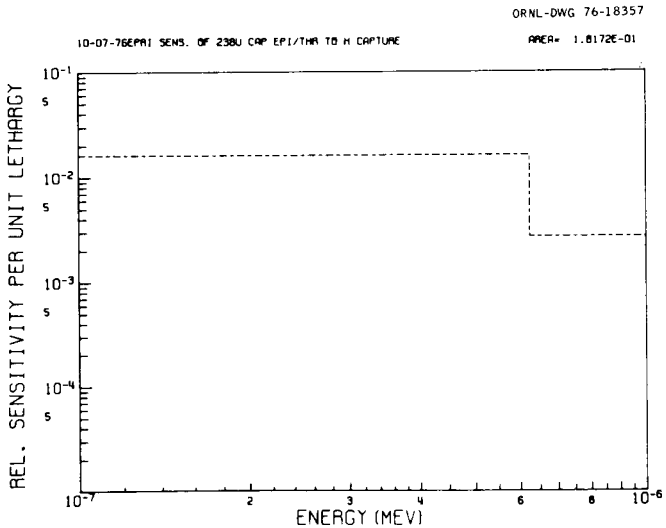

Fig. 17. The Energy Dependent Sensitivity Profile of $^{28}\rho$ in TRX-2 to H(n,γ).

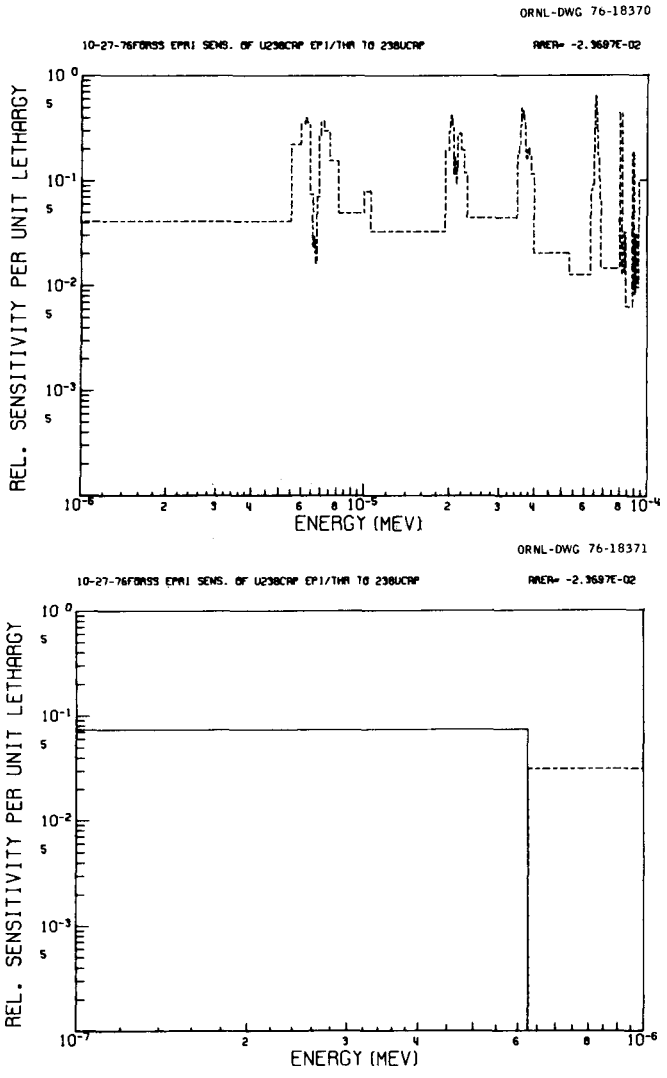

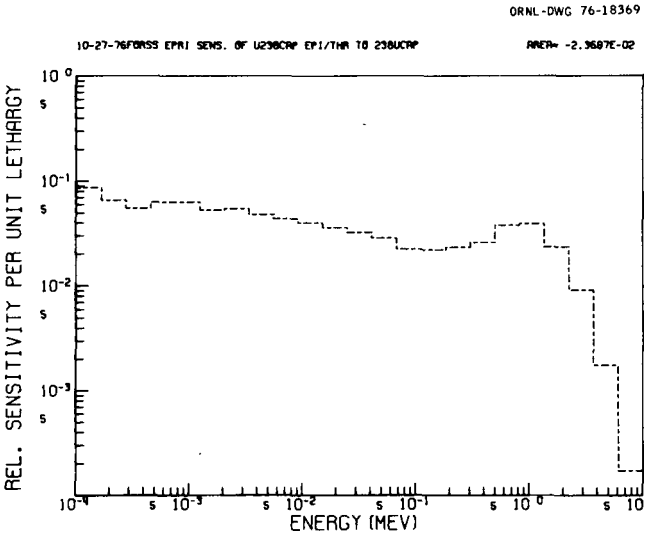

Fig. 18. The Energy Dependent Sensitivity Profile of $^{28}\rho$ in TRX-2 to $^{238}U(n,\gamma)$.

Table 8. Sensitivities for $^{28}\rho$ in the TRX-2 Thermal Lattice

Nuclide	Item	dR/R/dσ/σ Group 1[a]	Group 2[b]	Group 3[c]	Group 4[d]
H	σ_s	-0.084	-0.115	-0.845	0.010
^{235}U	σ_f	0.00002	0.00002	0.009	0.540
H	σ_c	0.0	0.0	0.005	0.094
^{235}U	σ_c	0.0	0.0	0.002	0.177
Moderator	DB^2	0.001	0.001	0.010	0.017
^{238}U	σ_c	0.102	0.114	0.563	-0.802
O	σ_s	-0.002	-0.001	-0.008	0.0009
Aℓ	σ_c	0.0	0.0	0.0002	0.008
^{238}U	σ_s	-0.002	-0.00007	0.005	0.002
Fuel	DB^2	0.0001	0.00006	0.0005	0.001
Clad	DB^2	0.0007	0.0006	0.0005	0.001
Void	DB^2	0.00001	0.00002	0.0002	0.0004
Aℓ	σ_s	0.0	-0.00003	-0.0007	0.0002
^{235}U	$\bar{\nu}$	0.0	0.0	-0.00001	-0.0003
^{238}U	σ_f	-0.0001	0.0	0.0	0.0
O	σ_c	0.0	0.0	0.0	0.0005
^{235}U	σ_s	-0.00001	0.0	-0.00004	0.00004
^{238}U	$\bar{\nu}$	-0.00002	0.0	0.0	0.0

[a] 10 MeV - 67.37 keV.
[b] 67.73 keV - 3.35 keV.
[c] 3.35 keV - 0.625 eV.
[d] 0.625 eV - 10^{-5} eV.

The effect of $^{235}U(n,f)$ on $^{28}\rho$ is generally negative in the large resonances due to competition with ^{238}U capture. Below the resolved resonance region ^{235}U fission has a positive effect by introducing neutrons above the energy range. It is also clear that a fission in ^{235}U introduces multiple high energy neutrons which must slow down through the resonance energy range.

C. Epithermal/Thermal ^{235}U Fission ($^{25}\delta$)

The sensitivities for $^{25}\delta$ to various reaction types are given in Table 9. Energy dependent sensitivity profiles are illustrated in Figs. 19, 20, and 21 for the three reaction types with the highest sensitivities. The processes of thermalization from neutron scattering with hydrogen, spectral

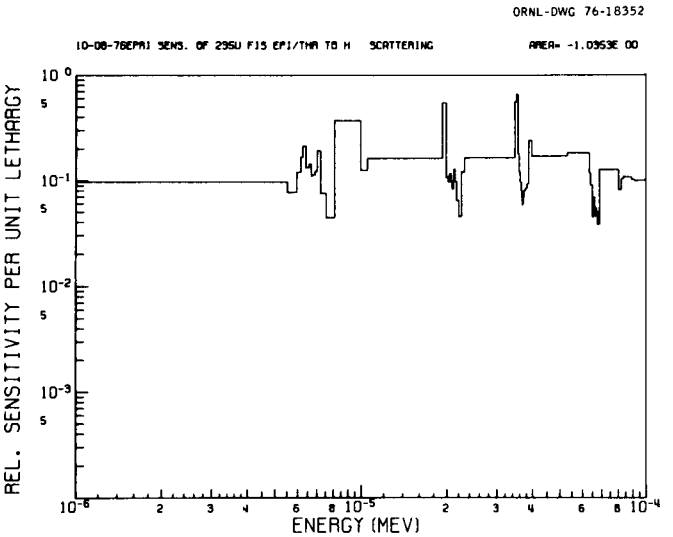

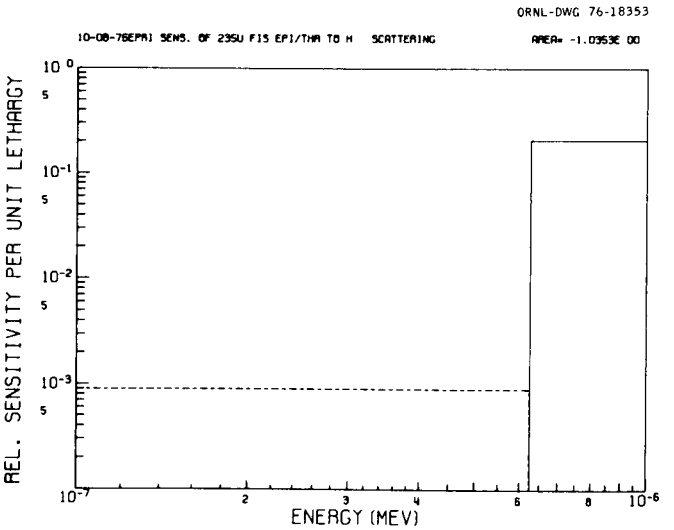

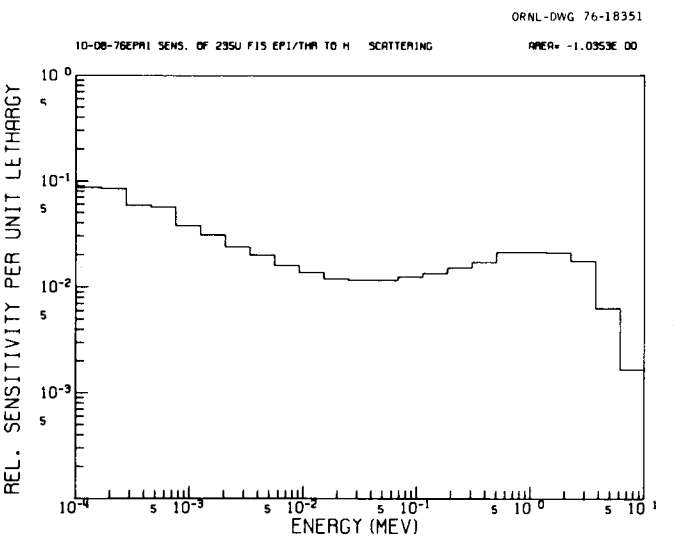

Fig. 19. The Energy Dependent Sensitivity Profile of $^{25}\delta$ in TRX-2 to H(n,n).

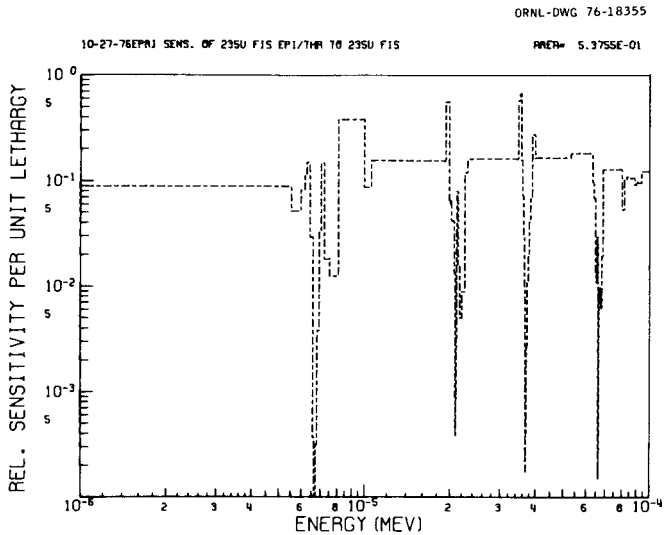

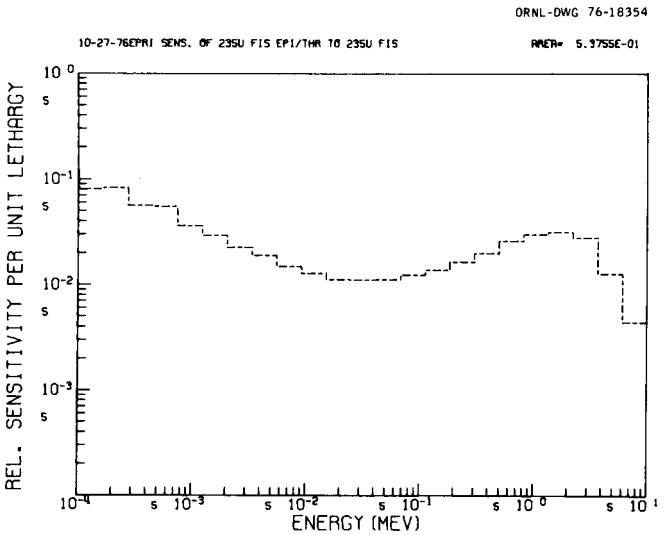

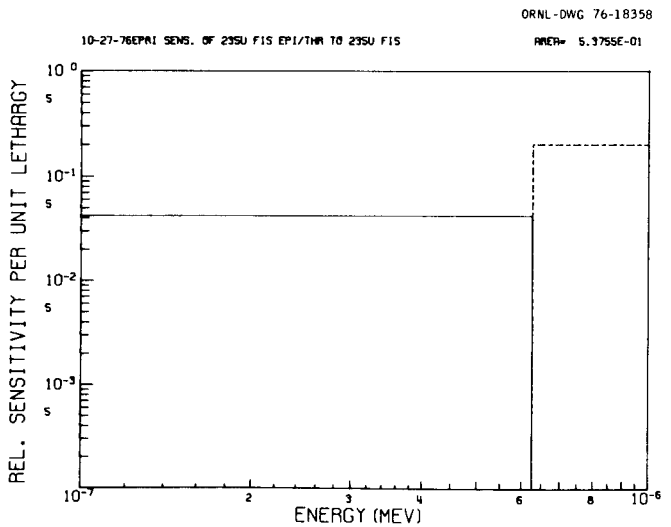

Fig. 20. The Energy Dependent Sensitivity Profile of $^{25}\delta$ in TRX-2 to $^{235}U(n,f)$.

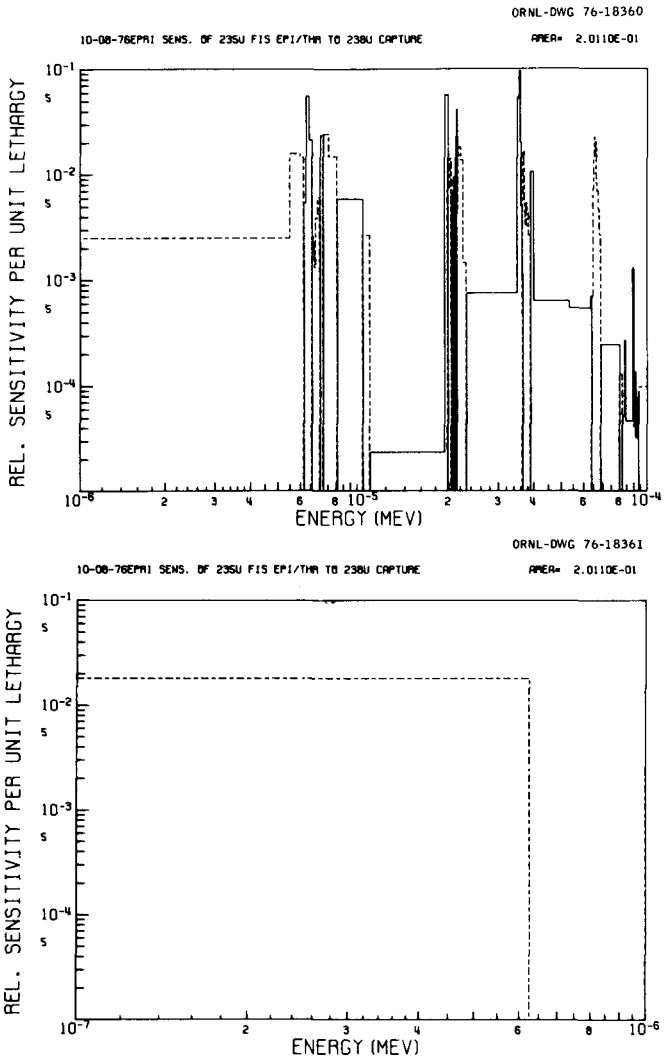

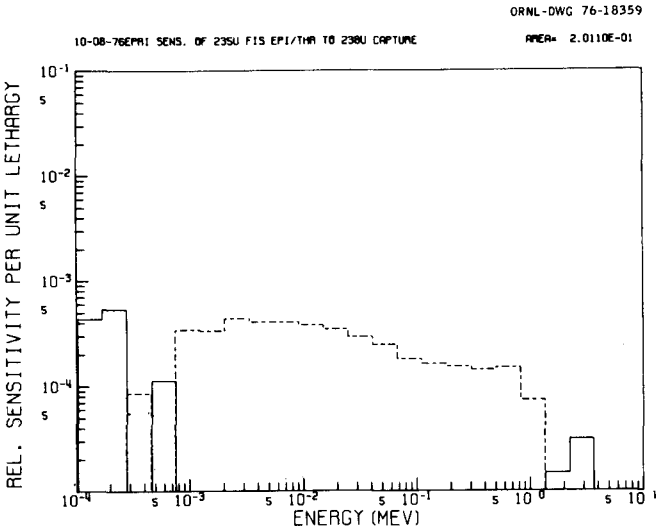

Fig. 21. The Energy Dependent Sensitivity Profile of $^{25}\delta$ in TRX-2 to $^{238}U(n,\gamma)$.

Table 9. Sensitivities for $^{25}\delta$ in the TRX-2 Thermal Lattice

Nuclide	Item	dR/R/dσ/σ Group 1[a]	Group 2[b]	Group 3[c]	Group 4[d]
H	σ_s	-0.074	-0.042	-0.929	0.002
^{235}U	σ_f	0.098	0.040	0.859	-0.460
^{238}U	σ_c	0.0004	0.001	0.002	0.198
H	σ_c	0.0	0.0	0.004	0.177
^{235}U	σ_c	0.00001	0.00003	-0.001	0.094
Moderator	DB^2	0.001	0.001	0.010	0.017
^{238}U	σ_s	-0.007	-0.0003	-0.008	0.002
O	σ_s	-0.003	-0.0004	-0.011	0.0009
Aℓ	σ_c	0.0	0.0	0.0001	0.008
Fuel	DB^2	0.0001	0.0002	-0.001	0.004
Clad	DB^2	0.0001	0.0002	-0.001	0.004
Aℓ	σ_s	-0.0004	-0.00001	-0.0007	0.0002
^{238}U	σ_f	-0.0008	0.0	0.0	0.0
Void	DB^2	0.00001	0.00003	0.00009	0.0004
^{235}U	σ_s	-0.00005	0.0	-0.0001	0.0004
^{235}U	$\bar{\nu}$	0.0	0.0	0.0	0.00003
O	σ_c	-0.00008	0.0	0.0	0.00005
^{238}U	$\bar{\nu}$	-0.00001	0.0	0.0	0.0

[a] 10 MeV - 67.37 keV.
[b] 67.73 keV - 3.35 keV.
[c] 3.35 keV - 0.625 eV.
[d] 0.625 eV - 10^{-5} eV.

hardening from fission, competition for thermal neutron fission by thermal ^{238}U capture are clearly evident. The direct effect of ^{235}U fission accounts for the negative value in the thermal range and positive in the epithermal range, Fig. 20.

D. ^{238}U Fission/^{235}U Fission ($^{28}\delta$)

The sensitivities of $^{28}\delta$ to various reaction types are given in Table 10. Energy dependent sensitivity profiles are illustrated in Figs. 22, 23, and 24 for the reaction types with the highest sensitivities, namely ^{238}U fission, H scattering, and ^{235}U fission. The general shape of these curves are

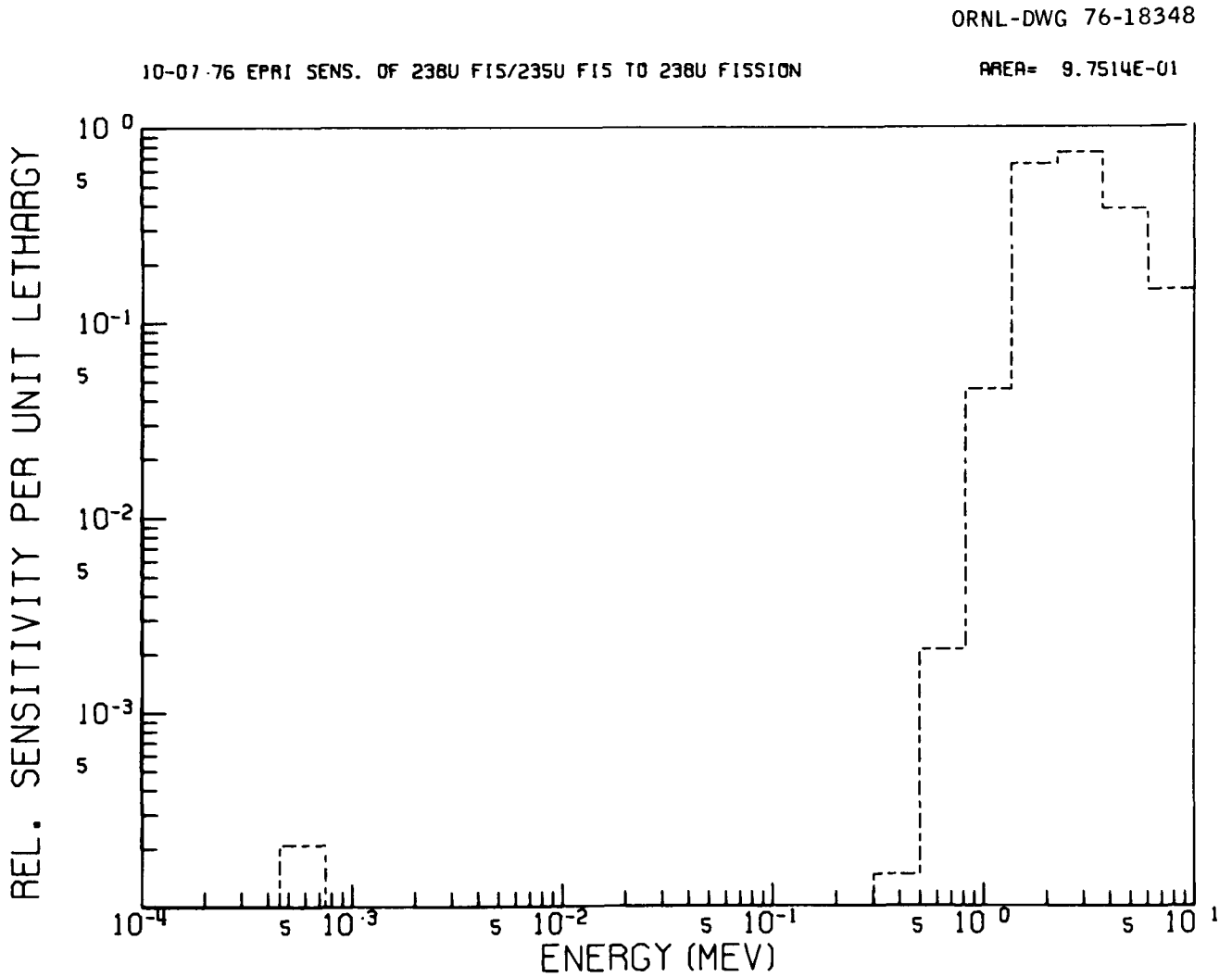

Fig. 22. The Energy Dependent Sensitivity Profile of $^{28}\delta$ in TRX-2 to $^{238}U(n,f)$.

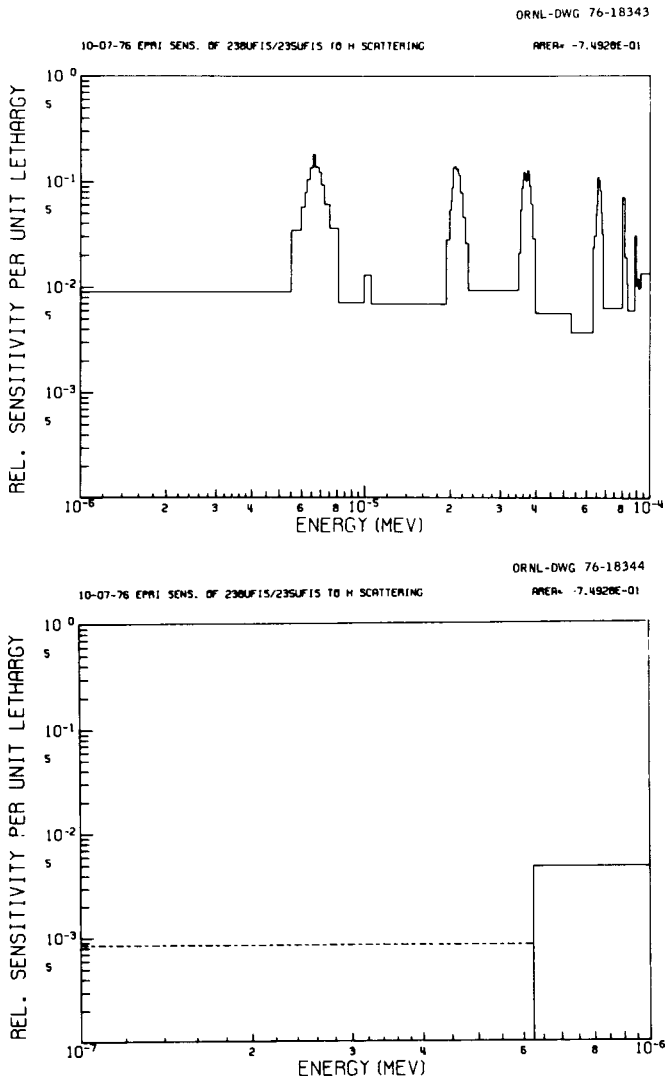

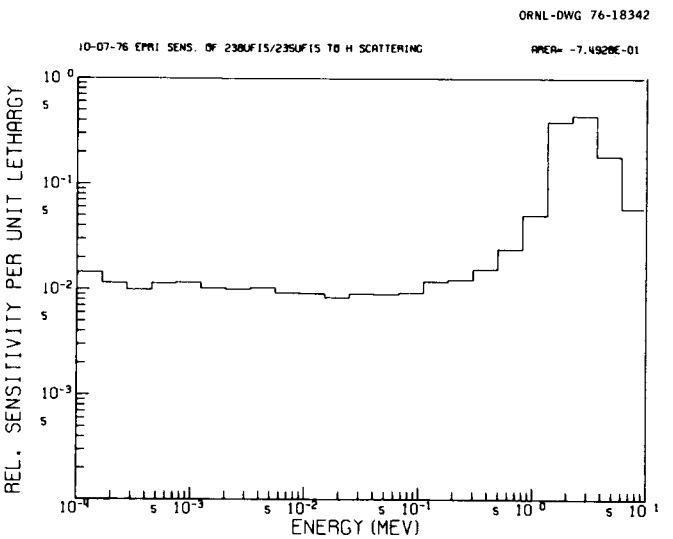

Fig. 23. The Energy Dependent Sensitivity Profile of $^{28}\delta$ in TRX-2 to H(n,n).

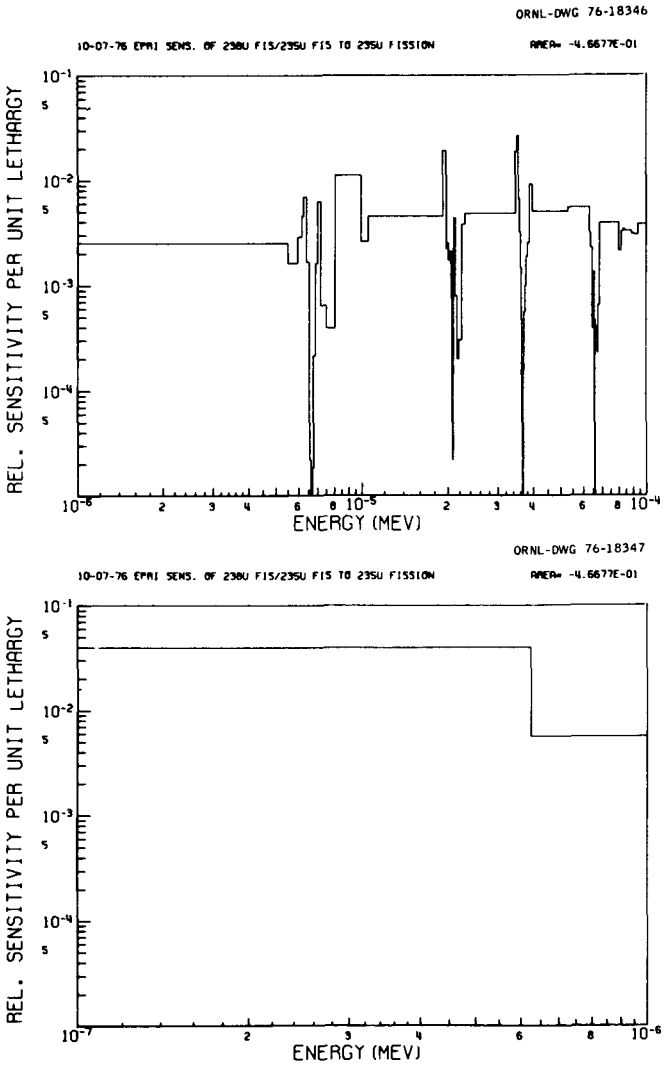

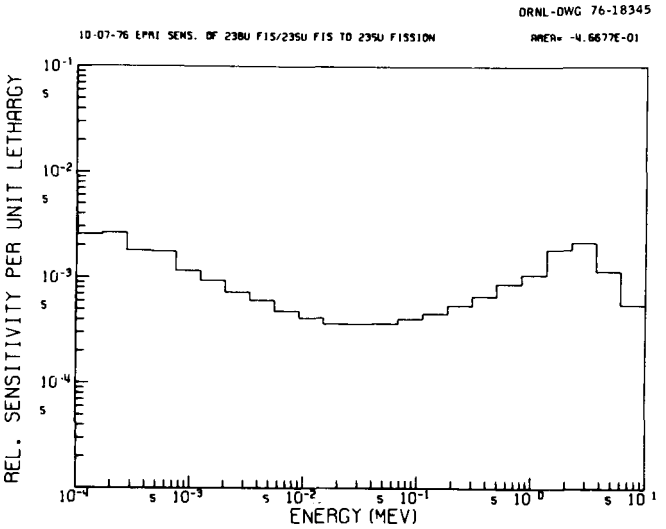

Fig. 24. The Energy Dependent Sensitivity Profile of $^{28}\delta$ in TRX-2 to $^{235}U(n,f)$.

Table 10. Sensitivities for $^{28}\delta$ in the TRX-2 Thermal Lattice

Nuclide	Item	(dR/R)/(dσ/σ) Group 1[a]	Group 2[b]	Group 3[c]	Group 4[d]
^{238}U	σ_f	0.975	0.00005	0.0001	0.0
H	σ_s	-0.599	-0.028	-0.132	0.009
^{235}U	σ_f	-0.005	-0.001	-0.026	-0.434
^{238}U	σ_c	0.010	0.015	0.073	0.186
^{238}U	σ_s	-0.196	-0.00002	0.0008	0.001
H	σ_c	0.00002	0.00007	0.006	0.167
^{235}U	σ_c	0.0002	0.0004	0.011	0.088
Moderator	DB^2	0.018	0.010	0.025	0.016
O	σ_s	-0.042	-0.0003	-0.001	0.0008
Fuel	DB^2	0.002	0.003	0.006	0.004
Aℓ	σ_s	-0.013	-0.00001	-0.0001	0.0002
Aℓ	σ_c	-0.0003	0.00006	0.0003	0.007
Clad	DB^2	0.001	0.0007	0.002	0.001
O	σ_c	-0.003	0.0	0.0	0.00005
Void	DB^2	0.00006	0.0004	0.0009	0.0003
^{235}U	σ_s	-0.001	0.0	0.0	0.00003
^{238}U	$\bar{\nu}$	-0.0008	0.0	0.0	0.0
^{235}U	$\bar{\nu}$	0.00001	0.0	0.00003	-0.0003

[a] 10 MeV - 67.37 keV.
[b] 67.73 keV - 3.35 keV.
[c] 3.35 keV - 0.625 eV.
[d] 0.625 eV - 10^{-5} eV.

consistent with a simple view of the uranium cross sections having a direct effect on the response definition (modified slightly by small flux effects) and hydrogen scattering feeding the ^{235}U thermal fission process.

Much interest has been generated of late on the effects that modification of the ^{238}U inelastic cross sections and spectra might have on spectrally sensitive thermal lattice parameters like $^{28}\delta$. Figure 25 illustrates the sensitivity of $^{28}\delta$ to the total inelastic cross sections while Figs. 26 - 28 present the three major contributors: inelastic continuum and the 21st and 22nd level. These levels correspond to 1.625 and 1.875 MeV respectively. The lower levels correspond to smaller energy degradations and do not significantly effect the flux spectrum.

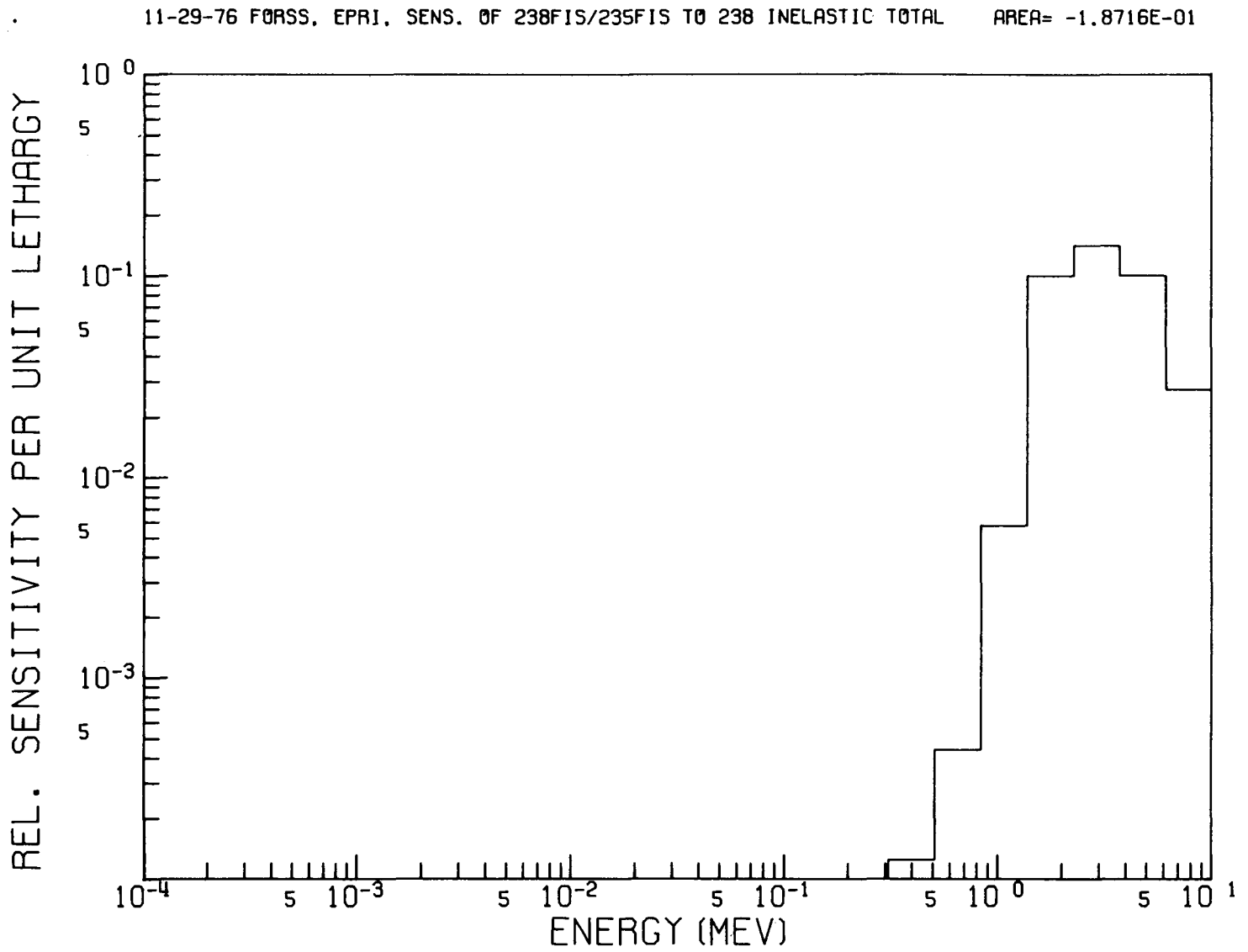

Fig. 25. The Energy Dependent Sensitivity Profile of $^{28}\delta$ in TRX-2 to $^{238}U(n,n)$ Total Inelastic.

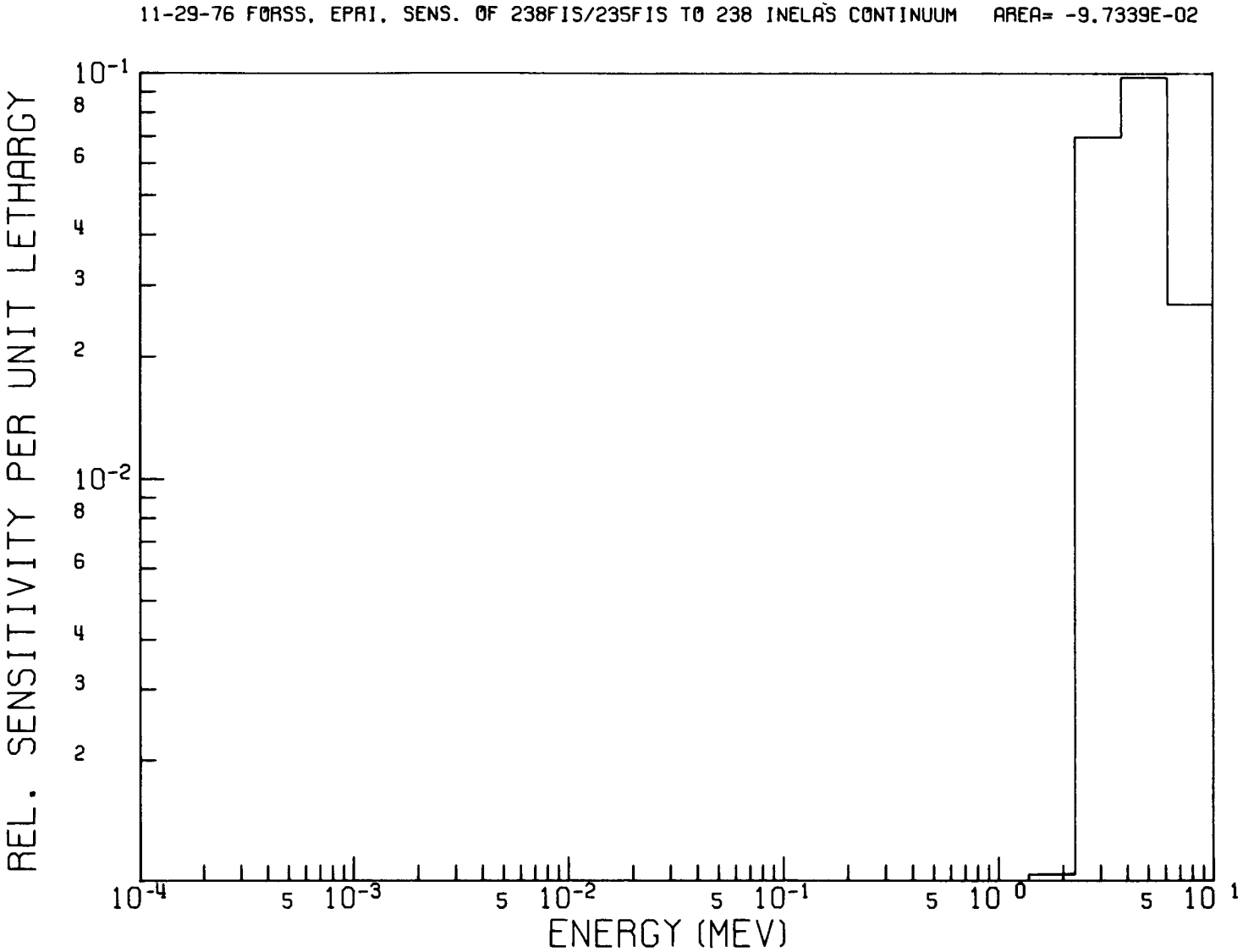

Fig. 26. The Energy Dependent Sensitivity Profile of $^{28}\delta$ in TRX-2 to $^{238}U(n,n)$ Inelastic Continuum.

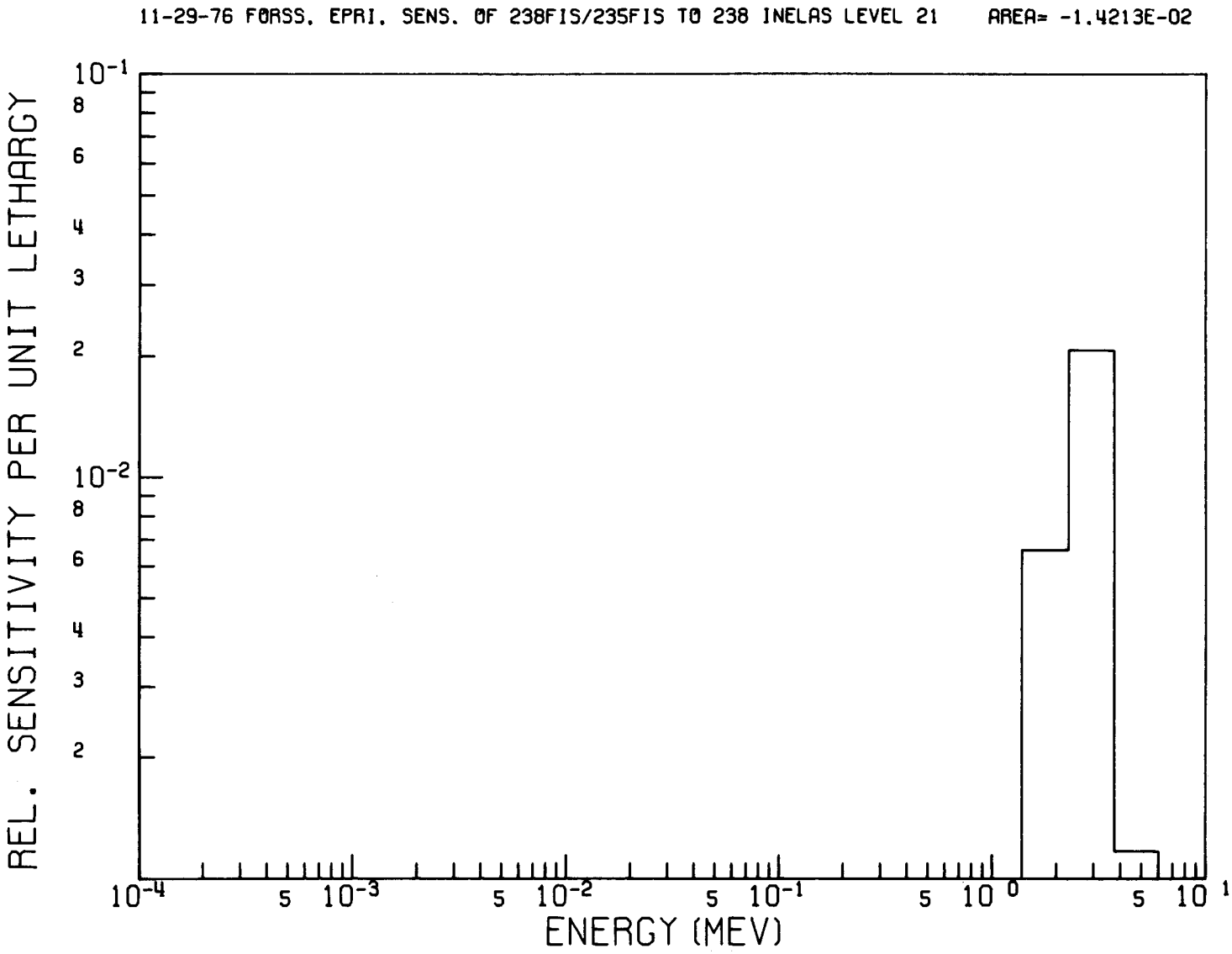

Fig. 27. The Energy Dependent Sensitivity Profile of $^{28}\delta$ in TRX-2 to $^{238}U(n,n)$ Inelastic Level 21.

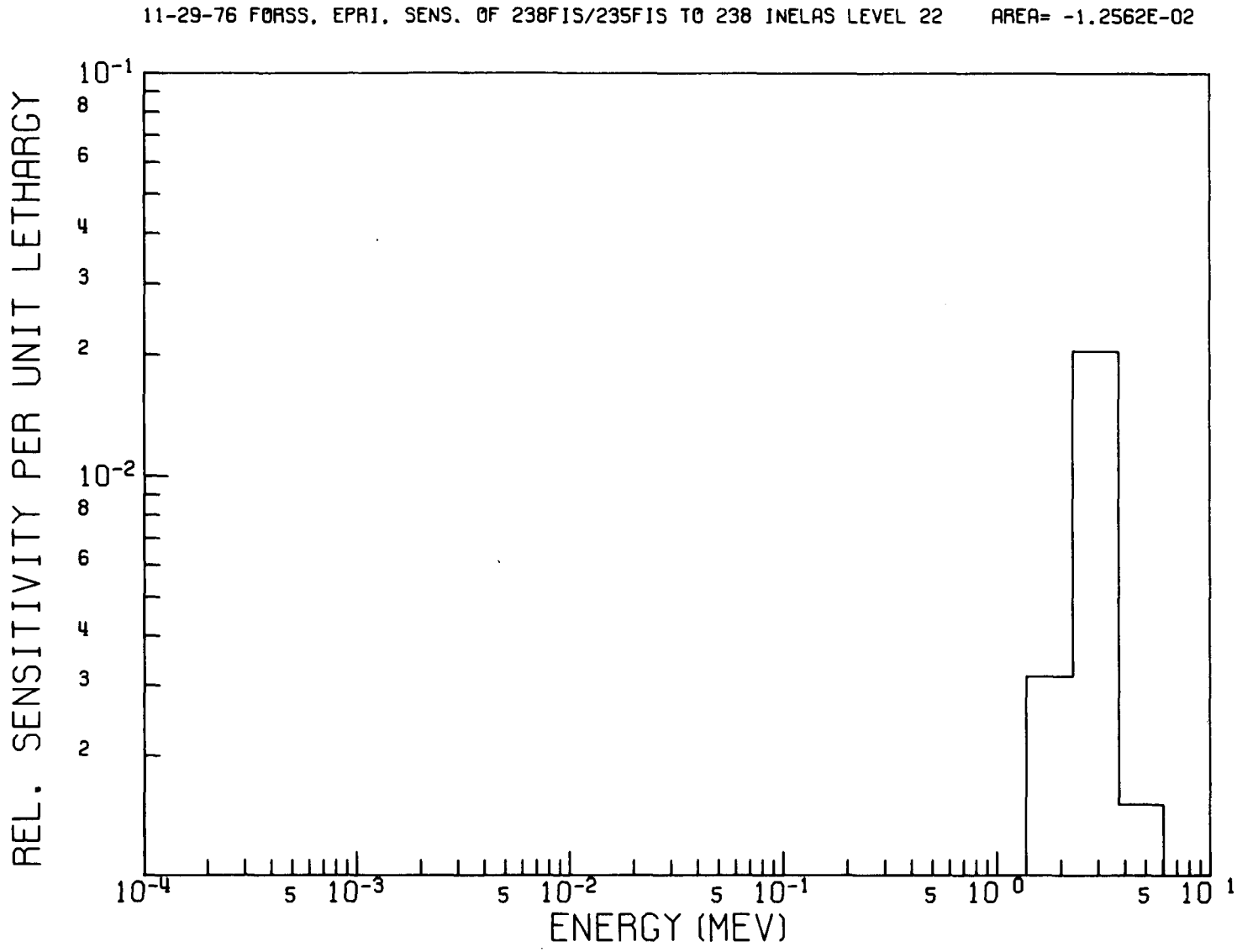

Fig. 28. The Energy Dependent Sensitivity Profile of $^{28}\delta$ in TRX-2 $^{238}U(n,n)$ Inelastic Level 22.

E. ^{238}U Capture/^{235}U Fission (CR)

The sensitivities for CR to various reaction types are given in Table 11. Energy dependent sensitivity profiles are illustrated in Figs. 29, 30, and 31 for the three reaction types with highest sensitivity, i.e., the two direct effects ^{238}U capture and ^{235}U fission and the major thermalization mechanism, H scattering.

Table 11. Sensitivities for CR in the TRX-2 Thermal Lattice

Nuclide	Item	Group 1[a]	Group 2[b]	Group 3[c]	Group 4[d]
^{238}U	σ_c	0.047	0.053	0.261	0.616
^{235}U	σ_f	-0.006	-0.002	-0.048	-0.723
H	σ_s	-0.035	-0.051	-0.340	0.004
H	σ_c	0.0	0.0	0.002	0.072
^{235}U	σ_c	0.0	0.0	0.001	0.038
Moderator	DB^2	0.0005	0.0005	0.004	0.007
O	σ_s	-0.0009	-0.0005	-0.003	0.0004
Aℓ	σ_c	0.0	0.0	0.00008	0.003
^{238}U	σ_s	-0.0007	-0.00003	0.003	0.0007
Fuel	DB^2	0.00004	0.00002	-0.0001	0.001
Clad	DB^2	0.00003	0.00002	0.0002	0.0005
^{235}U	$\bar{\nu}$	0.0	0.0	-0.00001	-0.0003
Void	DB^2	0.0	0.0	0.00007	0.0001
Aℓ	σ_s	0.00002	-0.00001	-0.0003	0.00009
O	σ_c	0.0	0.0	0.0	0.00002
^{238}U	σ_f	-0.00003	0.0	0.0	0.0
^{238}U	$\bar{\nu}$	-0.00002	0.0	0.0	0.0
^{235}U	σ_s	0.0	0.0	-0.00001	0.00002

[a] 10 MeV - 67.37 keV.
[b] 67.73 keV - 3.35 keV.
[c] 3.35 keV - 0.625 eV.
[d] 0.625 eV - 10^{-5} eV.

F. ^{238}U Resolved Resonance Parameter Sensitivities

The energy dependent sensitivity profiles provide a quantitative assessment of the rate of change in a particular response, R, with respect to the

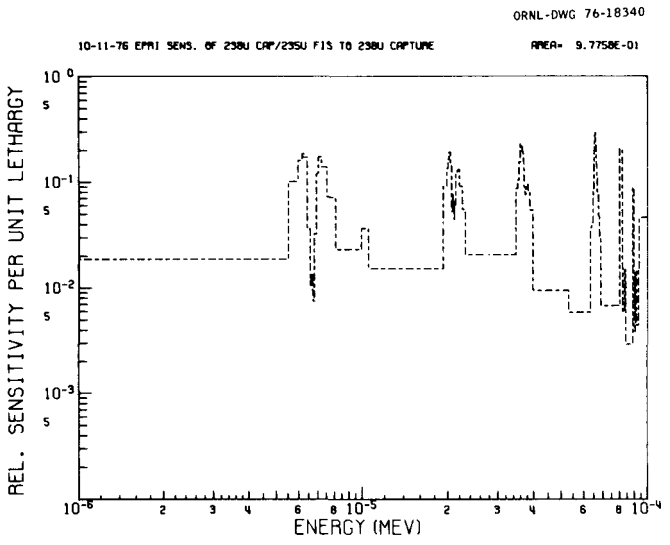

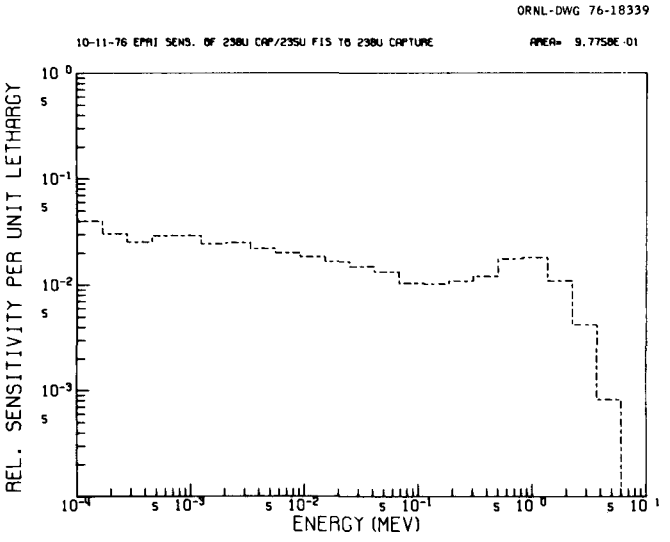

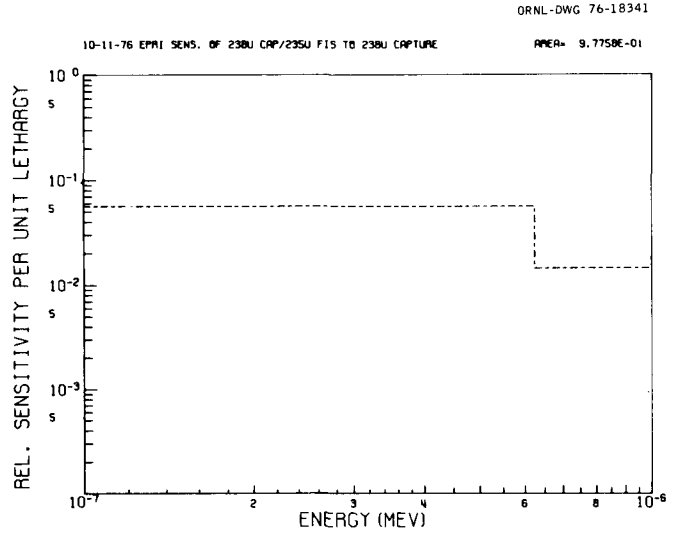

Fig. 29. The Energy Dependent Sensitivity Profile of CR in TRX-2 to $^{238}U(n,\gamma)$.

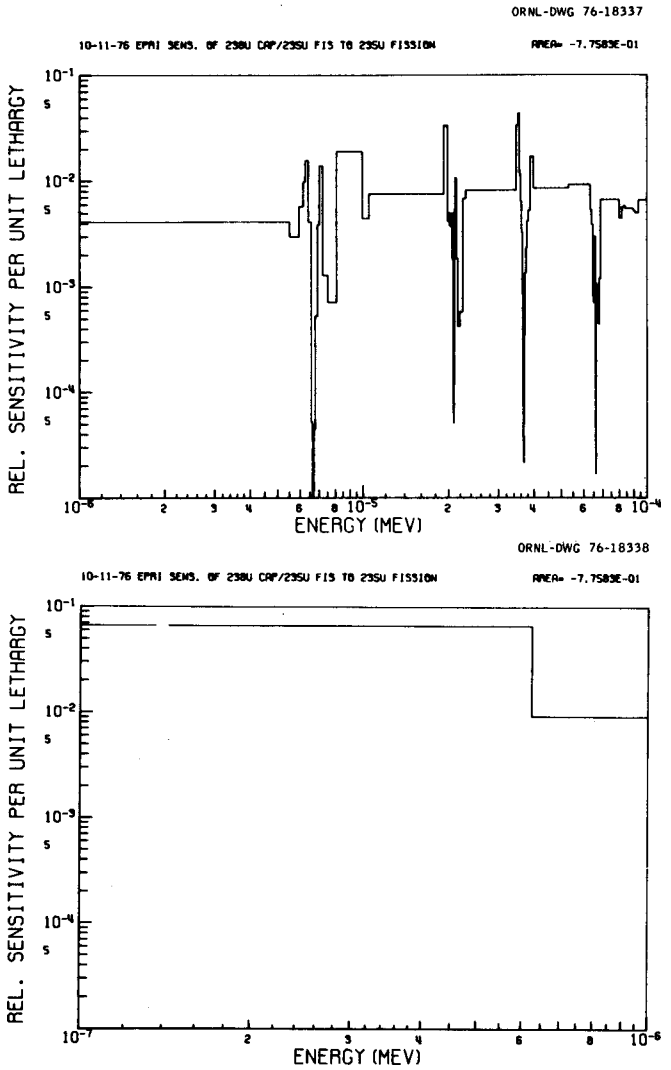

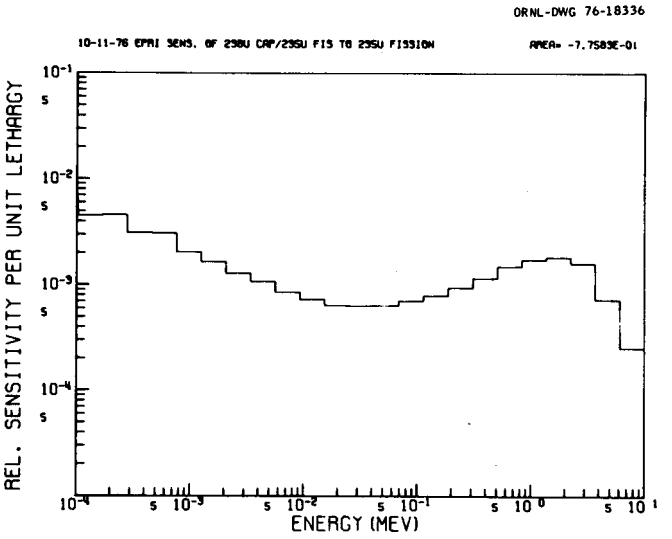

Fig. 30. The Energy Dependent Sensitivity Profile of CR in TRX-2 to $^{235}U(n,f)$.

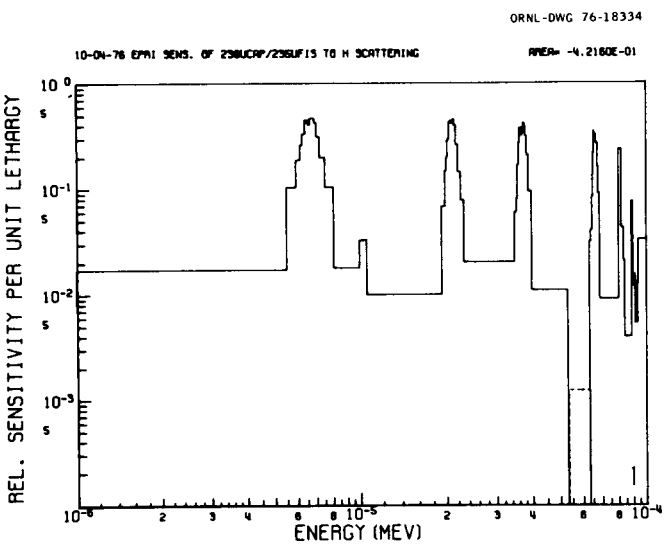

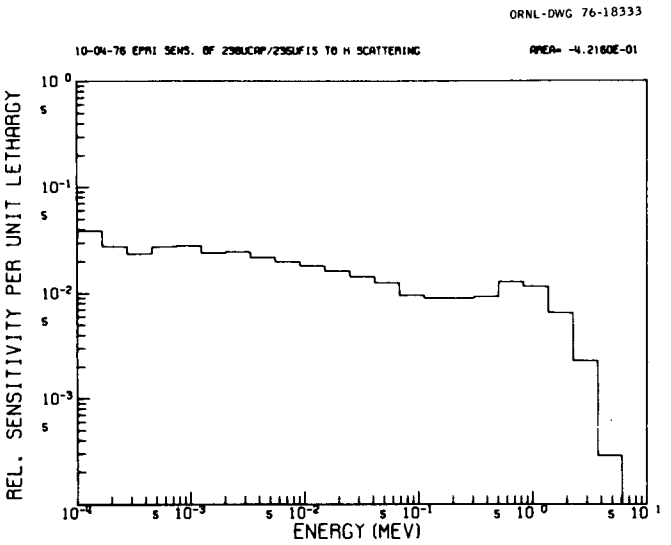

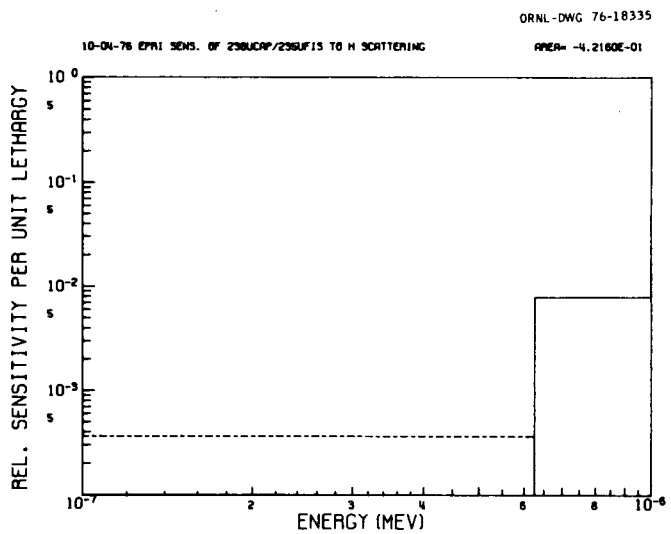

Fig. 31. The Energy Dependent Sensitivity Profile of CR in TRX-2 to H(n,n).

rate of change in some multigroup constant. Of more immediate interest is the sensitivity with respect to a specific resonance parameter, Γ_x. The latter can be obtained from

$$\frac{dR/R}{d\Gamma_x/\Gamma_x} = \sum_g \left(\frac{dR/R}{d\bar{\sigma}_g/\bar{\sigma}_g}\right) \frac{d\bar{\sigma}_g/\bar{\sigma}_g}{d\Gamma_x/\Gamma_x} \qquad (14)$$

The first term in each element of the sum is the sensitivity profile ($dR/R/d\bar{\sigma}_g/\bar{\sigma}_g$), whereas the second derivative ($d\bar{\sigma}_g/\bar{\sigma}_g/d\Gamma_x/\Gamma_x$) can be obtained numerically.

The numerical derivatives were obtained by direct recalculation of the group averaged cross section with a perturbed set of resonance parameters. This was done using the NPTXS and XLACS modules of the AMPX[14] system. The results of these calculations are given in Table 12 for the parameters of interest with respect to the capture and scattering widths of the first four resolved resonances.

Table 12. Performance Parameter Sensitivities to ^{238}U Resolved Resonance Parameters

E_o	6.67 eV		20.9 eV		36.8 eV		66.15 eV	
Parameter	Γ_n	Γ_γ	Γ_n	Γ_γ	Γ_n	Γ_γ	Γ_n	Γ_γ
k	-0.018	-0.018	-0.008	-0.008	-0.006	-0.006	-0.002	-0.002
$^{28}\rho$	0.149	0.147	0.068	0.066	0.055	0.055	0.020	0.020
$^{25}\delta$	0.004	0.004	-0.0007	-0.0007	-0.002	-0.002	0.0004	0.0004[a]
$^{28}\delta$	0.013	0.019	0.009	0.009	0.007	0.007	0.003	0.003
CR	0.069	0.068	0.031	0.031	0.026	0.026	0.009	0.009

[a]This value borders on the limit of computational precision.

It must be remembered that the sensitivity coefficients presented in Table 12 are appropriate to the methodology and analysis techniques described earlier in the report. Our sensitivity coefficients were compared to earlier reported results of Rothenstein,[7] and more recently Finch,[35] with regard to uniform reductions in resonance parameters for the first four levels. These results are presented in Table 13 in terms of percent change in integral parameters per percent increase in the resonance parameter of interest. Note that the ORNL results were obtained via perturbation theory (and checked by recalculation using transport theory) while the BNL and SRL values correspond to direct recalculation.

Table 13. Percent Changes in TRX-2 Integral Parameter for a Uniform 1% Increase in the Resolved Resonance Parameters of ^{238}U

Parameter Relative Sensitivity	k	$^{28}\rho$	$^{25}\delta$	$^{28}\delta$	CR
Change: a 1% Increase in Γ_n for the Four Lowest Energy Resonances in ^{238}U:					
ORNL	-0.034	0.292	0.002	0.038	0.134
BNL	-0.032	0.254	0.022	0.034	0.118
SRL	-0.034	0.200	0.030	0.120	0.090
Change: a 1% Increase in Γ_γ for the Four Lowest Energy Resonances in ^{238}U:					
ORNL	-0.034	0.288	0.002	0.038	0.135
BNL	-0.032	0.257	0.022	0.035	0.119
SRL	-0.034	0.220	0.037	0.120	0.095

Our results appear to agree somewhat better with the BNL values. The disagreement in the small value for the $^{25}\delta$ coefficient could arise from our numerical approximation to the $d\sigma/\sigma/d\Gamma_x/\Gamma_x$ derivative; this should be investigated. One should also investigate the possibility of loss of significance from subtraction of two responses (perturbed and unperturbed) of similar magnitude since this is the method used at BNL and SRL. The good agreement between the two labs, however, would seem to make this possibility remote. Since the ORNL values were also checked by direct recalculation, it is also possible that both sets of sensitivity coefficients are correct to within the approximation of their associated methodology. Preliminary results from SRL for sensitivities of the individual resonances show 20-40% differences (from Table 12) for some of the significant sensitivity coefficients. Both the SRL sensitivity coefficients and the ORNL sets have been used successfully to predict changes from a base case; again this seems to imply both sets of coefficients may be valid when used with the associated analysis technique. These differences are not yet understood (and may, in fact, be methods dependent), but have no significant impact on the results of subsequent sections in which these coefficients are used to reconcile differences between integral experiments, differential measurements, and calculated performance.

X. ^{238}U ALTERNATIVE DATA SETS

It was shown in the preceding section that the performance parameters, and particularly $^{28}\rho$, are sensitive functions of the values of the partial widths of the first few levels in ^{238}U. This sensitivity decreases rapidly with increasing resonance energy as might be expected because of the E^{-1} gross structure of the neutron energy spectrum.

A number of new high precision microscopic measurements were completed since the last ENDF/B evaluation of the low energy cross sections of ^{238}U; hence it seems appropriate to re-examine the ENDF/B description of those cross sections.

A careful examination of the presently available experimental data suggests values for the partial widths of the first three s-wave levels of ^{238}U somewhat different than those of ENDF/B-IV. Furthermore, in order to properly compute the results of neutron transmission measurements through thick ^{238}U samples a better cross section description is needed: specifically, a modification of the smooth background (file 3 of ENDF/B) and the use of a multilevel formula are required.

In Appendix A the presently available differential data are discussed in some detail and a description of the low energy cross sections of ^{238}U is recommended. This description was implemented by a series of modifications of the ENDF/B-IV parameters and procedures.

In order to compare the relative importance of the proposed modification of ENDF/B-IV, those modifications have been arranged in four successive steps defining four "alternative data sets." Those alternative sets are defined in Tables 14 and 15. The calculation of the TRX-2 performance parameters with those four sets will be the subject of the next section.

Before concluding this section two comments must be made: (1) Set D of Table 14 is not an adjusted set of modifications suggested by some integral experiment, but it results from an evaluation of the presently available differential data only. On the basis of these differential data the modifications defined by Set D are thought to give a much better description of the ^{238}U cross section than ENDF/B-IV. (2) Sets A, B, and C are not alternative sets of recommended parameters but are successive steps in going from ENDF/B-IV to

Table 14. Alternative ^{238}U Data Sets

Set A: The value of the capture width, Γ_γ, for the s-wave levels at 6.67 eV, 20.9 eV, and 36.8 eV were changed from their ENDF/B-IV values of 25.6 mV, 26.8 mV, and 26.0 mV respectively to 23.0 mV.

Set B: In addition to the modifications made for SET A, the value of the neutron width, Γ_n, for the s-wave levels at 20.9 eV and 36.8 eV were changed from their ENDF/B-IV values of 8.8 mV and 33.1 mV to 10 mV and 33.5 mV, respectively.

Set C: In addition to the modifications made for SET B the capture and scattering smooth files were changed from their ENDF/B-IV values in the range 0.625 eV to 2 keV to the values given in Table 15. Above 2 keV the ENDF/B-IV values were used.

Set D: This set is identical to SET C, including the smooth file, except that the resolved levels are treated with the multilevel Breit-Wigner formalism rather than the single level formalism.

Table 15. File 3 for Proposed Modification to ENDF/B-IV*

Energy (eV)	(n,γ) (barn)	Elastic (barn)
6.0000E-01	6.1238E-01	8.8003E 00
7.0000E-01	5.7773E-01	8.7841E 00
8.0000E-01	5.5098E-01	8.7675E 00
9.0000E-01	5.2992E-01	8.7506E 00
1.0000E 00	5.1313E-01	8.7334E 00
1.0000E 00	5.3565E-02	2.5685E 00
1.0000E 01	1.2422E-02	2.4279E 00
5.0000E 01	2.8458E-03	2.0534E 00
1.0000E 02	1.2814E-03	1.7809E 00
2.0000E 02	5.2214E-04	1.4523E 00
3.0000E 02	2.9954E-04	1.2420E 00
4.0000E 02	2.0112E-04	1.0865E 00
5.0000E 02	1.4797E-04	9.6215E-01
6.0000E 02	1.1560E-04	8.5777E-01
7.0000E 02	9.4235E-05	7.6712E-01
8.0000E 02	7.9297E-05	6.8642E-01
9.0000E 02	6.8397E-05	6.1320E-01
1.0000E 03	6.0180E-05	5.4573E-01
1.2500E 03	4.6697E-05	3.9493E-01
1.5000E 03	3.8888E-05	2.6066E-01
1.7500E 03	3.4151E-05	1.3570E-01
2.0000E 03	3.1337E-05	1.5148E-02

*Five significant figures are listed corresponding to ENDF/B format

Interpolation: log-log below 1 eV
linear-linear above 1 eV.

Set D. In particular, Set A is not recommended and will not yield a reasonable value for the infinite dilute capture resonance integral.

XI. RESULTS OF CALCULATIONS WITH THE ^{238}U ALTERNATIVE DATA SETS

The values of the performance parameters computed with ENDF/B-IV and with the four alternative data sets of Table 14 are compared in Table 16. The measured value of the performance parameters are also listed in the table.

Table 16. Alternative Data Set Results

Parameter	Experimental[a]	ENDF/B-IV	Set A	Set B	Set C	Set D
k_{eff}	1.0000	1.0012	1.0053	1.0041	1.0040	1.0046
$^{28}\rho$	0.837 ± 0.016	0.867	0.836	0.846	0.847	0.843
$^{25}\delta$	0.0614 ± 0.0008	0.0602	0.0602	0.0602	0.0602	0.0602
$^{28}\delta$	0.693 ± 0.0035	0.0698	0.0695	0.0696	0.0696	0.0695
CR	0.647 ± 0.006	0.645	0.634	0.638	0.638	0.637

[a]See ref. 31.

The proposed modification to the ^{238}U cross sections have an appreciable effect on the parameters k_{eff}, $^{28}\rho$, and CR but very little effect on $^{28}\delta$ and no significant effect on $^{25}\delta$. This is not surprising, since the capture cross section of ^{238}U affects directly k_{eff}, $^{28}\rho$, and CR but can affect the fission ratios only indirectly, though changes in the neutron energy spectrum.

The recommended ^{238}U cross section (Set D) yields a calculated value for $^{28}\rho$ in excellent agreement with the measured value. There is no significant difference between the values obtained for $^{28}\rho$ with Set B and Set D; this suggests that the refinements in cross section formalism which are required to properly account for differential transmission measurements through thick ^{238}U samples, are not required to compute $^{28}\rho$ for the TRX-2 lattice. Only for lattices with more self shielding than TRX-2 is the difference between Set B and Set D expected to be significant.

As shown in Table 16 there is a significant, 2%, discrepancy between the calculated and measured values of $^{25}\delta$. The calculation of this parameter is not significantly influenced by the proposed change in the ^{238}U cross sections, hence the discrepancy is probably associated with an error in some other cross section or in the calculational model.

The calculations of the performance parameters with the alternative data Sets A and B of Table 14 can be used as a check of the validity of the sensitivity coefficients $[(dR/R)(d\Gamma_i/\Gamma_i)]$ listed in Table 12. Since the fractional changes in the resonance widths in going from ENDF/B-IV to the alternative Sets A or B, are small, compared to unity, the performance parameters for the alternative data sets R can be obtained from the ENDF/B-IV values R by first order perturbation theory:

$$R' = R \prod_{i=1}^{n} \left[1 - \frac{dR/R}{d\Gamma_i/\Gamma_i} \left(\frac{\delta\Gamma_i}{\Gamma_i} \right) \right] \qquad (15)$$

In Table 17 the values of the performance parameters, computed with the first order perturbation approach defined by Eq. (15) are compared with the values compiled directly. The agreement between the two sets of calculation is considered reasonably good ($\leq$1% in predictive ability).

Table 17. Alternative Sets A and B: Comparison of the Direct Calculation to that Based on First Order Perturbation Theory (Inferred)

	Set A		Set B	
Parameter	Direct	Inferred	Direct	Inferred
k_{eff}	1.0053	1.0049	1.0042	1.0033
$^{28}\rho$	0.836	0.841	0.846	0.852
$^{25}\delta$	0.0602	0.0602	0.0602	0.0602
$^{28}\delta$	0.0695	0.0695	0.0695	0.0697
CR	0.634	0.635	0.638	0.639

XII. EVALUATED COVARIANCE FILES

Cross section error files (covariance matrices) were derived for the ^{235}U and ^{238}U cross sections. Those covariance matrices were folded with the sentivity profiles to obtain uncertainty estimates on the calculated performance parameters. The result of such calculations will be discussed in later sections, the error files are described in this section.

The error files for the ^{235}U cross sections were obtained by R. W. Peelle[36] and are discussed in detail in Appendix B. The covariance matrices were defined with respect to the pointwise cross sections by using a representation outlined by F. G. Perey.[37] In Tables 18 and 19 the group-to-group relative covariance of the cross section is given in matrix form. The element C_{ik} represents the value

$$C_{ik} = \left\langle \frac{(\sigma_i - \bar{\sigma}_i)(\sigma_k - \bar{\sigma}_k)}{\bar{\sigma}_i \, \bar{\sigma}_k} \right\rangle$$

where $\bar{\sigma}_i$ and $\bar{\sigma}_k$ are the evaluated cross sections in group i and group k respectively, and the average is over the probability distribution of the true values of σ_i and σ_k. The group's lower boundaries are indicated in the first column of the tables. The matrix is symmetric and only the lower half is tabulated. (Note that the relative variances have been multiplied by 10^4 for simplicity.) The correlation matrix can be obtained from the covariance matrix by dividing each element C_{ik} by $(C_{ii}C_{kk})^{1/2}$. Examples of correlation matrices are given in Figs. 32 and 33. In those figures the standard deviation, $C_{ii}^{1/2}$ are also given for each group.

The generation of the error files for the ^{238}U capture cross sections is discussed in Appendix C. The covariance matrix was defined with respect to the resonance parameters of the first few levels of ^{238}U and the parameters describing the background cross sections (file 3) for the recommended set of alternative parameters (set D of Table 14). We believe this set to represent the data more accurately than ENDF/B-IV, and our recommended set allows for construction of a symmetric (non-biased) covariance distribution.

The covariance matrix is shown in Table 20. The values and errors of the six first s-wave levels and of the p-wave level at 10.22 eV are given in eV.

Table 18. Relative covariance matrix for the $^{235}U(n,f)$ reaction. The lower portion of the symmetric matrix is tabulated after multiplying each element by 10^4.

Elow (eV)	Relvar × 10^4																							
1. E - 5	0.1																							
0.625	0.1	2																						
1.	0.1	2	5																					
1.8	0.1	2	4	5																				
5.0	0.1	2	4	4	7																			
10.	0.1	2	4	4	6	7																		
20.	0.1	2	4	4	6	6	8																	
40.	0.1	2	4	4	6	6	7	10																
80.	0.1	2	4	4	6	6	7	9	10															
200.	0.1	2	4	4	6	6	7	9	9	10														
400.	0.1	2	4	4	6	6	7	9	9	9	10													
1 E + 3	0.1	2	4	4	6	6	7	9	9	9	9	34												
3 E + 3	0.1	2	4	4	6	6	7	9	9	9	9	27.6	25											
10 E + 3	0.1	2	4	4	6	6	7	9	9	9	9	18	17	13.6										
30 E + 3	0.5	1	2	2	3	3	3.5	4.5	4.5	4.5	4.5	12	12	7.7	8.8									
0.1 E + 6	0	0	0	0	0	0	0	0	0	0	0	0	0	4	4	16								
0.15 E + 6	0	0	0	0	0	0	0	0	0	0	0	0	0	4	4	7.2	9							
0.2 E + 6	0	0	0	0	0	0	0	0	0	0	0	0	0	4	4	3.	5.4	9						
0.4 E + 6	0	0	0	0	0	0	0	0	0	0	0	0	0	0	0	4.9	5.25	6.3	12.25					
1 E + 6	0	0	0	0	0	0	0	0	0	0	0	0	0	0	0	0.7	0.75	1.1	2.6	6.25				
2 E + 6	0	0	0	0	0	0	0	0	0	0	0	0	0	0	0	0.6	0.9	1.4	2.6	3.	9			
4 E + 6	0	0	0	0	0	0	0	0	0	0	0	0	0	0	0	0	0	0	0.61	2.6	4.2	12.25		
10 E + 6	0	0	0	0	0	0	0	0	0	0	0	0	0	0	0	0	0	0	0	0.5	3.0	6.3	16	
15 E + 6	0	0	0	0	0	0	0	0	0	0	0	0	0	0	0	0	0	0	0	0.45	3.6	8.4	19.2	36
20 E + 6																								

Table 19. Relative Covariance matrix for the $^{235}U(n,\gamma)$ reaction. The lower portion of the symmetric matrix is tabulated after multiplying each element by 10^4.

Elow (eV)	Relvar × 10^4																		
1. E - 5	0.77																		
0.625	.7	169																	
1.0	.7	144	169																
1.8	.7	144	144	169															
5.0	.7	144	144	144	169														
10.	.7	144	144	144	144	169													
20.	.7	144	144	144	144	144	169												
40.	.7	144	144	144	144	144	144	169											
80.	.7	25	25	25	25	25	25	25	100										
200.	.7	25	25	25	25	25	25	25	50	64									
400.	.7	25	25	25	25	25	25	25	50	50	64								
1. E + 3	.7	25	25	25	25	25	25	25	50	50	50	64							
3. E + 3	.7	25	25	25	25	25	25	25	50	50	50	50	64						
10. E + 3	.7	25	25	25	25	25	25	25	50	50	50	50	50	100					
30. E + 3	.7	25	25	25	25	25	25	25	50	50	50	50	50	50	100				
0.1 E + 6	.7	25	25	25	25	25	25	25	50	50	50	50	50	50	50	225			
0.2 E + 6	.7	25	25	25	25	25	25	25	50	50	50	50	50	50	50	190	625		
0.5 E + 6	.7	25	25	25	25	25	25	25	50	50	50	50	50	50	50	180	500	1600	
1. E + 6	.7	25	25	25	25	25	25	25	50	50	50	50	50	50	50	180	450	1200	3600
4. E + 6	.7	25	25	25	25	25	25	25	50	50	50	50	50	50	50	120	400	960	2400
20. E + 6	.7	25	25	25	25	25	25	25	50	50	50	50							

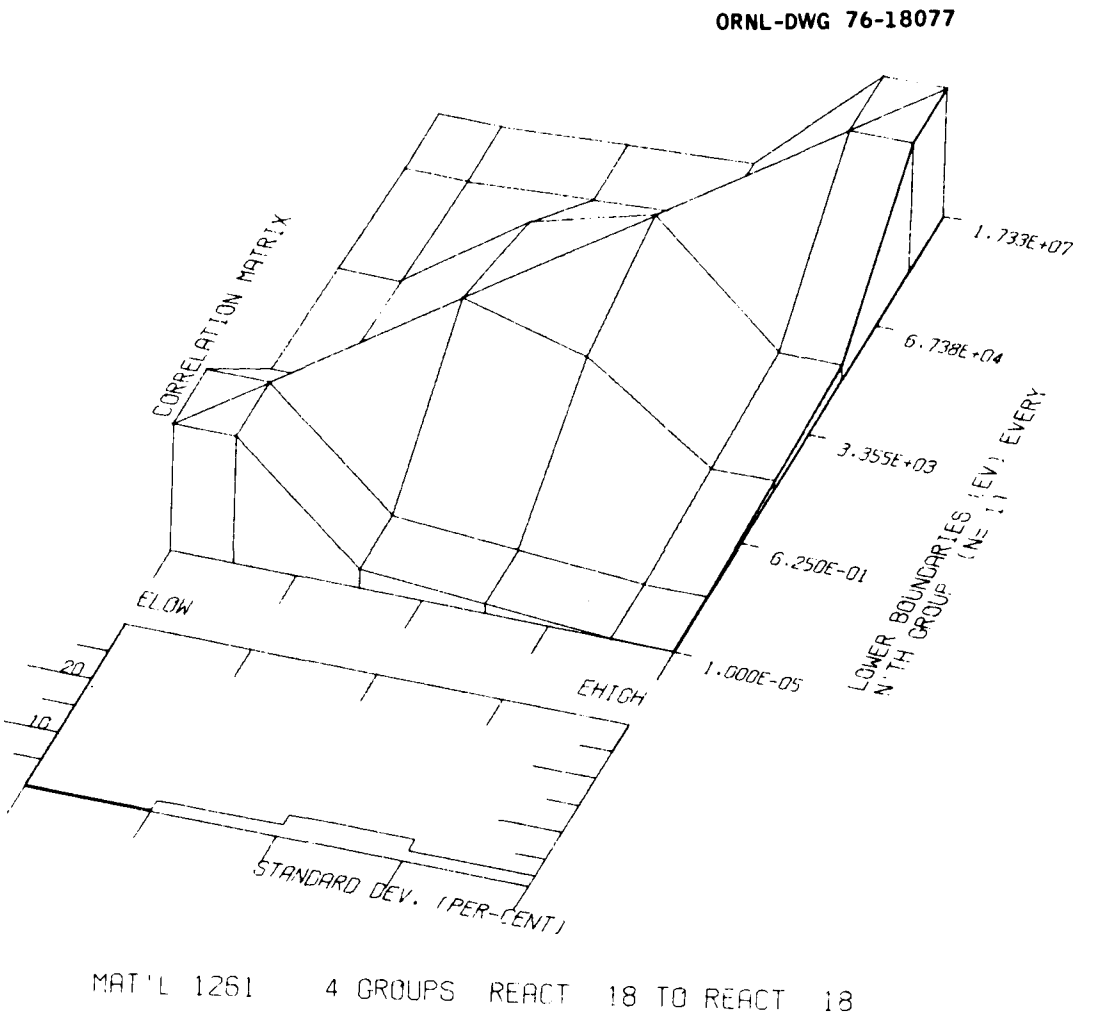

Fig. 32. The Correlation Matrix for the $^{235}U(n,f)$ Cross Section.

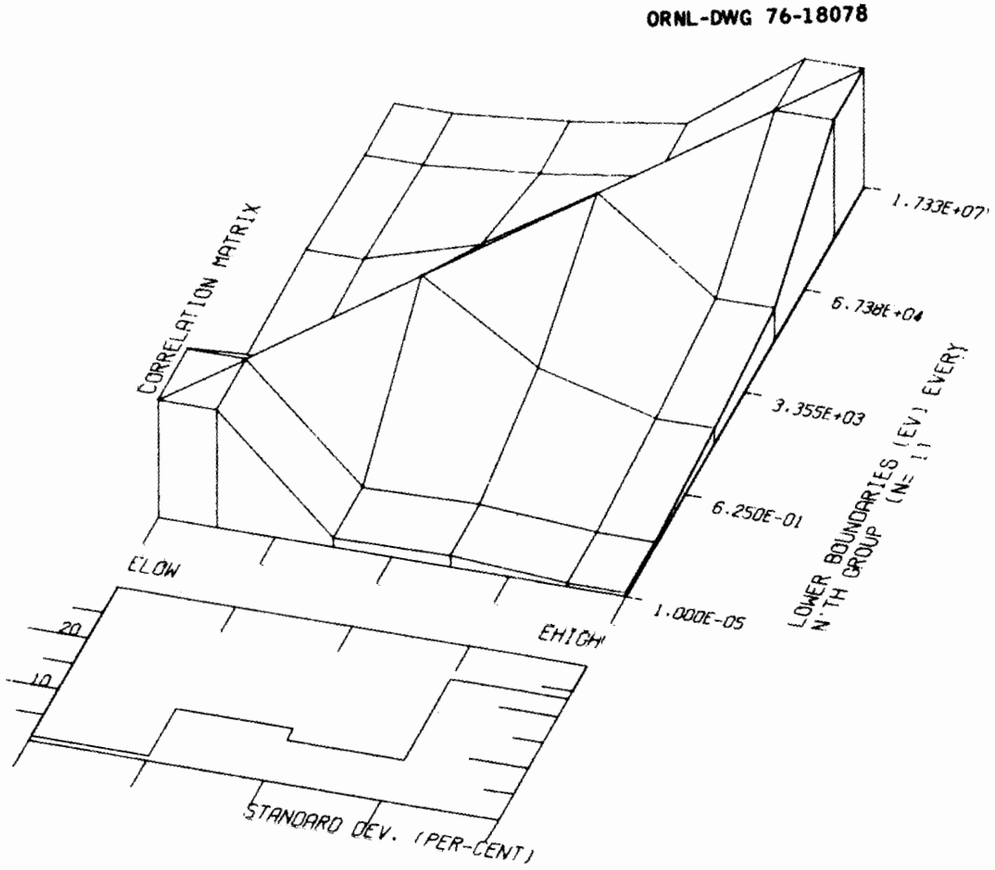

MAT'L 1261 4 GROUPS REACT 102 TO REACT 102

Fig. 33. The Correlation Matrix for the $^{235}U(n,\gamma)$ Cross Section.

Table 20. Covariance Matrix for ^{238}U Parameters

		Value	Error	Variance	Covariance
1	E_o	6.67	0.01	10^{-4}	
2	Γ_n	0.0015	2×10^{-5}	4×10^{-10}	
3	Γ_γ	0.023	0.0012	1.44×10^{-6}	$Cov(\Gamma_n\Gamma_\gamma) = -1.92*10^{-8}$
4	E_o	20.9	0.1	10^{-2}	
5	Γ_n	0.01	5×10^{-4}	25×10^{-8}	
6	Γ_γ	0.023	0.001	10^{-6}	$Cov(\Gamma_n\Gamma_\gamma) = -0.25*10^{-6}$
7	E_o	36.8	0.07	0.0049	
8	Γ_n	0.0335	0.001	10^{-6}	
9	Γ_γ	0.023	0.001	10^{-6}	
10	E_o	66.15	0.15	0.0225	All other covariances are 0
11	Γ_n	0.0253	0.001	10^{-6}	
12	Γ_γ	0.0235	0.001	10^{-6}	
13	E_o	80.74	0.07	0.0049	
14	Γ_n	0.002	0.0002	$4*10^{-8}$	
15	Γ_γ	0.0235	0.001	10^{-6}	
16	E_o	102.5	0.09	0.0081	
17	Γ_n	0.071	0.003	9×10^{-6}	
18	Γ_γ	0.026	0.003	9×10^{-6}	
19	E_o	10.22	0.03	$9X10^{-4}$	
20	Γ_n	1.55×10^{-6}	1.5×10^{-7}	2.25×10^{-14}	
21	Γ_γ	0.0235	0.002	4×10^{-6}	
22	b_n		0.2	4×10^{-2}	Correlated from 0 to 2 keV
23	b_γ		0.02	4×10^{-4}	
24	a	0.9184	0.025	6.25×10^{-4}	

The variances (square errors) are in eV^2. The parameters b_n and b_γ are smooth backgrounds in the elastic and capture cross sections respectively. Those backgrounds are given in Table 15. The errors on b_n and b_γ are in absolute value, in barn, the variances are in $barn^2$. Those errors are fully correlated between 0.6 eV and 2 keV (i.e., the capture cross section background may be raised or lowered by 0.02 barn over the entire range). The error on the spin up effective scattering radius â is given in 10^{-12} cm units. All the covariances are considered negligible except those between Γ_n and Γ_γ for the first two s-wave levels that are given in eV^2.

XIII. MULTIGROUP COVARIANCE FILES FOR ^{235}U

The covariance files for ^{235}U fission and ^{235}U capture were processed from the pointwise files described in the previous section, using the PUFF[38] covariance file processing code. (Since the primary uncertainties for ^{238}U were assessed directly in terms of resonance parameters, multigroup averaging of covariance files was not necessary in this case.) The neutron spectrum averaged over the fuel pin was used as a weight function for the multigroup processing. Uncertainty analysis was performed in the four group structure commonly employed by CSEWG data testers in analysis of thermal benchmarks. The 131 group sensitivity profiles were reduced four groups with flat weighting.

Figures 32 and 33 illustrate the correlation matrices for ^{235}U fission and capture, respectively, in the four group processed form. The four group energy boundaries are given in Table 21.

As would be expected for such a broad mesh these matrices are strongly diagonal, i.e., the magnitude of the matrix elements tend to be small for groups G and G' which are widely displaced in energy. Note that these matrices are actually evaluated for infinitely dilute cross sections, the analysis approximates the covariance file for the self-shielded cross section as being the same as for the infinitely dilute case.

Table 21. Four Group Energy Structure Used for Uncertainty Analysis

Group	Upper Energy (eV)
1	1.0000+7
2	6.7380+4
3	3.3546+3
4	6.2500-1
	1.0000-5

XIV. UNCERTAINTIES DUE TO NUCLEAR DATA

The calculated uncertainties for the TRX-2 lattice due to uncertainties in nuclear data are given in Table 22. These values reflect the uncertainties in the ^{235}U fission and capture cross sections over the entire energy range, the ^{238}U resolved resonance parameters for the lowest four levels, the thermal capture cross section of hydrogen, and the thermal capture cross section of ^{238}U. Uncertainties in the ^{238}U fission cross section were not considered in this analysis; this is an important consideration for $^{28}\delta$.

The uncertainties were obtained by folding the sensitivity profiles with the covariance matrices described in earlier sections. Standard deviations for thermal hydrogen capture and thermal ^{238}U capture were estimated to be 0.9% and 1.0% respectively. The covariance matrices for the ^{238}U parameters were developed with reference to alternative SET D; ENDF/B-IV was taken as the mean for the remaining reaction types and nuclides.

The magnitude of the uncertainties due solely to nuclear data are indeed small. As can be seen from Table 22 they are comparable to (and generally less than) estimated uncertainties in the integral measurements and are small with reference to calculational differences (methods approximations) between various reported results from different laboratories based upon the same data set. Only one example of differences due to methods is given in Table 22, but the reader can easily refer to Table 1 for additional justifications that methods differences can be larger than those associated with uncertainties in nuclear data.

Table 22. Uncertainties in TRX-2 Performance Parameters Due Solely to Nuclear Data

Parameter	Nominal Values ORNL	Nominal Values BNL	Experimental	1σ Uncertainty (%) Exp.	1σ Uncertainty (%) Nuclear Data	Methods[a] Differences (%)
k	1.0012	0.9921	1.0000		0.4	0.9
$^{28}\rho$	0.867	0.846	0.837	1.0	0.9	2.4
$^{25}\delta$	0.0602	0.0611	0.0614	1.3	2.0	1.5
$^{28}\delta$	0.0698	0.0663	0.0693	5.1	0.4	4.6
CR	0.637	0.640	0.647	0.9	0.8	0.9

[a](ORNL-BNL/ORNL) x 100.

XV. CONSISTENCY BETWEEN DIFFERENTIAL DATA AND TRX-2 PERFORMANCE PARAMETERS

We have shown in the preceeding section that the uncertainties in the calculated values of the TRX-2 performance parameters, due to uncertainties in nuclear data, were small compared to differences between independent calculations using the same data base. If we ignore those unknown "methods errors" we can adjust the microscopic data to minimize the weighted differences between our calculated value and the measured value of the performance parameters.

Such an adjustment was performed simultaneously on the five parameters k_{eff}, $^{28}\rho$, $^{25}\delta$, $^{28}\delta$, and CR and the infinitely dilute ^{238}U capture resonance integral RI.

The χ^2 per degree of freedom of the adjustment was 0.6, verifying the internal consistency between the differential data and the measured performance parameters.

The adjustment to the differential data is illustrated in Table 23. This adjustment is insignificant and approaches one standard deviation only for the

Table 23. Adjusted Multigroup and Resonance Parameters Based on Differential and TRX-2 Integral Measurements

Energy Group (eV)	Reaction	Old Value[a]	New Value	% Change/ Old Std. Dev.
1.0+07 - 6.7+04	$^{235}U(n,f)$	1.264±0.02	1.266±0.02	0.081
6.7+04 - 3.3+03	$^{235}U(n,f)$	2.671±0.10	2.710±0.08	0.371
3.3+03 - 6.25-01	$^{235}U(n,f)$	28.93±0.61	29.21±0.35	0.454
6.25-01 - 1.0-05	$^{235}U(n,f)$	230.4±1.15	229.4±0.92	-0.889
1.0+07 - 6.7+04	$^{235}U(n,\gamma)$	0.1408±0.03	0.1426±0.03	0.056
6.7+04 - 3.3+03	$^{235}U(n,\gamma)$	1.006±0.08	1.016±0.08	0.131
3.3+03 - 6.25-01	$^{235}U(n,\gamma)$	13.03±1.32	13.39±1.27	0.274
6.25-01 - 1.0-05	$^{235}U(n,\gamma)$	42.39±0.38	42.48±0.38	0.235
66.15	$^{238}U\ \Gamma_\gamma$	0.02350±0.001	0.02351±0.001	0.006
36.8	$^{238}U\ \Gamma_\gamma$	0.02300±0.001	0.02299±0.001	-0.006
20.9	$^{238}U\ \Gamma_\gamma$	0.02300±0.001	0.02309±0.001	0.087
6.67	$^{238}U\ \Gamma_\gamma$	0.02300±0.001	0.02338±0.001	0.317
66.15	$^{238}U\ \Gamma_n$	0.025300±0.001	0.02531±0.001	0.007
36.8	$^{238}U\ \Gamma_n$	0.03350±0.001	0.03351±0.001	0.006
20.9	$^{238}U\ \Gamma_n$	0.01000±0.0005	0.00995±0.0005	-0.101
6.67	$^{238}U\ \Gamma_n$	0.00150±0.00002	0.00149±0.00002	-0.275
6.25-01 - 1.0-05	$H(n,\gamma)$	0.25600±0.002	0.25670±0.002	0.320
6.25-01 - 1.0-05	$^{238}U(n,\gamma)$	1.925±0.02	1.944±0.02	0.935

[a]All group cross sections are in b, all widths are in eV.

thermal group cross sections for capture in ^{238}U and fission in ^{235}U. Those thermal cross sections were changed so as to reduce k_{eff} and increase CR. (It is interesting to note that the 0.4% reduction in the ^{235}U thermal fission cross section is consistent with a proposed 0.3% reduction for ENDF/B-V.[39])

In Table 24 the values of the integral parameters computed with the recommended and with the adjusted microscopic data are compared with the measured values. The integral parameters computed with the adjusted data have smaller errors (due to uncertainties in the multigroup cross sections) particularly for k_{eff}.

The results of Tables 23 and 24 show that small adjustments to the basic nuclear data will make our calculated values of the performance parameters agree well with the measured values. Any more general interpretation of the results of the adjustment must await a resolution of the "methods error" discussed previously.

Table 24. TRX-2 Performance Parameter Calculations

Parameter	Experimental	Recommended Data Set	Adjusted Data Set	Sample Methods Difference
k_{eff}	1.0000[b]	1.0046±0.0035	1.0003±0.0009	±0.009
$^{28}\rho$	0.837±0.016	0.843±0.007	0.845±0.006	±0.02
$^{25}\delta$	0.0614±0.0008	0.0602±0.0012	0.0610±0.0006	±0.0009
$^{28}\delta$	0.0693±0.0035	0.0695±0.0003	0.0698±0.0001	±0.003
CR	0.647±0.006	0.637±0.005	0.643±0.003	±0.006
RI[c]	275±5	278±3	277±2	

[a] $\frac{ORNL-BNL}{ORNL}$, see previous section.
[b] A 0.001 uncertainty was arbitrarily assigned to k_{eff}, because the magnitude of this uncertainty is required in the course of the adjustment.
[c] RI = ^{238}U infinitely dilute capture resonance integral.

XVI. DISCUSSION AND CONCLUSIONS

Sensitivity profiles were obtained for the five TRX-2 performance parameters with respect to the principal cross sections (or resonance parameters) of all the components of the reactor lattice. These sensitivity profiles are very useful in identifying those cross sections to which the performance parameters are most sensitive and in predicting how any change in the data base would affect the calculation of a given performance parameter.

Analysis of these profiles reveals the expected high sensitivity of all the performance parameters to ^{235}U fission and ^{238}U capture. Perhaps a more interesting feature that is immediately obvious is the extremely high sensitivity (near 1) of the lattice parameter to the hydrogen scattering cross section and the relatively high sensitivity to the hydrogen capture cross sections. Almost all of the sensitivity associated with the latter (> 90%) is in the thermal energy range. The high sensitivity of the scattering cross section is attributed to the importance of the thermalization process and resonance escape. The thermal capture cross section has a relatively high sensitivity for many parameters because it competes directly with the ^{235}U fission cross section for neutrons. A complete set of energy dependent sensitivity profiles can be found in ref. 34.

A review of the available differential cross section measurements led to a representation of the ^{238}U cross sections which differs from the ENDF/B-IV evaluation and one which, we believe, is more consistent with available differential measurements. This data set has Γ_γ for the s-wave levels of the 6.67 eV, 20.9 eV, and 36.8 eV constant at 23.0 mV, Γ_n for the 20.9 eV and 36.8 eV resonances at 10 and 33.5 mV, respectively, a file 3 smooth background to account for resonances not explicitly included in the resolved range and a resonance parameter representation intended for use in the multi-level Breit-Wigner description.

Covariance files were evaluated for those cross sections to which the performance parameters are most sensitive. The recommended ^{238}U modification to ENDF/B-IV made possible the development of a covariance file intended to characterize a normal distribution with the SETD values as the expectation values. The uncertainties in the calculated values of the performance parameters due to the estimated uncertainties in the nuclear data were obtained by folding the error file with the sensitivity profiles. These uncertainties in the

calculated values of the performance parameters were found to be comparable to the uncertainties in the measured values of the performance parameters and comparable to the difference between independent calculations of the performance parameter using the same data base. The estimated (1σ) standard deviations for computed k, $^{28}\rho$, $^{25}\delta$, $^{28}\delta$, and CR due to uncertainties in nuclear data were 0.4, 0.9, 2.0, 0.4, and 0.8% respectively. Uncertainties in the ^{238}U fission cross section were not considered when determining these values.

The TRX-2 performance parameters were computed with the ENDF/B-IV cross section and with our recommended ^{238}U cross section. The values computed with our recommended cross sections are consistent with the measured integral data, well within the uncertainties associated with the differential and integral data. An adjustment procedure applied simultaneously to the five integral parameters for TRX-2 and the infinitely dilute ^{238}U capture resonance integral, which minimized the weighted difference between the measured and computed values of the performance parameters, resulted in changes to the recommended data which were all smaller than one standard deviation and a χ^2 per degree of freedom of 0.6. It is interesting to note that the 0.4% reduction in the ^{235}U thermal fission cross section is consistent with the proposed 0.3% reduction for ENDF/B-V.[39]

There does not appear to be any significant difference (less than 0.5% for most of the performance parameters) between the results calculated using the multilevel formalism and those calculated using the single level Breit-Wigner formalism, thus indicating that multilevel treatment is not necessary for TRX-2 calculations. It should be noted that although the differences in the performance parameters were small, differences in the individual multigroup scattering cross section were significant.

We have already indicated in the introduction that there are appreciable differences in the value of a given performance parameter obtained by independent calculations, using the same data base. For TRX-2, reported differences have been as large as 16% for $^{25}\delta$. Such differences are larger than either the uncertainties in the measured value of the performance parameters, or our estimate of the errors in the calculation due to nuclear data uncertainties. These differences are thought to arise from various geometric models for the actual experiment (a hexagonal array of pins in a driver assembly of different pitch/diameter), different approaches to the estimation of the energy dependent

leakage (essential to the proper calculation of the eigenvalue) and a myriad of approximations associated with cross section processing and neutron transport (e.g., group structure, spatial mesh, etc.). It was beyond the scope of this six month study to quantify the methods approximations associated with the different calculational schemes. However, it is absolutely essential that benchmark calculations be established and numerical approximations associated with less rigorous schemes be meaningful. This was also the conclusion reached by McCrosson[40] in his summary of ENDF/B-IV thermal data testing.

REFERENCES

1. J. R. Askew, "The Current U.K. Position on Uranium Resonance Capture," Seminar on ^{238}U Resonance Capture, BNL-NCS-50451, p. 45, Brookhaven National Laboratory (March 1975).

2. J. Hardy, "Monte Carlo Analysis of TRX Lattices with ENDF/B Version 3 Data," Seminar on ^{238}U Resonance Capture, BNL-NCS-50451, p. 18, Brookhaven National Laboratory (March 1975).

3. "Benchmark Testing of ENDF/B-IV," ENDF-230, Vol. 1, Edited by E. M. Bohn, R. Maerker, B. A. Magurno, F. J. McCrosson, and R. E. Schenter (March 1976).

4. Seminar on ^{238}U Resonance Capture, Edited by S. Pearlstein, BNL-NCS-50451, Brookhaven National Laboratory (March 1975).

5. M. R. Bhat, "A Discussion of U-238 Resolved Resonance Parameters and Their Influence on Capture Cross Sections," Seminar on ^{238}U Resonance Capture, BNL-NCS-50451, Brookhaven National Laboratory (March 1975).

6. J. Hardy, Jr., Minutes of the Meeting of the Cross Section Evaluation Working Group, Edited by S. Pearlstein (May 11, 1976).

7. W. Rothenstein, "Thermal-Reactor Lattice Analysis Using ENDF/B-IV Data with Monte Carlo Resonance Reaction Rates," Nucl. Sci. Eng., 59, 337 (April 1976).

8. D. K. Olsen et al., "Precise Measurement, 0.52 to 4000 eV, and Analysis, 0.52 to 1088 eV, of Neutron Transmissions Through Seven Samples of ^{238}U," Trans. Am. Nucl. Soc., 23 (June 1976); also report accepted for publication in Nucl. Sci. Eng. (April 1977).

9. M. I. Liou and R. E. Chrien, "Low-Energy Neutron Resonance Parameters of U-238," BAPS Series II, Vol. 21, No. 1 (1976) and subsequent private communication of R. E. Chrien (May 1976).

10. G. deSaussure et al., "Note on the ENDF/B-IV Representation of the ^{238}U Total Cross Section in the Resolved Resonance Energy Range," Nucl. Sci. Eng., 61, 496 (1976).

11. E. T. Tomlinson and C. R. Weisbin, Letter to the Cross Section Evaluation Working Group Sensitivity Analysis Subcommittee for ENDF/B-V Thermal Data (February 3, 1976).

12. C. R. Weisbin, P. D. Soran, R. E. MacFarlane, D. R. Harris, R. J. LaBauve, J. S. Hendricks, J. E. White, and R. B. Kidman, "MINX: A Multigroup Interpretation of Nuclear X-Sections from ENDF/B," LA-6488-MS (ENDF-237) (September 1976).

13. N. C. Paik et al., "Physics Evaluations and Applications Quarterly Progress Report for Period ENding July 31, 1974, WARD-XS-3042-7 (July 1974).

14. N. M. Greene, J. L. Lucius, L. M. Petrie, W. E. Ford, III, J. E. White, and R. Q. Wright, "AMPX: A Modular Code System for Generating Coupled Multigroup Neutron-Gamma Libraries from ENDF/B," ORNL-TM-3706 (March 1976).

15. O. Ozer, Electric Power Research Institute, personal communication (May 1976).

16. J. E. White, R. Q. Wright, L. R. Williams, and C. R. Weisbin, "Data Testing of the 126/36 Neutron-Gamma ENDF/B-IV Coupled Library for LMFBR Core and Shield Analysis," Trans. Am. Nucl. Soc., 23, 507 (June 1976).

17. R. W. Roussin, C. R. Weisbin, J. E. White, N. M. Greene, R. Q. Wright, and J. B. Wright, "Progress on the Validation of the CTR Multigroup Data Package," Trans. Am. Nucl. Soc., 23, 14 (June 1976).

18. R. W. Roussin, C. R. Weisbin, J. E. White, N. M. Greene, R. Q. Wright, and J. B. Wright, "The CTR Processed Multigroup Cross Section Library for Neutronics Studies," ORNL/RSIC-37, Oak Ridge National Laboratory (to be published).

19. M. Raymund, "TEDIUM: Idealized Neutron Data for Testing Library Processing Codes," National Topical Meeting on New Developments in Reactor Physics and Shielding, p. 1048 (September 1972).

20. O. Ozer, "RESEND - A Program to Process ENDF/B Materials with Resonance Files into Point-Wise Form," BNL-17134, Brookhaven National Laboratory (1973).

21. D. E. Cullen, Lawrence Livermore Laboratory, personal communication (March 1976).

22. H. C. Honeck, "THERMOS: A Thermalization Transport Theory Code for Reactor Lattice Calculations," BNL-5826, Brookhaven National Laboratory (September 1961).

23. R. E. MacFarlane and R. B. Kidman, "LINX and BINX: CCCC Utility Codes for the MINX Multigroup Processing Code," LA-6219-MS, Los Alsmos Scientific Laboratory (1976).

24. A. Sauer, "Approximate Escape Probabilities," Nucl. Sci. Eng., 16(3), 329 (July 1963).

25. W. W. Engle, Jr., "A Users Manual for ANISN, A One-Dimensional Discrete Ordinates Transport Code with Anisotropic Scattering," ORGDP-K-1693 (March 1967).

26. Cross Section Evaluation Working Group, "Benchmark Specifications," BNL-19302 (ENDF-202), Brookhaven National Laboratory (1974).

27. L. M. Petrie and N. F. Cross, "KENO-IV - An Improved Monte Carlo Criticality Program," Oak Ridge National Laboratory, ORNL-4938 (November 1975).

28. J. Hardy, Jr., Bettis Atomic Power Laboratory, personal communication (August 1976).

29. W. E. Ford, III, C. C. Webster, and R. M. Westfall, "A 218-Group Neutron Cross-Section Library in the AMPX Master Interface Format for Criticality Safety Studies," ORNL/CSD/TM-4 (July 1976).

30. L. S. Kothari and V. P. Duggal, "Scattering of Thermal Neutrons from Solids and Their Thermalization Near Equilibrium," Advances in Nuclear Science and Technology, Vol. 5, 185-207 (1969).

31. "Studies of Thermal Reactor Benchmark Data Interpretation: Experimental Corrections," EPRINP-209, Prepared for EPRI by the Department of Mechanical Engineering, Stanford University (October 1976).

32. J. Hardy, Jr., Bettis Atomic Power Laboratory, personal communication (November 1970).

33. C. R. Weisbin, J. H. Marable, J. L. Lucius, E. M. Oblow, F. R. Mynatt, R. W. Peelle, and F. G. Perey, "Application of FORSS Sensitivity and Uncertainty Methodology to Fast Reactor Benchmark Analysis," Oak Ridge National Laboratory, ORNL/TM-5563 (1976).

34. E. T. Tomlinson, J. L. Lucius, and C. R. Weisbin, "A Compendium of Energy Dependent Sensitivity Coefficients for the TRX-2 Thermal Lattice" (to be published).

35. D. R. Finch, "Sensitivity Coefficients to ^{238}U Resonance Parameters for the TRX-2 and MIT-1 Thermal Benchmark Lattices," memo to W. E. Graves (October 1976) to appear in J. Hardy, Jr., "Compilation of Sensitivity Coefficients for CSEWG Thermal Reactor Benchmarks" (November 1976).

36. R. W. Peelle, Oak Ridge National Laboratory, personal communication (September 1976).

37. F. G. Perey, Oak Ridge National Laboratory, personal communication (May 1976).

38. C. R. Weisbin, E. M. Oblow, J. Ching, J. E. White, R. Q. Wright, and J. D. Drischler, "Cross Section and Method Uncertainties: The Application of Sensitivity Analyses to Study Their Relationship in Radiation Transport Benchmark Problems," Oak Ridge National Laboratory, ORNL-TM-4847 (ENDF-218) (August 1975).

39. B. R. Leonard, Jr., D. A. Kottwitz, and J. K. Thompson, "Evaluation of the Neutron Cross Sections of ^{235}U in the Thermal Energy Region," EPRI-NP-167, Electric Power Research Institute (1976).

40. F. J. McCrosson, "ENDF/B-IV Thermal Data Testing: Methods, Results, and Recommendations," Trans. Am. Nucl. Soc., 23, 584 (June 1976).

APPENDIX A
LOW ENERGY CROSS SECTIONS OF ^{238}U

I. Introduction

The purpose of this note is to review the measurements and evaluations of the low-energy cross sections of ^{238}U, particularly the resonance parameters of the first six s-wave levels and of the p-wave level at 10.22 eV. The results of these measurements are compared with ENDF/B-IV MAT 1262[1] and a modification of ENDF/B-IV MAT 1262 is suggested.

This suggested modification is by no means an adjustment: it is not designed to bring differential data in agreement with a particular integral experiment, but rather it is compelled by the results of new measurements which were not available to the ENDF/B-IV evaluators, and by a new analysis of the results considered by the ENDF/B-IV evaluators.

The suggested modifications to ENDF/B-IV concern only the parameters of the first three s-wave levels and the low-energy "smooth cross section" (File 3). The ENDF/B-IV parameters for those three levels were taken unchanged from an evaluation made by T. A. Pitterle in March 1971 for ENDF/B-II.[2-4] The ENDF/B-IV low-energy smooth cross section was evaluated by F. J. McCrosson following procedures used by B. R. Leonard in the evaluation of ENDF/B-II.[1,5,6] The modifications suggested in this appendix could be implemented only above 0.625 eV, as indicated in Table 15, because the thermal group cross sections could not be modified. As can be seen in Table A7, the proposed modifications below 0.625 eV are indeed very small.

The proposed modification to ENDF/B-IV is not an adjustment, but it consists in a minimum of changes from ENDF/B-IV which were selected because they were thought to have an impact on thermal assemblies. In our opinion, there are many desirable improvements to ENDF/B-IV but most of those were not included in the proposed modification because they were not thought to be important for thermal assemblies.

There are very large discrepancies among the measurements of the capture widths, Γ_γ. A discussion of the problems of the interpretation of the measurements suggests a partial explanation for the discrepancies.

The measurements of Γ_γ reported since 1970 are very consistent, but, for the first three s-wave levels they lead to values significantly lower than those given in ENDF/B-IV. They suggest a reduction of the ENDF/B-IV values of at least 10%.

The measurements of the neutron widths, Γ_n, are far more consistent than those of Γ_γ. There is no significant external correlation between the values reported for Γ_γ and Γ_n, so that the two parameters can be evaluated independently. The most recent measurements of Γ_n suggest that the ENDF/B-IV values for the levels at 20.9 eV and 36.8 eV should be increased by about 10%.

The measured values of the thermal capture and total cross sections are used to estimate the contribution of the bound levels to the low-energy cross sections. This leads to the construction of "smooth cross sections" to be used in place of the ENDF/B-IV low-energy smooth cross sections (File 3).

In conclusion, we show that the proposed modification of ENDF/B-IV will not significantly affect the value of the computed infinite dilution resonance integral. It will prevent the scattering cross section from assuming negative values, as it does in ENDF/B-IV. We suggest a procedure to test the proposed modification on thermal lattice parameters.

II. Capture Widths

1. Existing Measurements and Their Discrepancies

In Table A.1 we list the results of most of the measurements[7-25] and of a few evaluations[1,26-27] of the capture widths, Γ_γ, of the six first s-wave levels and of the p-wave level at 10.22 eV. Those measurements were carried out over a period of more than 20 years.

There are very large discrepancies between some of the results listed in the table: for the important level at 6.67 eV there are at least five standard deviations between the value reported by Jackson and Lynn,[14] 27.2 $\pm$ 0.4 mV, and that recently obtained by Liou and Chrien,[23] 21.8 $\pm$ 1.0 mV. Similar discrepancies may be observed for the other levels: compare underlined values in each column.

There seems to be no significant systematic trend associated with a particular experiment: the values of Lynn and Pattenden[9] are higher than the average for the levels at 6.67 and 20.9 eV but the reverse is true for the levels at 66.15 and 102.5 eV. Inversely the data of Rahn et al.[22] are lower than average at 66.15 eV but higher than average at 102.5 eV.

The five most recent sets of measurements[21-25] give very consistent results, but for the first three levels the values from those experiments are significantly lower than those of ENDF/B-IV.

Recently Block et al.[57,58] at RPI have performed a series of self indication measurements on samples of ^{238}U of various thicknesses and temperatures. These data have not been considered in the present analysis because no satisfactory analysis of the measurements is available at present (November 1976). Preliminary analysis of some of the measurements were done by D. Finch[58] and by the RPI group.[57] The results of these two preliminary analysis are not fully consistent; however, both recommend a decrease of values of Γ_γ for the first three s-wave levels, from the ENDF/B-IV values. This recommendation is qualitatively consistent with the proposed modifications discussed here.

2. Experimental Problems

We do not propose to review here the many techniques used to obtain resonance parameters, and the problems of those techniques. Excellent articles have been published on this subject.[28,29] But it seems useful to list a few of the problems specific to the low-energy levels in ^{238}U, as this may help understanding the discrepancies among experiments.

A. Thin Sample Capture Area. A method often used to determine resonance parameters is to compare the thin sample capture area, proportional to $\Gamma_n\Gamma_\gamma/(\Gamma_n + \Gamma_\gamma)$, with the thin sample transmission area, proportional to Γ_n to obtain Γ_n and Γ_γ. However, for the ^{238}U level at 6.67 eV the neutron width, $\sim$2 mV, is less than 10% of the capture width so that the quantity $\Gamma_\gamma/(\Gamma_n + \Gamma_\gamma)$ is almost unity and the capture area is very insensitive to the value of Γ_γ. For the level at 20.9 eV the ratio of the neutron width to the capture width is more favorable, but the area analysis is complicated by a poorly resolved p-wave level at 19.5 eV[22,24] and an important level in ^{235}U at 19.3 eV.[17] Many early measurements were done on natural uranium, and even the best depleted uranium samples, available today, contain a non-negligible amount of ^{235}U.

B. Shape Analysis. Shape analysis is often used to determine the total width, $\Gamma_\gamma + \Gamma_n$, of a resonance. However, for the low-energy levels of ^{238}U the room-temperature Doppler width is about twice as large as the natural width so that the shape of the resonances is almost entirely determined by the

Doppler broadening: for the 6.67 eV level the room temperature Doppler width is 54 mV, whereas the natural width is approximately 25 mV; the apparent width of the level, obtained by an appropriate convolution of the line shape with the Doppler broadening shape, is approximately 100 mV and is very insensitive to the exact value of the natural width.

In order to reduce (and to better understand) the Doppler broadening, measurements have been performed with the sample cooled below room temperature.[14,30] But the interpretation of such measurements is considerably complicated by crystal binding effects.

C. Thick Sample Measurements. The resonance parameters may also be obtained from a comparison of transmission (or self-indication) measurements through thick and thin samples. The transmission area through a thin sample is proportional to Γ_n and that through a thick sample to $\Gamma_n(\Gamma_\gamma + \Gamma_n)$ so that a comparison of the two types of transmission areas yields Γ_n and Γ_γ. However, a proper interpretation of thick sample transmission (or self-indication) measurements requires a multilevel formalism, and the parameters obtained are somewhat sensitive to the value of the scattering radius and to the parameters of the neighboring levels, particularly of the poorly known bound levels.[24]

3. Measurement of Jackson and Lynn[14]

The value $\Gamma = 27.2 \pm 0.4$ mV given by Jackson and Lynn for the level at 6.67 eV has a stated uncertainty considerably lower than any of the other values listed in Table A.1. The value is also higher than any of the other values listed for that level, and is discrepant with the values given by Levin and Hughes,[8] Radkevich et al.,[12] Michaudon et al.,[17] Liou and Chrien,[23] and Olsen et al.[24] Because of its small uncertainty, the value has been weighted heavily in most evaluations and in particular in ENDF/B-IV, and it has tended to "pull up" the evaluated value of Γ_γ for the 6.67 eV level.

One of the main motivations for the experiments of Jackson and Lynn was to study resonant absorption of neutrons by cristals: in their words, "a narrow resonance, whose nuclear parameters are known, may be regarded as a probe for measuring some features of the lattice oscillation spectrum."[14] The experiment consisted of transmission measurements through uranium metal and oxide samples of various thicknesses at the temperatures of 4, 77, and 293 deg K.

The resonance parameters were determined by shape analysis of the transmission data using a Breit-Wigner term convoluted with the lattice energy transfer function. The values were obtained assuming that the mean frequency of the uranium metal lattice corresponds precisely to $h\nu$ = 0.011 eV, no uncertainty was allowed for this assumption.[23]

It appears that any evaluation of the capture width of the 6.67-eV level should increase the uncertainty in the value of Jackson and Lynn, to allow for uncertainties in the model; furthermore, this value should be used with a Doppler broadening kernel similar to that which was used in the analysis of the experiment, and not with the free gas Maxwell-Boltzmann type kernel often used in reactor calculations.[31,32]

4. Proposed Evaluation of the Capture Widths

We have seen that there are large discrepancies among the measured capture widths. Some of the discrepancies may be associated, in part, with problems in the interpretation of the measurements: the value of Jackson and Lynn[14] was obtained by using a refined Doppler broadening theory, whereas all the other values were obtained using a free gas, effective temperature model; the values of Michaudon et al.[17] were obtained assuming that Γ_γ was the same for the levels of 6.67, 20.9, and 36.8 eV; all the values before 1976 were obtained using the single-level Breit-Wigner approximation, whereas multilevel effects were considered in the analyses of Liou and Chrien[23] and Olsen et al.[24]

It is obviously impossible to evaluate a set of Γ_γ which will agree with all measurements shown in Table A.1. There are good reasons to weight more the more recent measurements: modern time-of-flight techniques allow much better resolution and higher intensities than were available a decade ago. Recent measurements were also done with a wide range of thicknesses and used highly depleted uranium, whereas early measurements were done with natural uranium, and hence required large corrections for the ^{235}U contaminant. In Figs. A.1 and A.2 we compare the transmission data of Firk, Lynn, and Moxon[16] with those of Olsen et al.[24] in the vicinity of 350 eV. Note the improvements in resolution, statistical accuracy, and number of samples used. Many of the early values were obtained using scattering and capture measurements where multiple scattering corrections were ignored or roughly approximated, whereas the most recent values were derived primarily from transmission measurements which do not

Table A.1. Measured and Evaluated* Values of Γ_γ (mV) for the First Six S-Wave Levels of U-238 (and the P-Wave Level at 10.22 eV)

E_o (eV)	6.67	20.9	36.8	66.15	80.74	102.5	10.22
Harvey (55)		25±5	29±9	17±10			
Levin (56)	24±2	30±6	40±20				
Lynn (56)	26.1±1.5	28.8±2.3	24.9±4.2	18.6±2.7		15.5±5.4	
Fluharty (56)		25.9±12	27.7±24	39.1±26		24±26	
Bollinger(57)	26±3	21.9±2.3	29±10	25.6±9			
Radkevich (57)	21.15±1.30	36±3.5	34±10	25.5±12	21±15		
Rosen (60)						21±6	
Jackson (62)	27.2±0.4						
Moxon (62)			21.2±3.5	24.1±2		24.1±2	
Firk (63)			31.3±2.2	25.1±1.6		30.6±3.3	
Michaudon (63)	23±1	23±1	23±1				
Ashgar (66)	23.43±10.12	33.83±4	26.33±3	26.07±2	21.17±10	25.95±2	
Glass (62)			20.9±6	17.35±4		24.9±5	
Rohr (70)				19.6±3		26.1±2.3	
Maleski (72)				25±2		26±2	
Rahn (72)		22±3	23±2	21±2		28±3	
Chrien (76)	21.8±1	23.5±1.5	23.6±2	22.2±2	23.7±2.5	24.3±2.5	
Olsen (76)	23±0.8	22.8±0.8	22.9±0.8	23.2±0.8	24.3±1.3	24.1±0.9	22.2±2
Poortmans (76)		23.2±0.6	22.9±0.3	24.0±0.4		24.3±0.4	
*BNL-325 (65)	26±2	26±4	26±4	24±2	21±15	24±3	
*BNL-325 (73)	26±2	25±3	25±2	22±2		26±2	
Moxon (74)	26.9±0.37	25.7±1	26.55±1.2	23.56±0.76	21.17±8.9	25.78±0.94	
ENDF/B-IV	25.6	26.8	26.0	23.5	23.5	26.0	23.5
*SETD	23.0	23.0	23.0	23.5	23.5	26.0	23.5

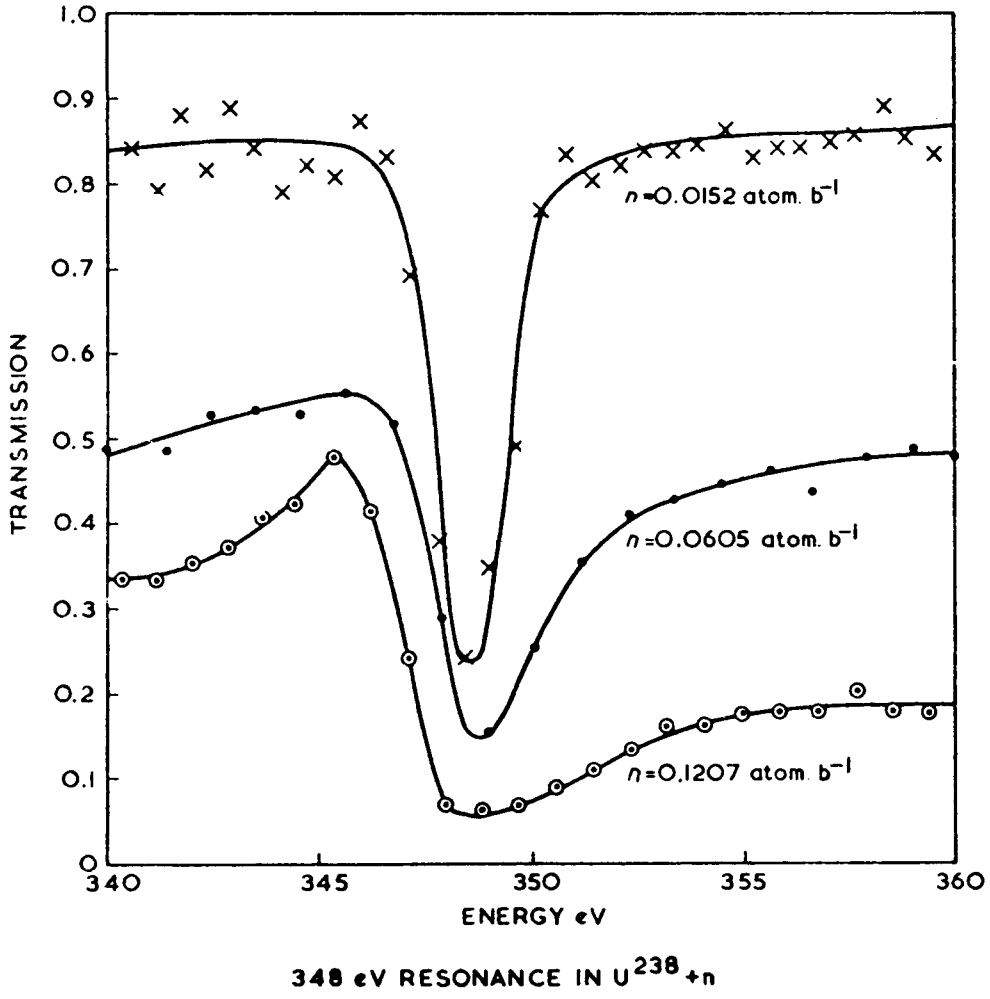

Fig. A.1. Typical Resonance Transmission Curves in the Region of Neutron Energy 340 eV to 360 eV.

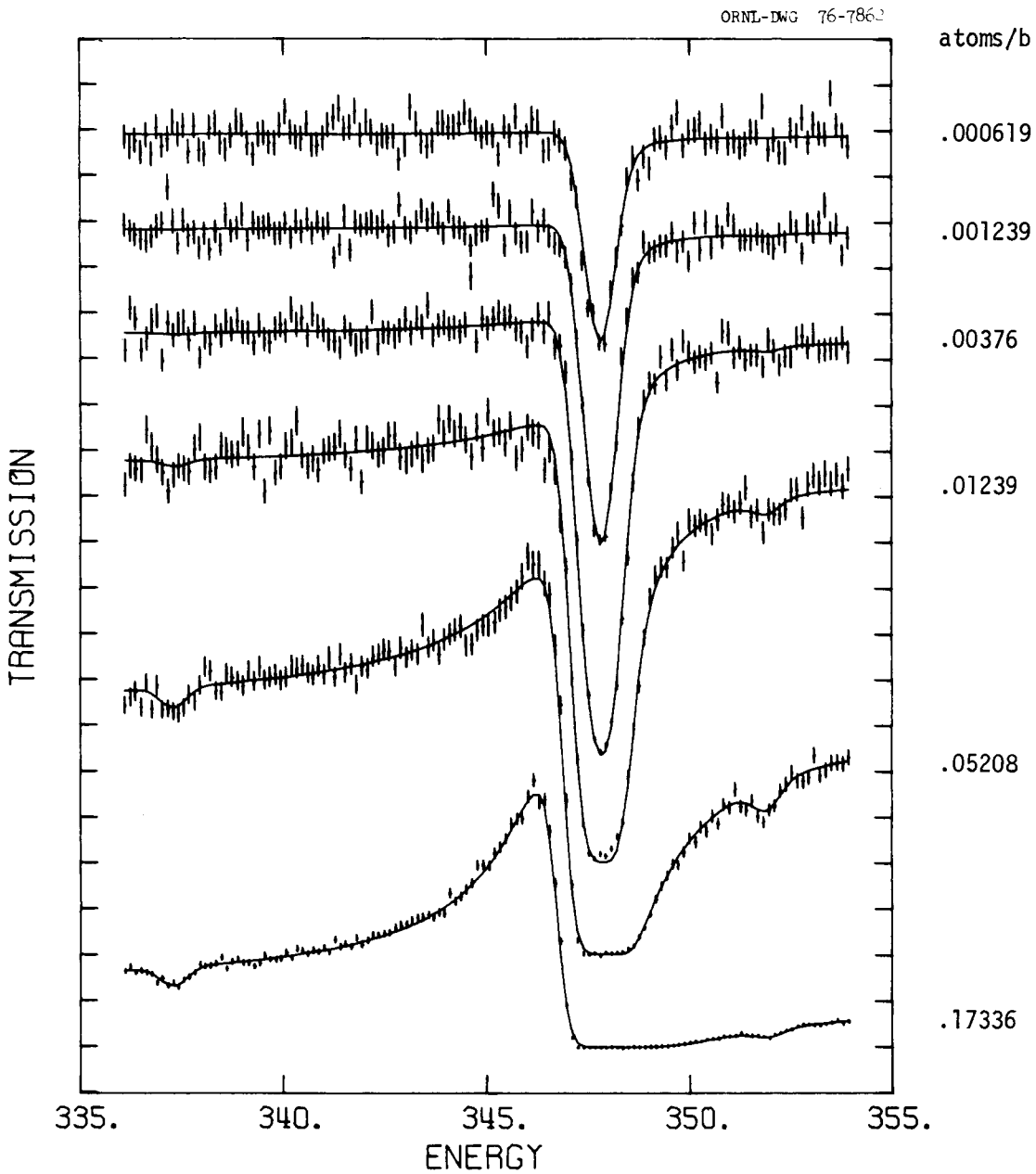

Fig. A.2. Least-Squares Fit to the 0.0127, 0.0254, 0.0762, 0.254, 1.08, and 3.62 cm Transmissions Around the 347.8 eV Resonance from a Seven-Sample Simultaneous Search on the Energy Region from 299.4 to 390.1 eV. The radiation width was held fixed at its ENDF/B-IV value of 23.5 mV and the neutron width converged to 80.0 $\pm$ 0.3 (stat) $\pm$ 1.6 (syst) mV.

require multiple scattering corrections. Finally the good agreement among the various values reported since 1970 suggests an improvement in the measurement techniques.

For the reasons previously discussed it seems appropriate to evaluate the capture widths of the first three s-wave levels in ^{238}U at 23 $\pm$ 1 mV. Those values are significantly lower than those of ENDF/B-IV and of most other evaluations, but they seem fairly consistent with presently available information.

III. Neutron Widths

1. Correlations Between Neutron and Capture Widths

In Table A.2 we list the results of most of the measurements[7-25,33-35] and of a few evaluations[1,26-27] of the neutron widths, Γ_n, of the six first s-wave levels and of the p-wave level at 10.22 eV. Because neutron widths can be obtained directly from thin samples transmission or capture area measurements, the relative accuracy of the neutron widths data is generally much better than that of the capture widths data. Yet there are discrepancies in the values listed in Table A.2. In particular, the values of Radkevich et al.[12] for the first three levels are discrepant with almost all the other data. (This discrepancy is not understood.)

Most transmission, self-indication, capture or scattering measurements will yield strongly correlated values of Γ_γ and Γ_n; in fact, many measurements yield only a relation between those two widths.[28] Nevertheless there is no significant external correlations between the values of Γ_γ and Γ_n reported in Tables A.1 and A.2: for instance, in the measurement of Lynn and Pattenden[9] a relatively high value of Γ_γ for the 6.67-eV level is associated with a relatively low value of Γ_n, whereas in the measurement of Jackson and Lynn[14] a relatively high value of Γ_γ is associated with a relatively high value of Γ_n.

The absence of significant external correlations between the values of Γ_n and Γ_γ reported by a given experimenter is partly due to the fact that each value is based on a number of experiments that have different internal correlations between the widths, and partly due to the fact that the capture widths have relatively large uncertainties obscuring any possible correlation.

Table A.2. Measured and Evaluated* Values of Γ_n (mV) for the First Six S-Wave Levels of U-238 (and the P-Wave Level at 10.23 eV)

E_o (eV)	6.67	20.9	36.8	66.15	80.14	102.5	10.22
Harvey (55)		8.5±0.4	32.5±1.9	25±2	2.1±0.7	65±9	
Levin (56)	1.54±0.10	8.3±0.7	30±4				
Lynn (56)	1.4±0.1	8.7±0.3	28.6±1.5	22.6±1.5	1.8±0.6	67.5±3	
Fluharty (56)		10.3±2	32.6±9	25.4±7	2.34±0.80	69±20	
Bollinger (57)	1.45±0.12	9.9±0.4	34±2.3	23.4±1.5	2.1±0.2	74±5	0.0014
Radkevich (57)	1.15±0.04	6.35±0.59	22±3.5	19.1±4.5	2.7±1.1		
Jackson (62)	1.52±0.01						
Moxon (62)			34.5±3	23.5±1.5	1.8±0.3	69±3	
Firk (63)			31±0.9	25.1±1.2		65.9±2	
Garg (64)	1.52±0.01	8.7±0.3	31±0.9	25±1	2.06±0.17	65.9±2	
Ashgar (66)	1.578±0.1	9.34±0.5	30.95±1.17	22.74±0.77	1.85±0.15	58.64±2	0.0014
Rohr (70)				24.8±1.5		72.6±0.5	
Carraro (70)				25.3±1	2±1.5	69.5±7	
Makeski (72)				24.0±1.5	2.2±0.2	70±3	
Rahn (72)	1.52±0.05	8.5±0.78	38±2	26±2	1.71±0.18	70±4	0.00177±0.0004
Nakajima (75)		10.1±1.0	33.4±1.7	25.5±1.3	2.25±0.18	71.3±4.3	
Chrien (76)	1.50±0.03	9.86±0.5	33.3±1.2	25.6±1.8	2.16±0.18	68±5	0.00165±0.00015
Olsen (76)	1.480±0.032	10.16±0.21	33.76±0.70	24.37±0.53	1.823±0.046	70.9±1.6	0.00168±0.00005
Poortsmans (76)		10.2±0.1	34.1±0.5	23.9±0.8	1.81±0.08	69.0±0.2	0.00167±0.00004
*BNL-325 (65)	1.52±0.02	8.5±0.5	31±0.9	25±1.2	2±0.2	68±3	0.0014
*BNL-325 (73)	1.52±0.02	8.7±0.5	32±1	26±1.5	2±0.2	70±3	0.00156±0.00001
*Moxon (74)	1.51±0.009	8.97±0.175	31.6±0.5	24±0.04	1.96±0.07	70.8±0.4	0.00156±0.00001
*ENDF/B-IV	1.50	8.8	31.1	25.3	2	71	0.00156
*SETD	1.50	10.0	33.5	25.3	2	71	0.00156

3. Proposed Evaluation of the Neutron Widths

The ENDF/B-IV values of the neutron widths of the first few levels of ^{238}U are in fair agreement with the bulk of the data shown in Table A.2, except perhaps for the levels of 20.9 eV and 36.8 eV. For those two levels the recent experiments of Nakajima et al.,[35] Liou and Chrien,[23] Olsen et al.,[24] and Poortmans et al.[25] yield a somewhat higher value. The excellent agreement between those four experiments (which extends over more levels than those listed in Table A.2) suggests that a value of 10 mV for the level at 20.9 eV and of 33.5 mV for that at 36.8 eV would be more consistent with the bulk of the information presently available.

IV. Thermal Cross Sections and "Smooth Cross Sections"

1. Thermal Cross Sections and Bound Levels

In Tables A.3 and A.4 we compare the computed and measured values of the total and capture cross sections at 0.0253 eV. The measured values were obtained from the last edition of BNL-325.[26A] Table A.5, taken from the work of Hunt, Robertson, and Ryves,[36] summarizes the measurements of the thermal capture cross section.[36-44] The total cross section in the thermal region corresponds to a coherent scattering amplitude of $(0.84 \pm 0.01) \times 10^{-12}$ cm, a value in excellent agreement with the results of three neutron diffraction measurements.[6,45-47] The potential scattering cross section was taken from ENDF/B-IV; it was evaluated by T. A. Pitterle[2] and corresponds to an effective scattering radius of $(0.9184 \pm 0.013) \times 10^{-12}$ cm, a value obtained by Uttley[48,49] and Lynn[50] from an analysis of the average total cross section in the keV region.

The calculations were done with the proposed modification of the ENDF/B-IV resolved resonance parameters: the capture widths of the first three s-wave levels were set at 23 mV, the neutron widths of the levels at 20.9 and 36.8 eV were set at 10 mV and 33.5 mV respectively. The contributions of the resolved levels between 1 and 4000 eV were computed explicitly using the single-level Breit-Wigner formula. The contributions of the bound levels with energies below -140 eV were approximated with a "picket-fence" model to be discussed in the next section. Resonance parameters for a set of seven assumed levels with energies between -140 eV and -20 eV were adjusted to yield the desired capture and total cross sections at 0.0253 eV. The resonance parameters of those seven hypothetical levels are listed in Table A.6.

Table A.3. Total Cross Section (in barns) at 0.0253 eV
(Computed with proposed modification of ENDF/B-IV)

Capture Cross Section	2.70±0.02
Potential Scattering	10.599
Resolved levels contribution	-4.276
Bound Levels with -4 keV < E_r < -150 eV	1.555
Bound Levels with E_r > -150 eV	1.032
Computed Total Cross Section	11.610
Measured Total Cross Section[26A]	11.60±0.16

Table A.4. Capture Cross Section (in barns) at 0.0253 eV
(Computed with proposed modification of ENDF/B-IV)

Resolved Levels Contribution	2.349
Bound Levels with E_r < -150 eV	0.060
Bound Levels with E_r > -150 eV	0.292
Computed Capture Cross Section	2.701
Measured Capture Cross Section[26A]	2.70±0.02

Table A.5. ^{238}U Capture Cross Section for Neutrons of Velocity 2200 m/sec

Reference	σ_s (barn)	Methods and Comments
Harris, Rose, and Schroeder (1954)	2.71±0.05	Reactivity measurements in CP3 using a sample of very low ^{238}U content. Cd ratio measurements by activation to correct for resonance absorption. Revised using $\sigma_A(B)$ = 757.7 b at 2200 m/sec for the standard.
Egelstaff (1954)	2.8±0.10	Transmission measurements with a slow neutron chopper. Sample of very low ^{235}U content was used.
Crocker (1955)	2.72±0.10	Activation in a thermal spectrum with $\sigma_0[Au]$ = 98.8 b. Corrected for fission activity by Ryves (1959).
Small (1955)	2.72±0.06	Local oscillator in well moderated spectrum. Measurements with natural and depleted uranium. Revised assuming $\sigma_A(M_nSO_4)$ = 13.73 b.
Cocking and Egelstaff (1955)	2.69±0.04	Transmission measurements using cold neutrons from a Bi filter extrapolated to 2200 m/sec. Sample was of a very low ^{235}U content.
Egelstaff and Hall (1955)	2.69±0.04	Transmission measurements at long wavelengths with slow neutron chopper. Sample was of very low ^{235}U content.
Palevsky (1955)	2.73±0.07	Transmission measurements at long wavelengths with slow neutron chopper. Sample was of natural uranium.
Bingham, Durham, and Ungrin (1968)	2.721±0.016	Relative to thermal fission cross section of ^{235}U.
Hunt et al. (1969)	2.69±0.03	Activation in a thermal spectrum <0.005% ^{235}U.

The choice of the parameters of the last bound levels (Table A.6) is, to a large extent, arbitrary. The highest of those levels must have a reduced neutron width, Γ_n^o, smaller than average since the scattering cross section at thermal energies is smaller than the potential scattering, but, within this constraint there are an infinite number of combinations that will yield the desired thermal values. Fortunately the low-energy cross sections are not sensitive to the specific values of the parameters of the bound levels, with one possible exception which will be discussed later.[51]

2. Smooth Cross Sections (File 3)

The measured thermal cross sections introduce some constraints on the parameters of the bound levels. Those bound levels, and the levels above the resolved region, define the smooth cross sections at low energies. Indeed the purpose of the low-energy File 3 is to account for the contributions to the cross sections of those levels which are not explicitly included in the resolved resonance file (File 3).[52]

We shall follow the format of the ENDF/B-IV evaluation for ^{238}U: below 1 eV the scattering and capture cross sections are defined entirely by their File 3 contribution. Above 1 eV the smooth cross-section contribution of File 3 is added to a resolved resonance contribution from File 2. Below 1 eV the smooth cross sections are computed by adding the contributions of the resolved levels (with energies between 1 and 4000 eV), of the seven hypothetical bound levels (Table A.6) and of a "picket fence" of uniform levels extending from $-\infty$ to -140 eV and from 4 keV to $+\infty$. Above 1 eV the smooth cross sections consist of the same contributions except that of the resolved levels between 1 and 4000 eV which is obtained explicitly from File 2. The modification of the ENDF/B-IV File 3 is defined only up to 2 keV: above that energy the values of the smooth cross sections are considered unimportant for thermal assemblies.

The contributions of the "picket-fence levels" to the capture cross section, $\delta\sigma_\gamma$, and to the scattering cross section, $\delta\sigma_n$ are approximated by:

$$\delta\sigma_\gamma = \frac{C}{\sqrt{E}} \frac{\Gamma_n^o}{D} \Gamma_\gamma \quad f_1(E) \tag{A.1}$$

$$\delta\sigma_n = C \frac{\Gamma_n^o}{D} [\Gamma_n^o f_1(E) - 4 k_o a f_2(E)] \tag{A.2}$$

Table A.6. Assumed Parameters of the Bound Levels Above -150 eV

E_r (eV)	Γ_n^o (mV)	Γ_γ (mV)	$\delta\sigma_s$ (E_{th})	$\delta\sigma_\gamma$ (E_{th})
-140	5.6	23.5	0.212	0.028
-120	5.6	23.5	0.248	0.038
-100	5.6	23.5	0.297	0.054
-80	0.5	23.5	0.033	0.008
-60	0.5	23.5	0.044	0.013
-40	0.5	23.5	0.066	0.030
-20	0.5	23.5	0.132	0.121
Total			1.032	0.292
Average	2.7	23.5		

where $C = \pi k_o^{-2}$, $k_o = 2.1875 \times 10^9$ cm^{-1} is the reduced wave number at 1 eV, $\Gamma_n^o = 2$ mV and $\Gamma_\gamma = 23.5$ mV are the average reduced neutron width and capture width respectively, D = 22 eV is the averaging spacing of s-wave levels and $a = 0.9184 \times 10^{-12}$ cm is the effective scattering radius.

$$f_1(E) = \frac{E^+ - E^- + D}{(E^+ - E + .5D)(E - E^- + .5D)} \tag{A.3}$$

$$f_2(E) = \ell n \left(\frac{E - E^- + .582D}{E^+ - E + .582D} \right) \tag{A.4}$$

$E^+ = 4000$ eV, $E^- = -140$ eV are the limits of the picket fence. These approximations have been discussed elsewhere.[53]

A listing of the smooth file, compared with that of ENDF/B-IV is shown in Table A.7. Note that the difference between the two files is appreciable only above 1 eV.

V. Discussion and Conclusion

1. Infinite Dilution Capture Resonance Integral

In Table A.8 we compare the values of the infinite dilution capture resonance integral as computed with ENDF/B-IV and with the proposed modification of ENDF/B-IV, with the measured value.

The measured value was taken from BNL-325 compilation.[26A,54] The ENDF/B-IV value was obtained numerically by J. E. White;[55] the value corresponding to the proposed modification was obtained by using the following analytic approximation for the contribution, δI_γ, of the low-energy smooth cross section and of the resolved resonance parameters:[26A]

$$\delta I_\gamma = .45\, \sigma_{n\lambda}(E_{th}) + 2\pi c \sum_\lambda \frac{\Gamma_{n\lambda}\, \Gamma_{\gamma\lambda}}{E_\lambda^2 (\Gamma_{\gamma\lambda} + \Gamma_{n\lambda})} \tag{A.5}$$

Table A.7. Comparison of Files 3, ENDF/B-IV and Proposed Modifications

Neutron Energy (eV)	Proposed Modification		ENDF/B-IV	
	Elastic Scattering (b)	Capture (b)	Elastic Scattering (b)	Capture (b)
10^{-5}	8.89	135	8.96	135
10^{-4}	8.89	42.8	8.95	42.8
10^{-3}	8.89	13.5	8.95	13.5
10^{-2}	8.89	4.29	8.95	4.28
0.0253	8.89	2.70	8.95	2.70
0.05	8.88	1.93	8.95	1.93
0.1	8.88	1.38	8.94	1.38
0.5	8.82	0.659	8.89	0.665
0.7	8.78	0.578	8.87	0.586
0.8	8.77	0.551	8.85	0.560
0.9	8.75	0.530	8.84	0.539
1.	8.73	0.513	8.82	0.523
1.	2.57	0.0536	2.51	0.0277
10	2.43	0.0124	2.29	0.00729
100	1.78	0.00128	0	0
680	0.784	0.00010	0	0
700	0.767	0.00009	0	0.005
980	0.559	0.00006	0	0.02
1000	0.546	0.00006	0	0.05
2000	0.015	0.00003	0	0.11

Table A.8. Infinite Dilution Capture Resonance Integral

$$R.I. = \int_{0.5\ eV}^{\infty} \sigma_{n\gamma}(E)\,\frac{dE}{E}$$

1.	Computation with Proposed Modification of ENDF/B-IV	
	1/v-part of cross section	1.215 b
	Unresolved resonances	2.357 b
	Resolved p-waves	0.565 b
	Resolved s-waves	274.32 b
	Total	278.457 b
2.	Computed with ENDF/B-IV[55]	278.355 b
3.	Experimental Value	275±5 b

where $\sigma_{n\gamma}(E_{th})$ = 2.7 b is the capture cross section at 0.0253 eV and the other symbols have been defined previously.

The accuracy of the calculations is estimated to be ±2; both calculations agree with the measured value.

2. Procedure to Test the Proposed Modification

In testing the proposed modifications to ENDF/B-IV with thermal lattice parameters it was desirable to proceed step-wise as some of the proposed changes will have opposite effects on integral parameters: for instance, the decrease in the capture widths and increase in the neutron width will affect the ratio of epithermal to thermal captures in opposite directions.[56]

The switching from the single level to the multilevel formalism is not expected to have an appreciable effect on integral parameters; however, this hypothesis must be tested directly, since it is impractical to express the uncertainties associated with a formalism in the format of a covariance file.

A covariance error file is discussed in Appendix C for the proposed modification of ENDF/B-IV.

3. Shape of the ^{238}U Cross Section in the Thermal Region

A final comment must be made concerning the shape of the capture cross section in the thermal region. We have stated that the shape of the low-energy cross sections is not a sensitive function of the parameters of the bound levels. Indeed for most choices of parameters the capture cross section is essentially proportional to $E^{-1/2}$. It is, however, possible to choose a set of bound levels which will yield too low a value for the capture cross section at 0.0253 eV. The missing capture could then be accounted for by a p-wave level, or small s-wave level, in the thermal energy region or just below. With such a hypothesis the capture cross section below 0.1 eV would not be proportional to $E^{-1/2}$, and this may have an important impact on the calculation of thermal lattice parameters. In our opinion the present experimental information does not rule out the possibility of a small level near zero energy. This possibility is excluded from the present proposed modification of ENDF/B-IV.

References for Appendix A

1. ENDF/B-IV MAT 1262, 92-U-238 Evaluated September 1973 by N. C. Paik (WARD) - Distributed August 1974.

2. T. A. Pitterle, "Evaluation of U-238 Neutron Cross Sections for the ENDF/B Version II File," WARD-4181-1 (March 1971).

3. T. A. Pitterle, "Evaluation of U-238 Neutron Cross Sections for the ENDF/B-File," Second International Conference on Nuclear Data for Reactors, Helsinki, 15-19 June 1970, Vol. II, p. 687 (IAEA, Vienna, 1970).

4. T. A. Pitterle, N. C. Paik, and C. Durston, "Evaluation and Integral Testing of Modifications to ENDF/B Version II Data," WARD-4210T4-1 (December 1971).

5. B. R. Leonard, Jr., "Thermal Cross Sections of the Fissile and Fertile Nuclei for ENDF/B-II," BNWL-1586 (June 1971).

6. B. R. Leonard, Jr., "Energy-Dependent Cross Sections in the Thermal Region," National Topical Meeting on New Developments in Reactor Physics and Shielding, Sept. 12-15, 1972, CONF-720901, Book 1, p. 81 (USAEC Technical Information Center).

7. J. A. Harvey, D. J. Hughes, R. S. Carter, and V. E. Pilcher, Phys. Rev. 99, 10 (1955); also private communication from J. A. Harvey (1976).

8. J. S. Levin and D. J. Hughes, Phys. Rev. 101, 1328 (1956).

9. J. E. Lynn and N. J. Pattenden, Proc. International Conf. on Peaceful Uses of Atomic Energy 4, 210 (1956).

10. R. G. Fluharty, F. B. Simpson, and O. D. Simpson, Phys. Rev. 103, 1778 (1956).

11. L. M. Bollinger, R. E. Cote', D. A. Dahlberg, and G. E. Thomas, Phys. Rev. 105, 661 (1957).

12. I. A. Radkevich, V. V. Vladimirsky, and V. V. Sokolovsky, J. Nuc. Energy 5, 92 (1957).

13. J. L. Rosen, J. S. Desjardins, J. Rainwater, and W. W. Havens, Phys. Rev. 118, 687 (1960).

14. H. E. Jackson and J. E. Lynn, Phys. Rev. 127, 461 (1962).

15. M. C. Moxon and C. M. Mycock (1962), quoted in Refs. 26A and 26B.

16. F. W. K. Firk, J. E. Lynn, and M. C. Moxon, Nucl. Phys. 41, 614 (1963).

17. A. Michaudon, H. Derrien, P. Ribon, and M. Sanche-Cauvin, Nucl. Phys. 69, 545 (1965).

18. M. Asghar, C. M. Chaffey, and M. C. Moxon, Nucl. Phys. 85, 305 (1960).

19. N. W. Glass, A. D. Schelberg, L. D. Tatro, and J. W. Warren, "U-238 Neutron Capture Results from Bomb Source Neutrons," in Neutron Cross Section and Technology Proceedings of Conference, Washington, D.C., March 1968, NBS Special Publication 299, Vol. 1, p. 573 (1968).

20. G. Rohr, H. Weigmann, and J. Winter, Nuclear Data for Reactors, Helsinki, IAEA Vienna, 1, 413 (1970).

21. K. L. Maletski, L. B. Pikel'ner, I. M. Salamatin, and E. I. Sharapov, Sovt. J. At. Energy 32, 45 (1972).

22. F. Rahn et al., Phys. Rev. C6, 1954 (1972).

23. H. I. Liou and R. E. Chrien, "Epithermal Neutron Capture in ^{238}U," BNL-21696 (1976); see also R. E. Chrien, H. I. Liou, and J. Kopecky, "Neutron Capture in ^{238}U," Contributed Paper PH1/D22, 1976 International Conference on Interactions of Neutrons with Nuclei, July 6-9, 1976, The University of Lowell, Lowell, Mass. (Proceedings published by TIC, ERDA-1976; CONF-76015).

24. D. K. Olsen, G. deSaussure, R. B. Perez, and F. C. Difilippo, "Resonance Parameters of the 6.67, 20.9, and 36.8 eV Levels in U-238," Trans. Am. Nucl. Soc., Vol. 23 (June 1976); see also D. K. Olsen, G. deSaussure, R. B. Perez, E. G. Silver, F. C. Difilippo, R. W. Ingle, and H. Weaver, "Precise Measurement, 0.52 to 4000 eV, and Analysis, 0.52 to 1088 eV, of Neutron Transmissions Through Seven Samples of U-238," accepted for publication in Nucl. Sci. Eng., April 1977.

25. F. Poortmans, E. Cornelis, L. Mewissen, G. Rohr, R. Shelley, T. Van der Veen, G. Vanpraet, and H. Weigmann, "Cross Sections and Neutron Resonance Parameters for ^{238}U Below 4 keV," Contributed Paper PG2/B18, 1976 International Conference on Interactions of Neutrons with Nuclei," July 6-9, 1976; The University of Lowell, Lowell, Mass. (Proceedings published by TIC, ERDA-1976: CONF. 76015.)

26A. S. F. Mughabghab and D. E. Garber, BNL-325, Third Edition, Vol. 1 (June 1973).

26B. J. R. Stehn, M. D. Goldberg, R. Weiner-Chasman, S. F. Mughabghab, B. A. Magurno, and V. M. May, BNL-325, Second Edition, Suppl. No. 2 (1965).

27. M. Moxon, "Evaluation of U-238 Resonance Parameters," in Specialists Meeting on Resonance Parameters of Fertile Nuclei and Pu-239, Saclay 20-22 May 1974, Proceedings edited by P. Ribon NEANDS(E)163U, January 1975, p. 159.

28. "Experimental Neutron Resonance Spectroscopy," Edited by J. A. Harvey, Academic Press, New York and London, 1970.

29. "Neutron Time-of-Flight Methods," Proceedings of a Symposium, Saclay, 24-27 July 1961, Edited by J. Spapen, published by: European Atomic Energy Community (EURATOM), Brussels, Sept. 1961.

30. A. Michaudon, H. Derrien, C. LePipec, and P. Ribon, "Etude de l'interaction resonnante de neutrons d energie voisine de 6, 7 eV avec le noyau d' uranium 238 dans l'oxyde d'uranium a basse temperature," C. R. Academie des Sciences, vol. 255, p. 2086 (October 22, 1962).

31. W. E. Lamb, Phys. Rev. 55, 190 (1939).

32. A. W. Solbrig, Am. J. Phys. 29, 257 (1961).

33. J. B. Garg, J. Rainwater, J. S. Peterson, and W. W. Havens, Phys. Rev. 134, B985 (1964).

34. G. Carraro and W. Kolar, Nuclear Data for Reactors, Helsinki, IAEA Vienna, I, 403 (1970).

35. Y. Nakajima, A. Asami, M. Mizumoto, T. Fuketa, and H. Takekoshi in Nuclear Cross Sections and Technology, Proceedings of a Conference, NBS Special Publication 425, p. 738 (1975).

36. J. B. Hunt, J. C. Robertson, and T. B. Ryves, Nucl. Energy 23, 705 (1969).

37. S. P. Harris, D. Rose, and H. D. Schroeder, ANL-LAT=109 (1954).

38. P. A. Egelstaff, J. Nucl. Energy 1, 92 (1954).

39. V. S. Crocker, J. Nucl. Energy 1, 234 (1955).

40. V. G. Small, J. Nucl. Energy 1, 319 (1955).

41. S. J. Cocking and P. A. Egelstaff, NRDC-84, part 2 (1955).

42. P. A. Egelstaff and J. W. Hall, NRDC-84, part 2 (1955).

43. H. Palevsky, unpublished, quoted in Proc. Geneva Conf. 4, 147 (1955).

44. C. B. Bigham, P. W. Durham, and B. N. Andric, EANDS (Conf. 134) (1968).

45. R. B. Roof, G. P. Arnold, and K. A. Gschneider, Acta. Cryst. 15, 351 (1962).

46. M. Atoji, J. Chem. Phys. 35, 1950 (1961).

47. K. D. Rouse and B. T. M. Willis, Acta. Cryst. B24, 177 (1968).

48. C. A. Uttley, Proc. International Conf. on Nucl. Phys., Paris, p. 700 (1964).

49. C. A. Uttley, "Total Neutron Cross Section Measurements," in Nuclear Data for Reactors, Program at AERE for Period 1 July 1963 - 31 December 1963, EANDC-(UK) 35L, p. 2 (1964).

50. J. E. Lynn, Proc. Phys. Soc. (London), 82, 903 (1963).

51. For a more detailed discussion, see M. F. James and J. S. Story, "Contribution of Negative Energy and Distant Resonances in the Resolved Resonance Region," Nuclear Data for Reactors, Conference Proceedings, Paris, 17-21 October 1966, IAEA Vienna 1967, Vol. II, p. 359.

52. ENDF/B formats are defined in ENDF-102, "Data Formats and Procedures for Evaluated Nuclear Data File, ENDF," Revised by D. Garber, C. Dunford, and S. Pearlstein, BNL-NCS-50496 (October 1975).

53. G. deSaussure, D. K. Olsen, and R. B. Perez, "Note on the ENDF/B-IV Representation of the U-238 Total Cross Section in the Resolved Resonance Energy Region," Nucl. Sci. Eng. 61, 496 (1976).

54. See also J. Hardy, G. G. Smith, and D. Klein, Nucl. Sci. Eng. 14, 358 (1962)

55. J. E. White, private communication (June 1976).

56. M. R. Bhat, "A Discussion of U-238 Resolved Resonance Parameters and Their Influence on Capture Cross Sections," in Seminar on U-238 Resonance Capture, BNL-NCS-50451, p. 255 (March 1975).

57. R. C. Block et al., Results presented at the CSWEG meeting of October 26-28, 1976.

58. D. Finch, private communication of October 6, 1976.

APPENDIX B

Uncertainty Files for ^{235}U Cross Sections

R. W. Peelle

To perform the required sensitivity studies it is necessary to obtain fairly complete if approximate covariance matrices for the group cross sections; procedures outlined by Perey[1] allow these to be obtained from ENDF-format uncertainty files which refer to the pointwise cross section. Up to now, sufficiently inclusive files for ^{235}U have not been available.

The points below outline the assumptions and methods employed for this complete but first-cut analysis.

1. Since the first proposed analysis uses only one thermal group for the energy region up to 0.625 eV, no attempt is made to determine uncertainties and correlations in energy for a finer mesh in the thermal region. Since Leonard[2] has analyzed the cross sections in the thermal range, an attempt is made to provide results consistent with his analysis. Should energy-dependent uncertainties and correlations become available from Leonard's ongoing work, the results of this study can be updated to permit alternate group structures to be employed in future work.

2. Uncertainties in capture are provided in an approximate way in case sensitivity studies should show them to be of importance. At least for the thermal group, the correlations between capture and fission should be shown explicitly.

3. Uncertainties in scattering are ignored, i.e., the analysis can assume they are null.

4. For the fission resonance region above 0.625 eV and up to 1 keV the analysis is based on average cross sections (flat weight, infinitely dilute) from various experiments as tabulated by Bhat[3] in his evaluation work toward ENDF/B-V. In the resonance region these average cross sections are taken over standard intervals which bracket the major resonances.

5. For fission, Difilippo has produced an uncertainty file for $^{235}U(n,f)$ in the 1-keV to 100-keV range using SUR;[4] a program which is based on the

"external" method of uncertainty analysis discussed by Perey et al.[5] This existing file is adopted following collapse to control the size of the covariance matrix in a region of low importance to thermal reactor benchmark analysis. For capture uncertainties, the values are based on the ENDF/B-IV analysis by Peelle.[6]

6. Above 0.1 MeV, though the region is assumed of little importance for thermal reactors, rough uncertainty estimates are provided to assure that the analyst is not fooled by any deceptively low output uncertainties.

7. No distinction will be made between the data base available now and that which was available for the ENDF/B-IV analysis. However, comparison could be made at least for the thermal group and possibly the epithermal groups between presently determined uncertainties, current best values likely to be used for version V, and version IV values.

A brief description of the methods used and results obtained is given in the sections below. It will be seen that the methods employed were largely qualitative. The results are intended to be adequate for analysis of thermal reactors, but are likely not to be fully adequate for sensitivity studies on fast reactors.

Variance and Covariance for $^{235}U(n,f)$ and $^{235}U(n,\gamma)$ in the Thermal Group

B. Leonard has analyzed cross sections in the thermal region in terms of 2.2 km/sec values and Westcott g factors.[2] Though the practice seems somewhat inconsistent with the idea of point covariance files, in this study a single relative uncertainty will be quoted which is combined from the uncertainties quoted for these two factors (0.29 and 0.11%, respectively). The 0.31 percent uncertainty obtained by Leonard[2] for fission is based on the output of a constrained least square fit -- note that alternatively one perhaps should employ the larger 0.5 percent uncertainty which was input to this fit based on fission cross section measurements alone. This additional margin might also compensate for as yet undetermined a cross section processing uncertainty.

The evaluated capture cross section given by Leonard was largely determined by spectrum-averaged capture/fission measurements, so the "alpha" uncertainty of 0.83 percent must be combined with the fission uncertainty to give a capture uncertainty value of 0.88 percent. The relative covariance linking capture and fission for the thermal energy range is then $0.0031^2 = 0.096 \times 10^{-4}$.

It may well be that the cross section uncertainties given above are far too small for application in the present problem, even if they are appropriate for pointwise cross sections. The effective average thermal group cross section (taken as an input for the present research) depends upon the energy spectrum within the thermal group; the uncertainty in the true spectrum may imply a much larger uncertainty in the group cross section than for the underlying microscopic cross sections. Adjusted cross sections obtained using the methods of this study, for example, cannot be taken as fully usable until this question of thermal group microscopic cross section uncertainties can be studied and resolved.

Relative Covariance for Fission at Energies Above the Thermal Group

Table 18, p. 65, gives the lower half of the relative covariance matrix for the $^{235}U(n,f)$ cross section (times 10^4). The elements were obtained by study of the scatter among the results of various experiments, except for the (1,1) element discussed above and except for the region from 1 to 100 keV.

Since the SUR method,[4] in effect, calculates the covariance matrix of a sample consisting of the existing data sets and infers that this is equal to the covariance matrix of the evaluated cross section, its estimates may tend to be high in cases where many data sets are available and a distinction might be recognized between the expected statistical distributions of the data and of the mean of the data -- the mean more resembling the evaluated cross sections. For this reason the block of the matrix between 1 and 100 keV may have values which are too large. The values given for this region were taken from the results of the prior work of Perey et al.[5]

From 0.6 eV to 1 keV the diagonal elements were deduced from tabulations prepared by Bhat[3] and from comments made by assembled experts of the CSEWG Standards Committee and the June 1976 NEANDC/NEACRP Specialists Meeting on Fast Fission Cross Sections (held at ANL). The off-diagnonal elements in the region below 100 keV were deduced by recognizing that for a large share of the available data the normalization is built up from thermal energies toward higher energies, so that for example a relative uncertainty at 10 eV remains a component of the uncertainty at 10 keV.

Because of the difference in methods employed, cross sections at energies above 100 keV were judged almost completely statistically independent of those below this energy. Uncertainties above 0.1 MeV were based on inspection of the range of scatter of data on comparison graphs prepared by W. Poenitz[32] for the above mentioned NEACRP/NEANDC meeting. Off-diagonal elements were judged on the basis of the fraction of the relevant measurement sets which include data in both of the pertinent energy ranges; this method may tend to overestimate off-diagonal elements.

Except for the thermal energy group, no covariances are given between fission and capture cross sections. Similarly, the files for both fission and capture exclude uncertainties from sources such as standard cross sections or instruments which may in fact also induce such correlations between different reaction types. The net effect is to tend to cancel the effects of these omissions for estimation of the uncertainty in an integral parameter such as the ^{235}U capture/fission ratio.

In the unresolved resonance energy region and up to 100 keV the covariance matrix given in Table F for neutron capture in ^{235}U is based on the analysis in the author's evaluation for ENDF/B-IV.[31] The off-diagonal elements in this region reflect the fact that a normalization uncertainty appears to be a strong component of the total. Above 0.1 MeV the uncertainties were estimated almost without references to the data base, and probably represent an upper limit. If uncertainties propagated from these estimates for the higher energies should be important for any application, the covariance values should be reviewed and probably updated.

In the resonance region the construction of an uncertainty file was confused by existence of an apparent bias between the most recent evaluation work and ENDF/B-III or IV. Leonard[27] has noted that in fitting the capture data below 1 eV he found it necessary to normalize upward the ORNL-RPI[33] results by 14%, while making a small downward correction to the work of Gwin.[34] While Leonard's analysis did not cover the energy region above 1 eV, the renormalized data sets agree within 3% for capture integrals over standard regions up to 60 eV except for 8 to 9 percent deviations in the region 0.7 to 1.8 eV. Since the ENDF/B versions follow closely the ORNL-RPI results given by deSaussure, there is the implication that ^{235}U capture cross sections now in use may be low by 10 to 15% through the whole resonance region. The uncertainty file therefore

shows a fully correlated 12% uncertainty from 0.6 to 80 eV, combined for diagonal elements with a 5% component to reflect the scatter among the measurements. However, the discrepancy is more likely a bias than an uncertainty, so sensitivity coefficients in this region should be examined closely to see what problems may be caused by thermal reactors by this uncertainty or bias.

Summary

Complete uncertainty files compatible with ENDF/B formats for File 33 have been provided for neutron capture and fission in ^{235}U. Only in the energy region below 0.6 eV is the covariance between capture and fission properly accounted for. Covariance components arising from uncertainties in standard cross sections are not included unless they have affected the scatter among the currently available data sets; for applications not dominated by the thermal energy group a more logically derived uncertainty file is still required. The analysis highlighted the well-known discrepancy among measurements of neutron capture in the resonance region; it now appears likely that ENDF/B-IV resonance parameters yield neutron capture cross sections systematically low by about 12%.

For energy regions about one lethargy unit wide, the diagonal covariance matrix elements for fission, from 1 eV to several MeV, correspond to relative standard deviations in the range 2 to 4%. Relative estimated uncertainties for capture cross sections in similar intervals from 1 eV to 0.2 MeV range from 8 to 25%.

References for Appendix B

1. F. G. Perey, "Format Manual for ENDF/B-V Files 31, 32, and 33" (1977); see also, F. G. Perey, "Estimated Uncertainties in Nuclear Data - An Approach," Proceedings of a Conference on Nuclear Cross Section and Technology, Volume II, edited by R. A. Schrack and C. D. Bowman, p. 842 (October 1975).

2. B. R. Leonard, Jr., D. A. Kottwitz, and J. K. Thompson, "Evaluation of the Neutron Cross Sections of ^{235}U in the Thermal Region," EPRI-NP-167 (1967).

3. M. R. Bhat, "Evaluation of the ^{235}U Fission Cross Section from 100 eV to 20 MeV," Proceedings of the NEANDC/NEACRP Specialist Meeting on Fast Neutron Fission Cross Sections of U-233, U-235, U-238, and Pu-239, June 28-30, 1976, Argonne National Laboratory, edited by W. P. Poenitz and A. B. Smith, ANL-76-90, p. 307 (1976).

4. F. C. Difilippo, "SUR, A Program to Generate Error Covariance Files," ORNL-TM-5223 (1976).

5. F. G. Perey, G. deSaussure, and R. B. Perez, "Estimated Data Covariance Files of Evaluated Cross Sections, Examples for ^{235}U and ^{238}U," in Advanced Reactors: Physics, Design, and Economics, Ed. J. M. Kallfelz and R. A. Karam, Pergamon Press, 1975.

6. R. W. Peelle, "An Evaluation for ENDF/B-IV of the Neutron Cross Sections for ^{235}U from 82 eV to 25 keV," ORNL-4955 (ENDF-233) (1976).

7. W. P. Poenitz and P. T. Guenther, Argonne National Laboratory, Supplement to ANL-76-90, Proceedings of the NEANDC/NEACRP Specialists Meeting on Fast Neutron Fission Cross Sections of U-233, U-238, and Pu-239 (1976).

8. G. deSaussure et al., "Measurement of the Neutron Capture and Fission Cross Sections and of Their Ratio Alpha for U-233, U-235, and Pu-239," Nuclear Data for Reactors, Vol. II, p. 233, IAEA, Vienna, 1967.

9. R. Gwin et al., Nucl. Sci. Eng., 59, 79 (1976).

APPENDIX C

Error File for the Low Energy Cross Sections of ^{238}U

1. Introduction

In this appendix we discuss our estimates of the uncertainties in the low energy cross sections of ^{238}U. An "error file" is defined in terms of the resonance parameters of the first six ^{238}U s-wave levels, of the p-wave level at 10.22 eV and of a few parameters describing the cross section backgrounds (file 3). The error file is intended to be folded with the appropriate sensitivity coefficients to obtain the uncertainties in the TRX-2 performance parameters due to uncertainties in the ^{238}U microscopic data. Errors were established only for those quantities which are known or thought to be important to the calculation of the TRX-2 performance parameters; hence the file is not adequate for other applications, such as the calculation of fast assemblies.

Our experience with cross section error files is very limited, and this is probably the first error file defined in terms of low energy resonance parameters. We hope that all the relevant uncertainties and their correlations have been properly identified and evaluated, but our confidence is definitely limited by lack of experience.

We find it impossible to establish meaningful symmetric errors around the ENDF/B-IV values of the resonance parameters of ^{238}U, because we believe that these values are biased. For instance, for the capture width of the level at 6.67 eV, ENDF/B-IV has a value of 25.6 mV. We would estimate the error around this value to be approximately $^{+0}_{-3}$ MeV. Since the sensitivity analysis presently requires symmetric errors, we must define the errors around those values which we believe are most likely to be correct; those are the recommended values defined by SET D of the alternative data sets discussed in Appendix A.

The error file discussed here is based only on differential cross section measurements and does not include the information from the infinite dilute resonance integral or from other "integral parameters." In Appendix A we have shown that our recommended set of parameters yields a value of the infinite dilute resonance integral consistent with the measurement of this quantity.

2. Error Estimates

The errors in the resonance energies are not considered very important: those resonance energies are surely known to better than 0.1 eV and changes in the resonance location within this bound are not expected to affect the calculated value of the performance parameter more than one part in 10^5. For the errors in the resonance energies the values of the 1973 edition of BNL-325[1] were adopted. Those values are, for most cases, somewhat larger than the values obtained by Moxon[2] from the dispersion between independent measurements.

The errors on the neutron and capture widths were evaluated with the same guidelines that were used in the evaluation of the parameters themselves. The data considered are listed in Tables A.1 and A.2 of Appendix A. The errors were obtained from the uncertainties quoted for the measurements completed in the past five years; but were somewhat arbitrarily increased to account for the fact that the average values of earlier measurements differ significantly from those of the more recent measurements (see discussion in Appendix A).

The errors on the smooth background cross section, b_n and b_γ, were obtained from the uncertainties in the thermal capture cross section and in the scattering cross section. The measurements considered in the evaluation of these data have been discussed in Appendix A. Since the smooth backgrounds represent essentially the contribution of distant levels to the cross sections, the absolute error in those backgrounds must be considered uniformly correlated over the entire energy range (0.025 to 2 keV).

The error on the effective radius a was obtained from the uncertainties in the measurements of Uttley,[3,4] Lynn,[5] Hughes and Zimmerman[6] and from the investigations of Olsen *et al.*[7] where the effects of changing in the scattering radius of the transmission measurements were studied. The correlation coefficients between the partial widths of the first three s-wave levels and the effective scattering radius a, obtained from a least-square fit to seven transmission measurements by Olsen *et al.* are given in Table C.1. The most important correlations are the negative correlations between the capture and neutron widths of the levels at 6.67 eV and 20.9 eV. The correlation coefficients of Table C.1 are specific to a given set of transmission measurements and to a particular method of analyzing the data. Moreover, those correlation coefficients are obtained

Table C.1. Correlation Coefficients Between the Effective Scattering Radius $\hat{a}$, and the Partial Widths of the First Three s-wave Resonances of ^{238}U Obtained from a fit of Seven Transmission Measurements

E_o								
	$\hat{a}$	1.00						
6.67 eV	Γ_γ	0.12	1.00					
	Γ_n	-0.06	-0.81	1.00				
20.9 eV	Γ_γ	0.03	0.08	-0.06	1.00			
	Γ_n	0.12	-0.05	0.10	-0.51	1.00		
36.7 eV	Γ_γ	-0.12	0.00	-0.10	0.03	-0.09	1.00	
	Γ_n	0.39	0.01	0.07	0.04	0.19	-0.37	1.00

from the statistical uncertainties in the data and do not include the effect of possible systematic errors. Hence, the coefficients of Table C.1 do not necessarily represent the correlation coefficients of the evaluated parameters. Nevertheless, for lack of information on the correlation patterns of other experiments, and because those measurements which were most weighted in determining the evaluated parameters are similar to those of Olsen et al., we assume that the correlations between evaluated resonance parameters are negligible, except for those between the neutron and capture widths, which are estimated to be -0.8 and -0.5 respectively, for the levels at 6.67 and 20.9 eV, on the basis of the values listed on Table C.1 (corresponding covariances are given in Table 20 of the main text).

3. Discussion and Conclusions

The errors listed in Table 20 of the main text are somewhat conservative estimates: in some cases the errors have been increased to represent the dispersion between believable data and recent evaluations. A significant reduction of the errors listed could probably be achieved, but this would require a considerable effort. In particular, it would involve (1) a readjustment of all the evaluated values (in this study the changes from ENDF/B-IV were kept at a minimum), (2) a detailed study of all the measurements to identify possible

sources of systematic errors, and (3) a complete investigation of possible correlations among parameters by least-square fitting experimental data using different constraint on the parameters and different cross section models.

Such an extensive study is beyond the scope of the present investigation. It also does not seem warranted unless a similar study is made on the other parameters affecting the calculation of the performance parameters, such as the cross sections of other materials, the formalisms used, the calculation techniques, and so on.

References for Appendix C

1. S. F. Mughabghab and D. E. Garber, BNL-325, Third Edition, Vol. 1 (June 1973).

2. M. Moxon, "Evaluation of U-238 Resonance Parameters," in Specialists Meeting on Resonance Parameters of Fertile Nuclei and Pu-239, Saclay 20-22 May 1974, Proceedings edited by P. Ribon NEANDS(E)163U, January 1975, p. 159.

3. C. A. Uttley, Proc. International Conf. on Nucl. Phys., Paris, p. 700 (1964).

4. C. A. Uttley, "Total Neutron Cross Section Measurements," in Nuclear Data for Reactors, Program at AERE for Period 1 July 1963 - 31 December 1963, EANDC-(UK) 35L, p. 2 (1964).

5. J. E. Lynn, Proc. Phys. Soc. (London), 82, 903 (1963).

6. D. J. Hughes and R. L. Zimmerman, "Neutron Resonances in Heavy Nuclei," p. 356 in Nuclear Reactions, Vol. I. Ed. P. M. Endt and M. Demeur, North Holland Publishing Company, Amsterdam, 1959.

7. D. K. Olsen, G. deSaussure, R. B. Perez, and F. C. Difilippo, "Resonance Parameters of the 6.67, 20.9, and 36.8 eV Levels in U-238," Trans. Am. Nucl. Soc., Vol. 23 (June 1976); see also, D. K. Olsen, G. deSaussure, R. B. Perez, E. G. Silver, F. C. Difilippo, R. W. Ingle, and H. Weaver, "Precise Measurement, 0.52 to 4000 eV, and Analysis, 0.52 to 1088 eV, of Neutron Transmissions Through Seven Samples of U-238," accepted for publication in Nucl. Sci. Eng., April 1977.